The completion of this thesis
was supported by the
Randy Seeling Award
given, in his memory, to another
outstanding graduate student
of the Geology Department,
University of Minnesota, Duluth.

STRATIGRAPHY AND HYDROTHERMAL ALTERATION OF ARCHEAN VOLCANIC ROCKS AT THE HEADWAY-COULEE MASSIVE SULFIDE PROSPECT, NORTHERN ONAMAN LAKE AREA, NORTHWESTERN ONTARIO

A Thesis Submitted to the Faculty of the Graduate School

of the University of Minnesota

by

STEVEN ARVID OSTERBERG

In Partial Fulfillment of the Requirements

for the Degree of

Master of Science

October 1985

ABSTRACT

The Headway-Coulee massive sulfide prospect of northwestern Ontario is situated within the Superior Province of the Canadian Shield. Rocks at the prospect form part of the Archean Wabigoon greenstone belt and consist of an intensely hydrothermally altered succession of mafic and felsic volcanic and intrusive rocks. Subaqueously deposited pillowed and amygdaloidal to massive and autobrecciated mafic lava flows form a 1-2 km thick succession which is locally interlayered with, and overlies a thin sequence of felsic volcanic rocks. The felsic volcanic rocks are laterally limited (2 km) and are composed dominantly of bedded ash tuffs capped by massive to brecciated and flow-banded lavas. The tuffs are fine-grained, generally fragment-poor, and vary from laminated to thickly-bedded. An extensive polymictic diamictite deposit, which contains clasts of granite, mafic and felsic volcanic rocks, and iron formation, is interlayered with the felsic volcanic rocks and is believed to represent a debris flow deposit which had its source to the southwest of the study area.

Based on their fine-grain size, limited lateral extent, and thin to thickly-bedded nature, the felsic tuffs are interpreted to be products of hydrovolcanic eruptions. Based on stratigraphic relationships the deposits are believed to have formed on the submerged flanks of two adjacent tuff cones. It is envisioned that the capping felsic lavas formed either under low water/magma ratio conditions as access of water to the erupting magma was restricted, and/or under high water/magma ratio conditions within a water flooded vent or on the submerged flanks of the cones.

The majority of the volcanic rocks were intensely altered by hydrothermal solutions during the waning stages of felsic volcanism. Alteration in the rocks is relatively widespread and is subconcordant to stratigraphically conformable in distribution. The altered rocks have been subdivided into four distinct mineral zones. The zones, in order of formation and increasing alteration intensity, are: (1) least altered, (2) quartz-sericite, (3) iron chlorite, and (4) chloritoid.

The progressive alteration of the rocks was studied by mass balance comparisons of the altered rocks and their less intensely altered, stratigraphic equivalents. These comparisons indicate that Al was generally immobile, and that volume losses during alteration range from 0 to approximately 50%; the largest volume losses occurred during alteration of the felsic ash tuffs. Major chemical trends involved in alteration of the rocks include large gains in K and loss of Na during sericitization, and generally addition of Fe, and loss of Ca and Na during formation of iron chlorite and subsequent development of the chloritoid alteration type.

Based on the distribution of the alteration types as well as the alteration mineralogy and chemistry it is proposed that, by shallow circulation through porous volcanic rocks, an acidic, K-rich fluid evolved and caused widespread sericitization within the study area. Deeper circulation evolved an Fe-rich fluid which was discharged along synvolcanic faults from a pressurized reservoir at depth. The solution chemically reacted with the sericitized rocks to produce the iron chlorite assemblage, and the pre-metamorphic equivalent of the chloritoid assemblage. The chloritoid assemblage developed as pre-meta-

morphic, coexisting iron chlorite + hydrous Al-silicate became unstable and reacted to form chloritoid during regional greenschist facies metamorphism.

ACKNOWLEDGEMENTS

The author wishes to express his gratitude to Dr. R.L. Morton of the University of Minnesota-Duluth for serving as principal thesis advisor, and for offering his advice and sense of direction during the course of this study. Dr. J.M. Franklin of the Geological Survey of Canada deserves recognition for his efforts in the initiation and completion of this project.

Drs. J.C. Green and J.A. Grant of UM-Duluth served as thesis committee members and provided numerous helpful ideas and comments which improved the final draft of the thesis.

Several people at the Geological Survey of Canada, including Steve Green, Dr. K.H. Poulsen, and Ms. J. Donnelly offered their generous advise and assistance; special appreciation is extended to Ms. C. Anglin for her help and advice at numerous times during this project.

I would also like to extend my thanks to my fellow graduate students at UM-Duluth for numerous interesting and sometimes entertaining discussions during my graduate study. C. Reichhoff assisted in the sketching of diagrams in the thesis.

Finally I wish to express my deepest appreciation to my parents for their steady encouragement throughout the years.

The Geological Survey of Canada provided financial support for this project.

TABLE OF CONTENTS

LIST OF ILLUSTRATIONS

I. INTRODUCTION

I.1 Purpose of Study

Since the late 1940's several mining companies have explored for massive sulfide-type mineralization at the Headway-Coulee prospect in the Northern Onaman Lake area, northwestern Ontario. Exploration was mostly by geophysical survey and diamond drilling; little attention was paid to the volcanic rocks underlying the property. This project was undertaken to study the physical volcanology and hydrothermal alteration of the rocks exposed at the Headway-Coulee prospect. Specific objectives of the study are:

(1) to determine volcanic deposit types and their stratigraphic relationships;

(2) to develop a model of the volcanic environment in which the rocks were deposited;

(3) to define mineralogical and chemical alteration in the rocks, and to develop an alteration model.

I.2 Location, Access, and Physiography

The Headway-Coulee prospect is located within the District of Thunder Bay approximately 265 km northeast of the city of Thunder Bay (Fig. 1). The prospect is reached by travelling north from TransCanada Highway 11 on a private gravel road which branches off Highway 11 approximately 9 km east of the village of Jellicoe (Fig. 1).

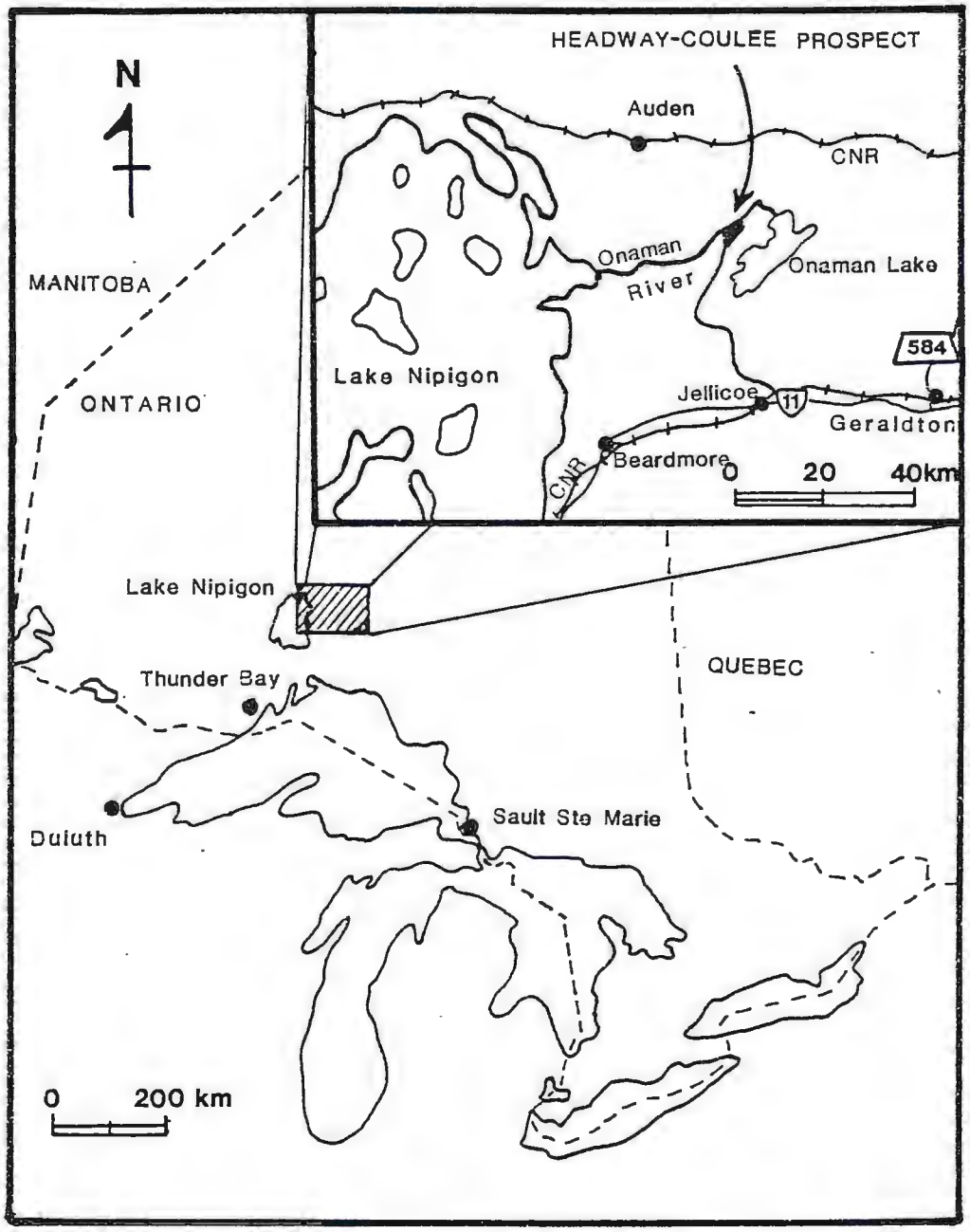

Figure 1. Location of the Headway-Coulee massive sulfide prospect, Northern Onaman Lake Area, northwestern Ontario.

The topography of the study area is typified by low hills generally composed of till and stratified drift, and broad gentle bedrock ridges mantled by glacial deposits of variable thickness (DiLabio, 1982). Muskeg swamps are found between the hills and ridges. Bedrock outcrops form approximately 7% of the study area and are unevenly distributed throughout. Much of the study area was clear-cut in the 1970's leaving large open areas with only limited tree growth. Where not clear-cut dominant tree vegetation is spruce and balsam in swamps, and aspen and birch on higher ground.

I.3 Methods of Study

Geologic mapping and rock sampling were conducted during July and August of 1983. The area mapped covers approximately 8 square km (Fig. 2). Mapping was done along a cut and flagged grid established by Noranda Exploration Company in 1972; results were compiled on a 1:4800 (1"=400') scale base map. Additional mapping was completed by pace and compass traverse off the cut grid, and compiled on mylar overlays to 1:4800 scale air photographs. Detailed mapping on 1:240 (1"=20') and 1:480 (1"=40') scale base maps was completed at specific sites of interest.

Three hundred and five rock samples were collected, from which one hundred and ninety-five thin sections were cut and studied for identification of mineralogy, textures, alteration, and degree of metamorphism. The modal mineralogy of thin sections studied is tabulated in Appendix I.

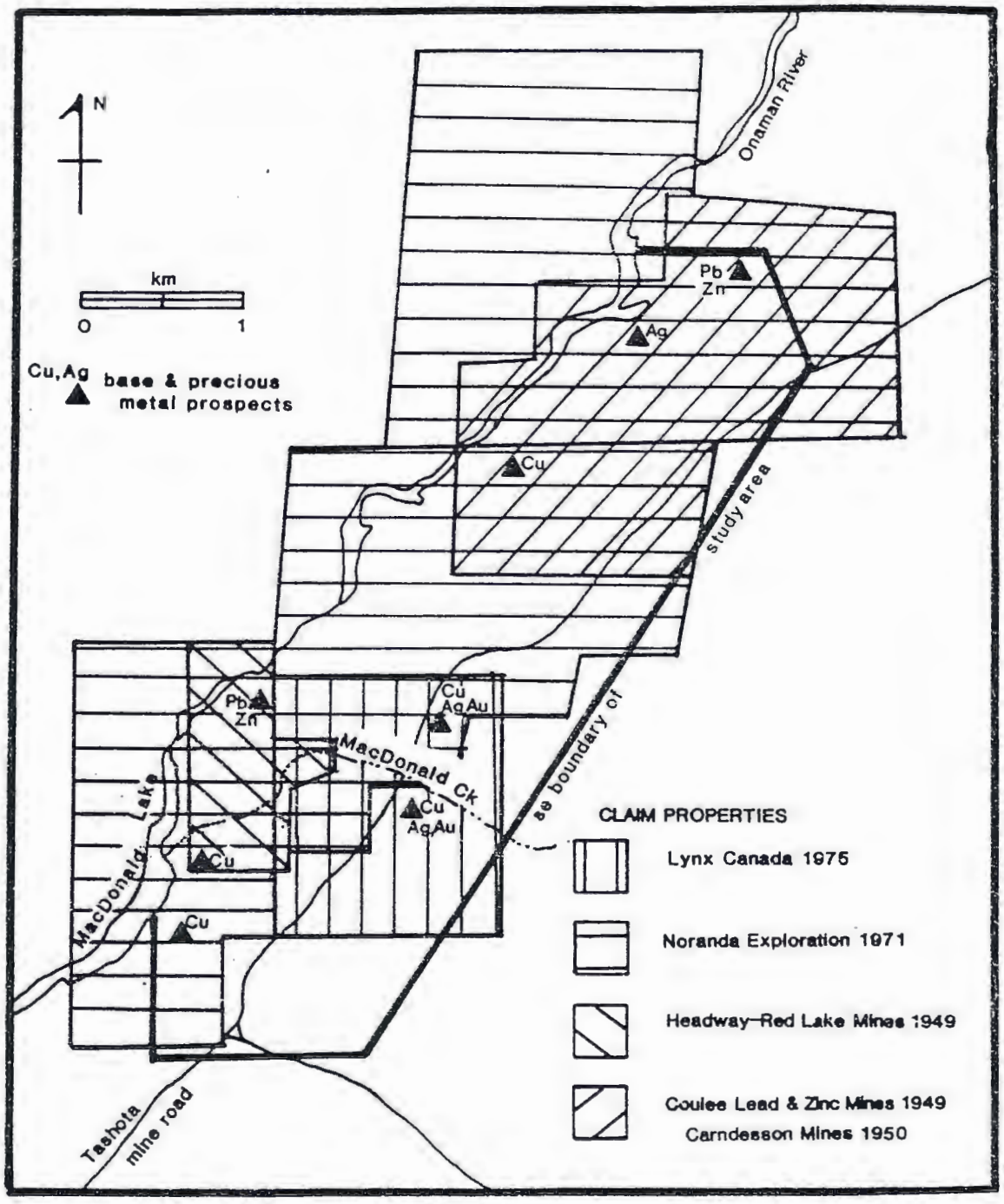

Figure 2. Location of exploration claims and base and precious metal prospects (after Thurston, 1980).

One hundred and seventeen rock samples were analyzed for major oxides and trace elements by the Geological Survey of Canada. Analytical methods used and sample results are described and listed in Appendix II. Specific gravities for these samples were measured on a modified beam balance for use in mass balance comparisons. Results are also compiled in Appendix II.

A suite of 13 samples was studied by x-ray diffraction for identification of Al-silicate, chlorite and carbonate species; four of these samples, along with 12 additional samples were stained with a potassium ferricyanide solution to help identify carbonate species. The results are listed in Appendix III.

Microprobe mineral analyses were made on nine polished thin sections to determine variations in the mineral compositions of chlorite, chloritoid, sericite, and carbonate species throughout the study area. Results of this study are included in Appendix III.

Locations of thin section, and polished thin section samples, and samples collected for whole rock analyses are shown on Plate 1.

I.4 Previous Work

Geological observations in the vicinity of the study area first began when Hopkins (1917) did reconnaissance mapping by traversing the Onaman and North Onaman Rivers, and the east boundary of the Nipigon Forest Reserve.

Gledhill (1925) mapped in the region and classified the area's rocks into 5 groups: Keewatin greenstones and iron formation; Laurentian gneisses; Timiskaming sediments including slate, graywacke,

and conglomerate; Algoman felsic intrusive rocks; and Keweenawan diabase. Gledhill (1925) was the first to report the presence of felsic metavolcanic rocks along the Onaman River northeast of MacDonald Lake (within the present study area).

The Ontario Geological Survey maintained a mapping party in the region during the summer of 1972, the fall of 1973 (Thurston, 1980), and the summer of 1976 (Amuken, 1980). These surveys more closely defined the map units outlined by Gledhill.

The region has had a long history of mineral exploration with interest focused on several base and precious metal prospects among which are those of the present study area (Fig. 2). Initial base and precious metal discoveries were made by prospectors in the early 1900's. Coulee Lead and Zinc Mines Ltd. began exploration on claims in the northeastern portion of the present study area in 1949 by carrying out basic geologic mapping, a dip needle survey, and diamond drilling on what were believed to be northeast-trending shear zones largely within felsic metavolcanic rocks (Fig. 2). The Coulee property was optioned in 1950 to Carndesson Mines Ltd. which continued exploration by diamond drilling in 1952.

In the southwestern portion of the study area, just northeast of MacDonald Lake are claims originally staked by prospectors in the late 1930's and purchased by Headway Red Lake Gold Mines Ltd. in the late 1940's (Fig. 2). Geological and geophysical surveying led to the discovery of base metal showings in 1949-1950. Diamond drilling by Headway, and subsequently by Headvue Mines Ltd. outlined two zones of low-grade lead-zinc mineralization.

The Headway and Coulee properties were optioned to Noranda Exploration Company Ltd. in 1971. Noranda staked additional claims, and geological, geochemical, and geophysical surveys were completed on the property in 1971 and 1972. Noranda diamond drilled anomalies outlined by these surveys including the mineralized showings identified by Headway and Headvue.

In 1975 a syndicate composed of Lynx-Canada Explorations Ltd., Dejour Mines Ltd., and Canadian Reynolds Metals Company Ltd. leased claims from Headway, and staked additional claims concentrated around the intersection of the Tashota Mine road and MacDonald Creek (Fig. 2). Prospecting by Dave Thorsteinson and Nolan Cox (personal communication, 1983), and geophysical surveying by the syndicate led to the discovery of a zone of chalcopyrite and pyrrhotite mineralization just southeast of the intersection of the creek and the mine road.

The syndicate identified a second mineralized zone about 30 meters east of the mine road and 200 meters north of MacDonald Creek consisting of a series of quartz veins mineralized with chalcopyrite and minor pyrrhotite within mafic flows (Fig. 2).

I.5 Regional Geology

The Headway-Coulee prospect is located within the eastern portion of the Archean Wabigoon greenstone belt (Fig. 3). The prospect is situated between the east-trending Geraldton-Beardmore metavolcanic-metasedimentary succession to the south, and the east-trending Tashota-Onaman metavolcanic-metasedimentary succession to the north (Fig. 4) (Pye et al., 1966).

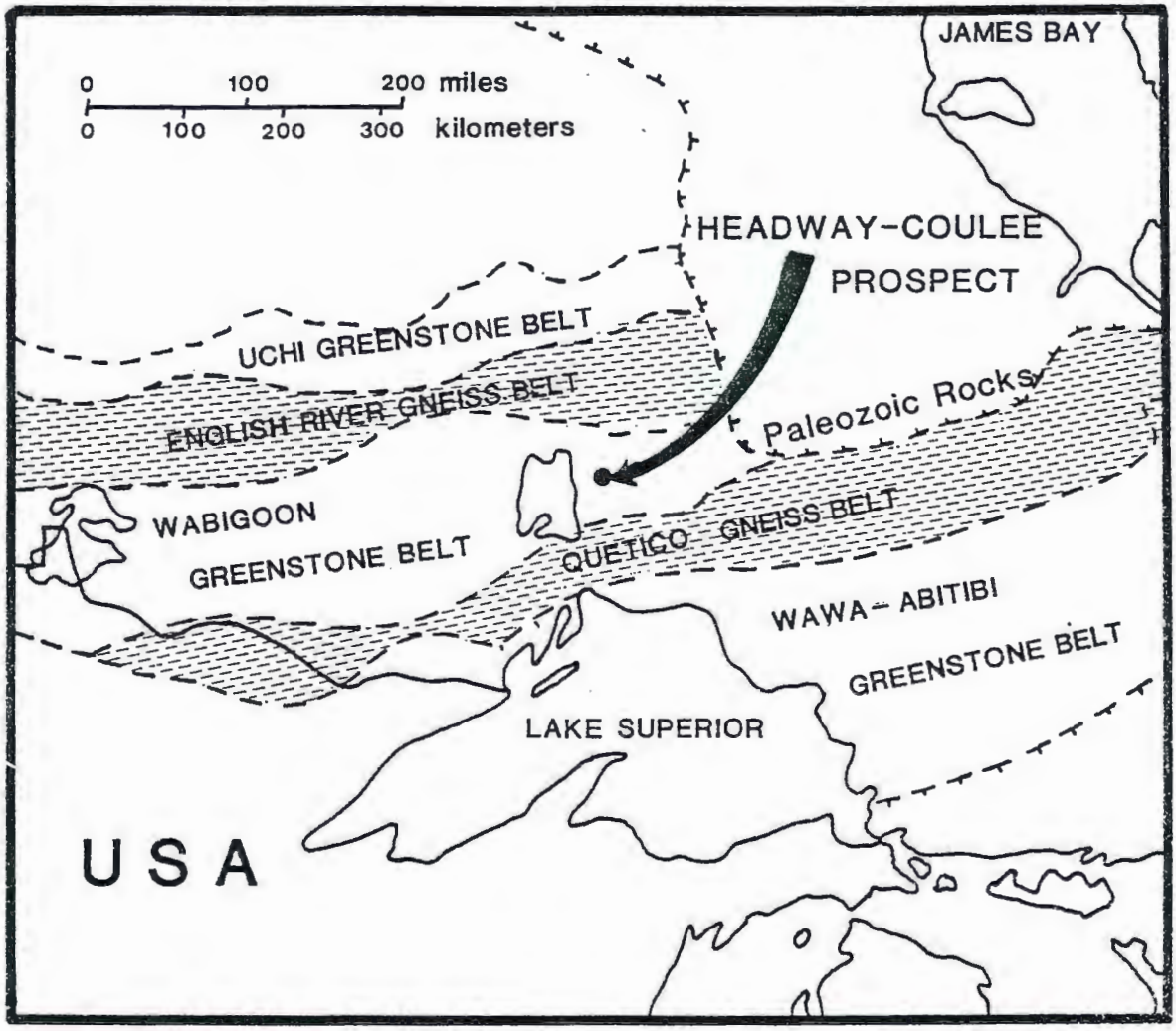

Figure 3. Greenstone and gneiss belts of northwestern Ontario (after Condie, 1981).

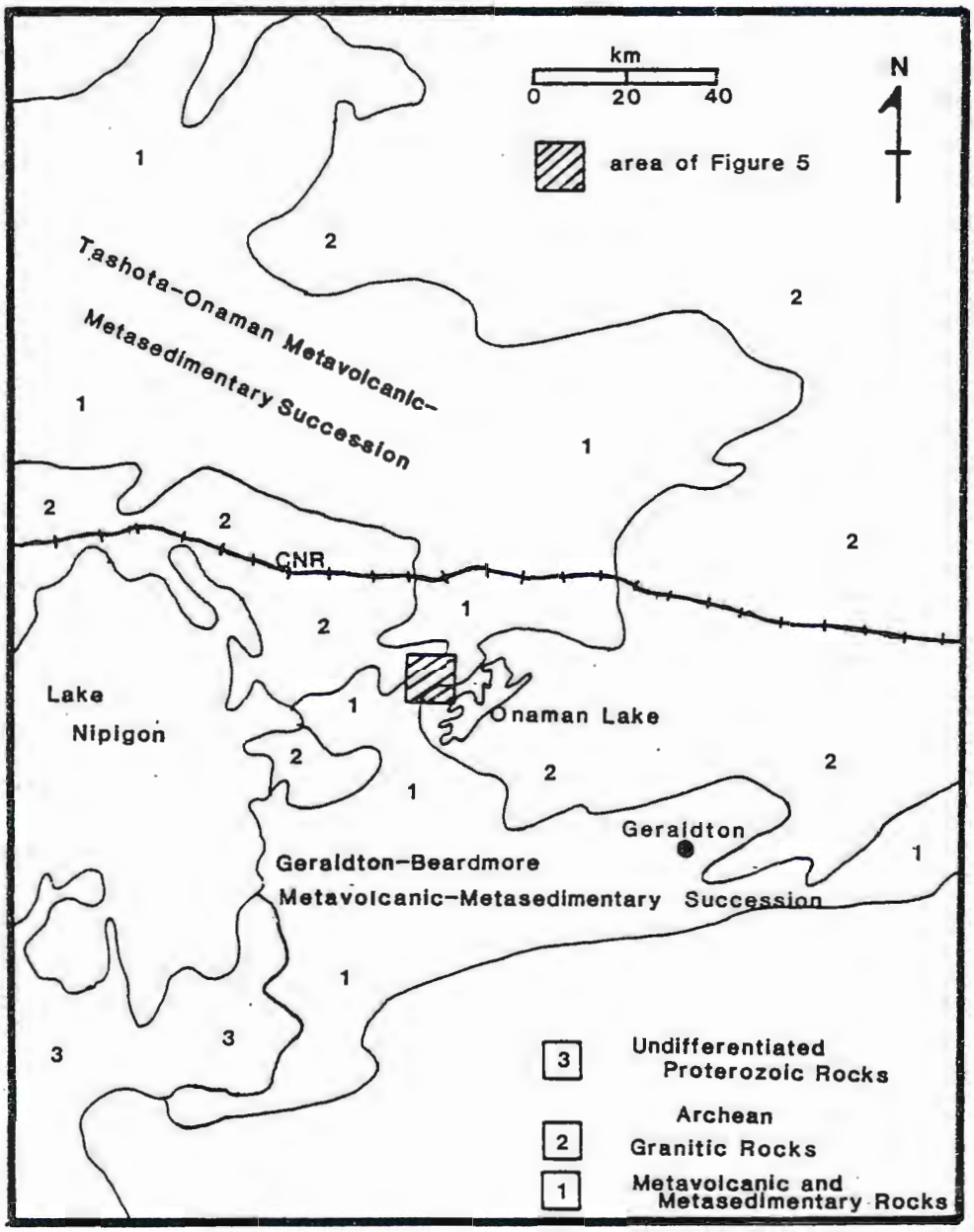

Figure 4. Location of the Headway-Coulee prospect between the Tashota-Onaman and the Geraldton-Beardmore metavolcanic-metasedimentary successions (after Pye et al., 1966).

In the vicinity of the current study area, metavolcanic and metasedimentary rocks form a northeast-southwest trending succession bounded by large granitic plutons (Fig. 5). Mafic metavolcanic rocks, dominantly lava flows, constitute approximately 80% of this succession.

Felsic metavolcanic rocks occur only within an 8 km long and 150-200 meter wide zone northeast of MacDonald Lake (Fig. 5). These steeply dipping, northwest facing rocks are composed of crystal-lapilli tuffs, chloritoid-sericite schists, and minor flow-banded rhyolites (Thurston, 1980). Metasedimentary rocks are present within the vicinity of the study area, the major occurrences of which are oxide facies iron formation associated with mafic flows near the Tashota Mine, and a clastic metasedimentary succession southwest of the study area (Fig. 5) (Amuken, 1980; Thurston, 1980). The clastic succession consists of conglomerates intercalated with wackes, mudstones, and tuffs (Amuken, 1980).

Numerous intrusive rocks also occur within the metavolcanic-metasedimentary succession including quartz-feldspar porphyry, gabbro, and lamprophyre. Granitic rocks occur adjacent to the metavolcanic-metasedimentary successions and are interpreted to have intruded the supracrustal rocks (Amuken, 1980; Thurston, 1980). Proterozoic diabase dikes cut the metavolcanic, metasedimentary, and granitic rocks in the region (Amuken, 1980; Thurston, 1980) and represent the latest stage of igneous activity in the area.

Rocks of the Northern Onaman Lake area have been subjected to regional greenschist facies metamorphism except along contacts with the

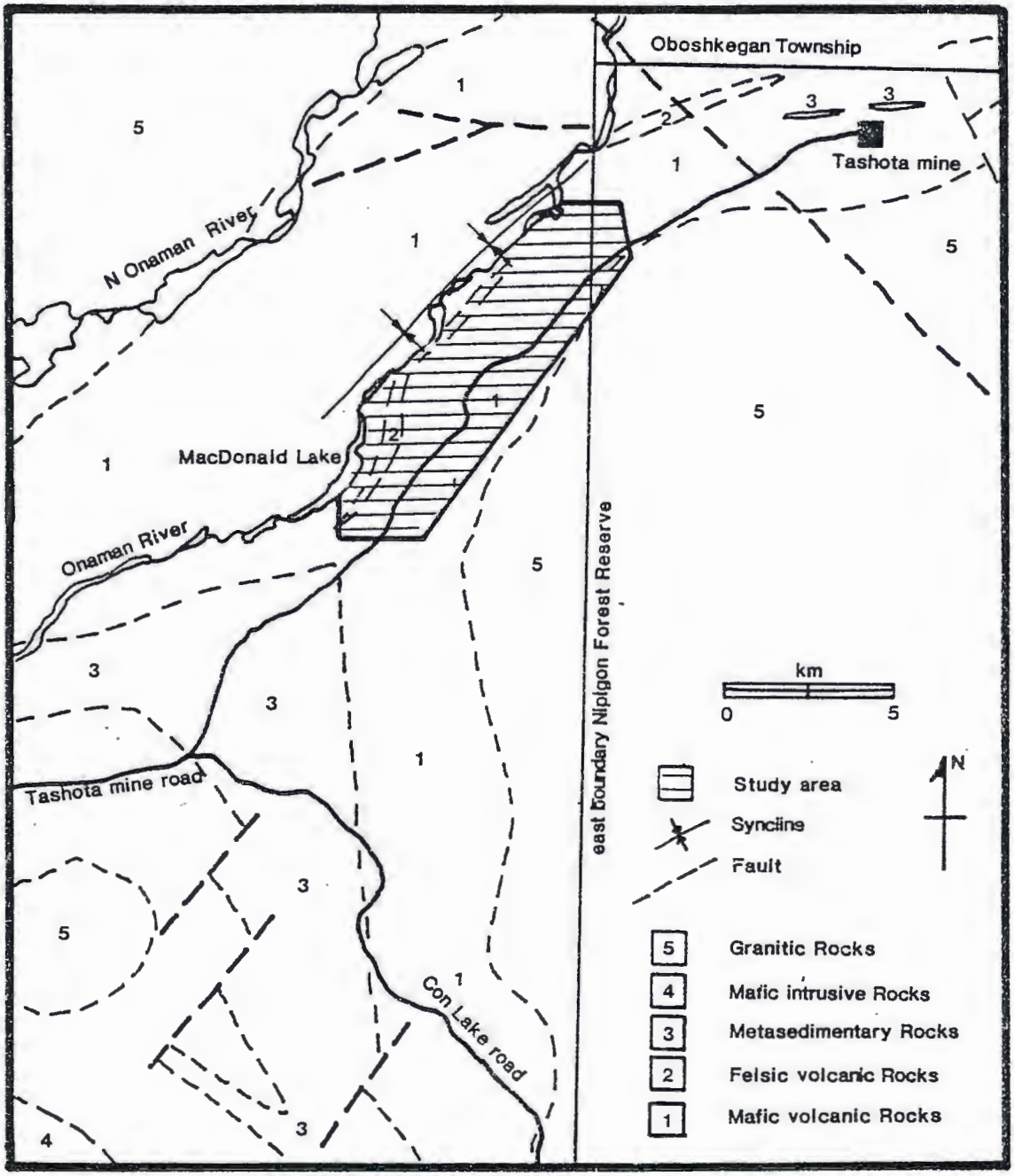

Figure 5. Generalized geology of the Northern Onaman Lake area, northwestern Ontario (after Amuken, 1980; Thurston, 1980).

granitic intrusive rocks where they are locally of amphibolite grade (Thurston, 1980).

Gledhill (1925) and Thurston (1980) postulated the existence of a northeast-trending, upright, isoclinal syncline which trends parallel to the metavolcanic belt and has formed as a result of intrusion of the surrounding granitic rocks (Fig. 5). A set of minor folds which plunge northwesterly throughout the region were reported by Flaherty (1936). Several faults have been mapped within the area, most of which either trend northeasterly where parallel to, or northwesterly, where perpendicular to the strike of the volcanic-sedimentary stratigraphy (Fig. 5) (Amuken, 1980; Thurston, 1980).

Quaternary glaciation has left the Northern Onaman Lake area relatively flat with extensive deposits of sand, sandy till, and occasional bouldery hills formed as outwash deposits associated with the Onaman interlobate moraine in Oboshkegan Township (northeast of the study area, see Fig. 5) (Zoltai 1965). Varved clays, deposited in Glacial Lake Nakina, the last remnant of which is Onaman Lake, occupy the lower part of the Onaman River valley, extending into the present study area. Muskeg swamps between the Onaman River and Onaman Lake are also underlain by such clays.

II. LITHOLOGY AND STRATIGRAPHY

II.1 Introduction

The distribution of the rock units within the study area is shown on Plate 1, and modal mineral abundances of representative samples are listed in Appendix I. The rocks have all undergone greenschist facies metamorphism, and for the purpose of brevity, the prefix meta is not used in the remainder of this text. In addition to metamorphism, most of the rocks have undergone relatively intense hydrothermal alteration; anomalous modal abundances of quartz, sericite, chlorite, carbonate, kyanite, and chloritoid reflect this alteration. In spite of metamorphism and alteration numerous primary textures are visible on outcrop and in thin section; these permit interpretation of original volcanic deposit types.

Mafic volcanic rocks underlie 70% of the study area and consist of pillowed and massive to amygdaloidal lava flows and flow breccias which form a 1-2 km thick stratigraphic succession. This succession is locally interrupted by a narrow, lens-shaped horizon (30-200 m x 5 km) of felsic rocks which interfingers with, and/or is terminated by mafic ava flows to both the northwest and southeast (Plate 1). The felsic volcanic rocks are composed of laminated to bedded ash tuffs, and minor lava flows.

II.2 Description of Lithologic Units

MAFIC VOLCANIC ROCKS

Mafic Lava Flows (Unit 1 on Plate 1)

Poorly exposed mafic lava flows are the dominant rock type in the study area and form a relatively thick succession which extends northwest from the granite pluton (Plate 1). Foliation is generally well developed in these flows, and is especially prevalent immediately beneath and above the felsic horizon.

In outcrop, mafic lava flows vary from fine to medium-grained and range from dark green to pale or reddish-brown in color. Flows vary in structure from massive to pillowed and, less commonly, brecciated; amygdules are locally recognizable in outcrop. Pillowed lavas are most common, and are composed of oval, spherical or highly irregular (Fig. 6), tightly packed pillows which range from <15 cm to >1 m in diameter. In less intensely altered rocks pillows may be outlined by 2-3 cm thick, dark green chloritic selvages. Where alteration is relatively intense and the rocks deformed, pillows may be stretched up to 1.5-2 m in plan view and pillow rinds may impart a banded appearance to the rock. Although generally not abundant, material from between pillows typically consists of irregular fragments, up to 3 cm in diameter, set in a fine-grained chloritic matrix.

Pillow breccia, which is interlayered with the pillowed flows, is occasionally recognized. In these deposits fragment-supported clasts are poorly sorted, range from 4-20 cm in diameter, and appear similar in color, texture, and grain size to the associated pillowed flows. Larger fragments may contain visible portions of pillow rinds.

Figure 6. Irregular-shaped pillows within mafic lava flows. Knife is 8 cm long.

Amygdules, where observed, are 2 mm to 1 cm in diameter, constitute 1-15% of the pillowed flows and are composed dominantly of quartz. Similarly sized, or larger, round to oval pits were occassionally seen on outcrop and are believed to represent weathered-out carbonate amygdules (Fig. 7).

In thin section, the pillowed flows and associated fragmental material mineralogically reflect the variable intensity of hydrothermal alteration throughout the map area. Flows interpreted as least altered are composed of a fine-grained (<1 mm) assemblage of actinolite (15-44%), epidote (15-35%), chlorite (20-35%), and albite (5-20%), with accessory quartz, calcite and opaques (Appendix I). The flows are generally aphyric in texture, although amphibole and plagioclase microphenocrysts may constitute up to 5% of the rock and locally exhibit a glomeroporphyritic habit. The plagioclase phenocrysts, and their sericite pseudomorphs, commonly occur as long (up to 0.5 mm), narrow, spiny crystals (Fig. 8) which may exhibit hollow cores and spiky or swallow-tail terminations. These textures are believed to indicate rapid quenching coincident with subaqueous deposition (Bryan, 1972; Pierce, 1974; Gelinas and Brooks, 1974; Yeats et al., 1973). More intensely altered pillowed flows typically consist of fine-grained (<1mm), granoblastic-polygonal quartz (+ albite?) (10-55%), and anhedral carbonate (0-13%), with foliated, wispy to bladed sericite (5-40%), chlorite (0-40%), and stilpnomelane (0-7%) dispersed throughout (Appendix I). Albite was not recognized in altered mafic lava flows, however fine-grained, untwinned albite which is petrographically indistinguishable from fine-grained quartz may be present.

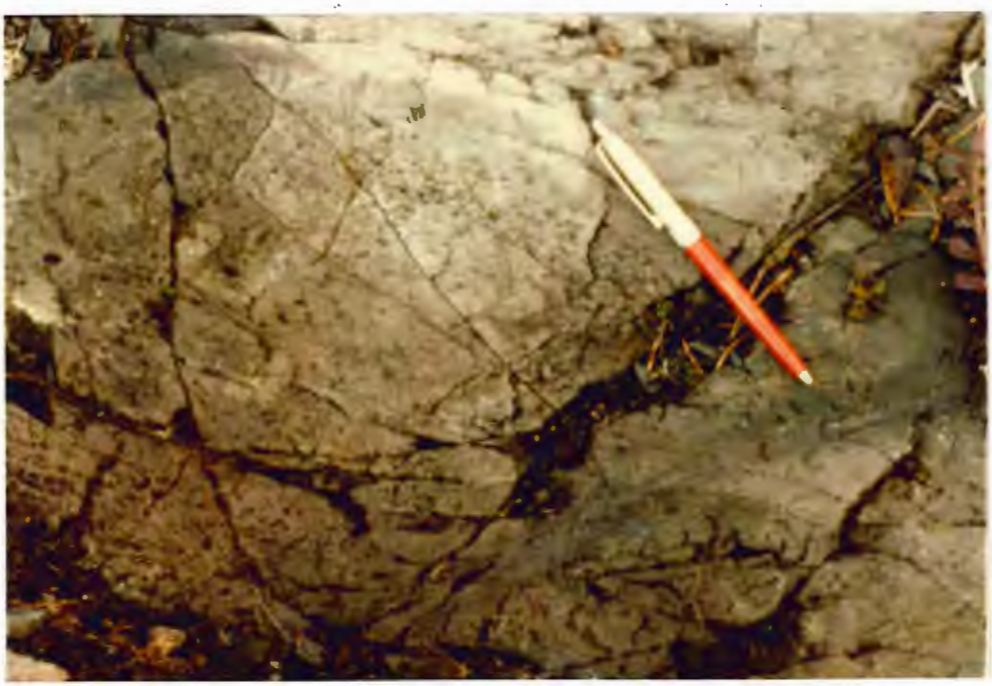

Figure 7. Amygdaloidal, pillowed mafic lava flow. Pen is 13 cm in length.

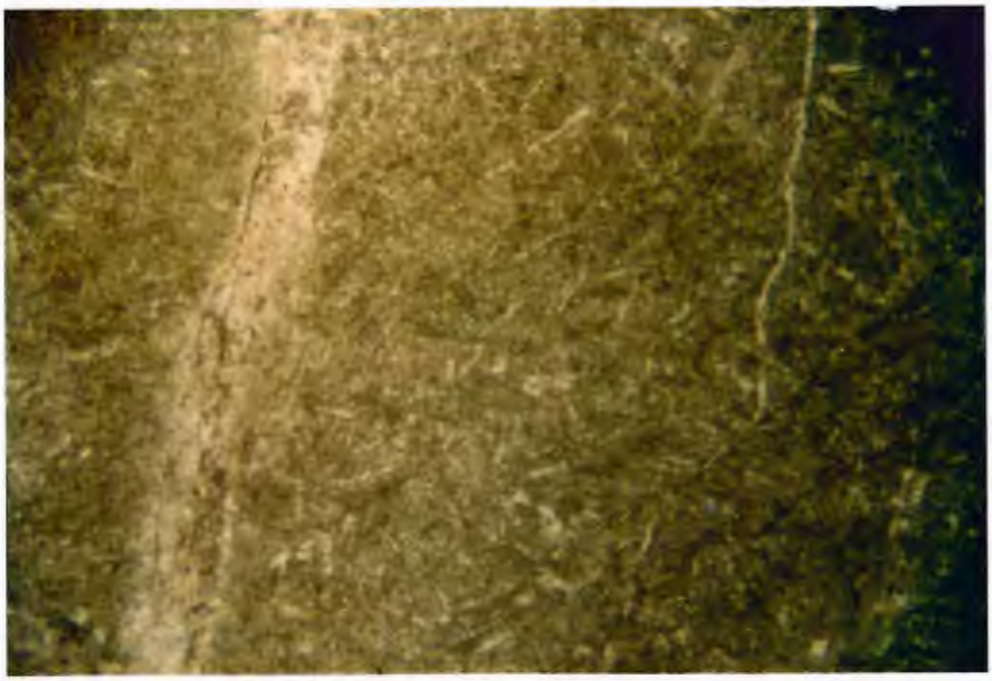

Figure 8. Photomicrograph of narrow, spiny, quenched plagioclase crystals in mafic lava flows. Plane polarized light, field of view: 4.8 x 4 mm.

Opaque minerals (0-8%), within the altered pillowed flows, occur as sub-parallel, lath-shaped crystals (up to 0.25 mm long and 0.1 mm wide) and, subhedral, blocky grains (0.1-0.3 mm) which are milky white or reddish-brown in reflected light. These may represent altered ilmenite and/or magnetite grains. Euhedral pyrite cubes (up to 1.5 mm in diameter) are also present. Chloritoid (1-25%) occurs as 1-2 mm bow-tie twinned porphyroblasts, or less commonly as 1-2 mm tabular grains.

Under the microscope, amygdules within the pillowed flows have a round to oval form and are filled by very fine-grained (<0.1 mm) mosaics of recrystallized quartz, or, less commonly, by varying amounts of chlorite, carbonate, and chloritoid (Fig. 9). Where the amydaloidal rocks are altered and highly recrystallized, the amygdules appear to merge with the matrix.

In thin section, samples collected from between pillows exhibit 0.5-2 mm wide blocky and angular fragments and are believed to represent altered hyaloclastite. These fragments are composed of fine-grained (<0.1 mm) recrystallized quartz, and iron oxide (hematite?), and are set in a chlorite and iron oxide-rich groundmass.

Massive mafic lava constitutes approximately 10% of the lava flows and occurs interlayered with pillowed flows. Thickness of individual flows is difficult to estimate due to the poor exposure, but certain exposed stratigraphic sections indicate a thickness of up to 10 meters. Autobrecciated flows were not observed associated with massive flows, possibly due to lack of exposure. The massive flows are similar in amygdaloidal content, composition, and mineralogy to the associated pillowed flows.

FELSIC VOLCANIC ROCKS

Felsic volcanic rocks within the study area are divided into two cycles on the bases of lithologic types and stratigraphic position. For the purpose of description the cycles are referred to as I and II.

Cycle I Felsic Volcanic Rocks

Laminated to bedded tuffs, quartz-crystal tuffs, and a quartz-porphyritic lava flow comprise a stratigraphic package of rocks in the southwestern portion of the study area. These are separated from rocks of Cycle II by a polymictic diamictite deposit (unit 4, page 32).

Laminated-Bedded Tuffs (Unit 2a on Plate 1)

Intensely altered, laminated-bedded ash tuff deposits volumetrically form most (90%) of the Cycle I rocks (Plate 1). The tuffs occur mainly as a poorly exposed, relatively thick (150-200 m), but laterally limited (1.5-2 km) unit. As well, there are four localized deposits of tuff which occur as thin lenses (up to 10 m thick) within mafic lava flows northeast of MacDonald Lake (Plate 1). At one outcrop (grid location 49 sw, 3+60 nw) mafic lava is exposed as three pillowed tongues, 20-90 cm in thickness, within ash tuff (Plate 1). This relationship has been reported elsewhere (SW Alaska, SW British Columbia, Iceland) and is believed to represent mafic magma which has intruded wet ash or sediment (Snyder and Fraser, 1963; Allen, 1980a, 1982).

On outcrop the rocks of unit 2a vary from dark green to pale brown and typically range from thinly-laminated to thickly-bedded. Individual beds range from <5 mm to 40 cm in thickness; most are <5 cm thick (Fig. 10). Although typically laminated or bedded in appearance, many

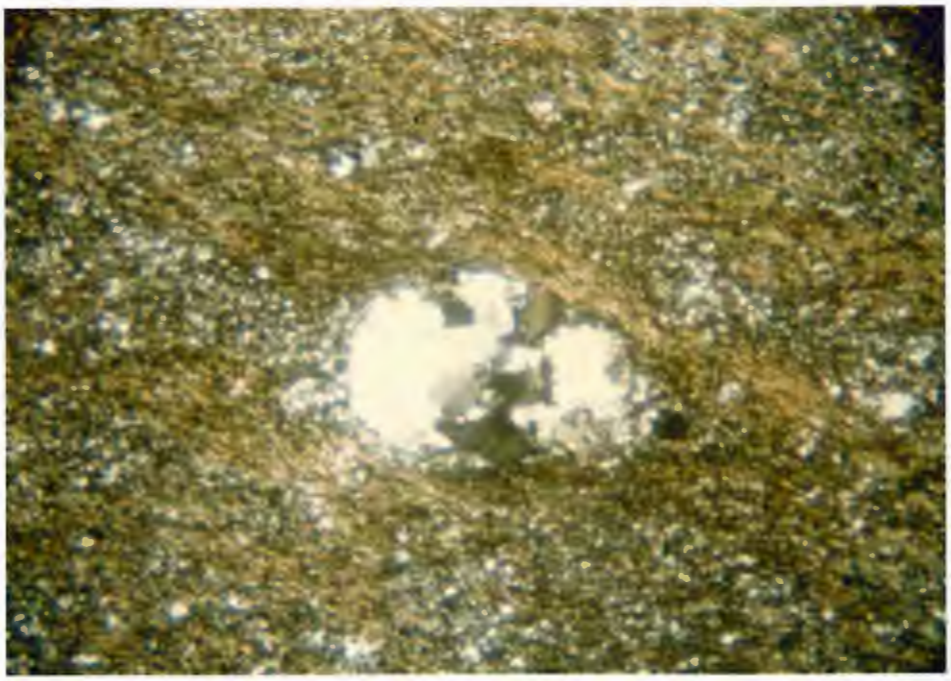

Figure 9. Photomicrograph of quartz amygdule within altered mafic lava flow. Crossed polars, field of view: 4.8 x 4 mm.

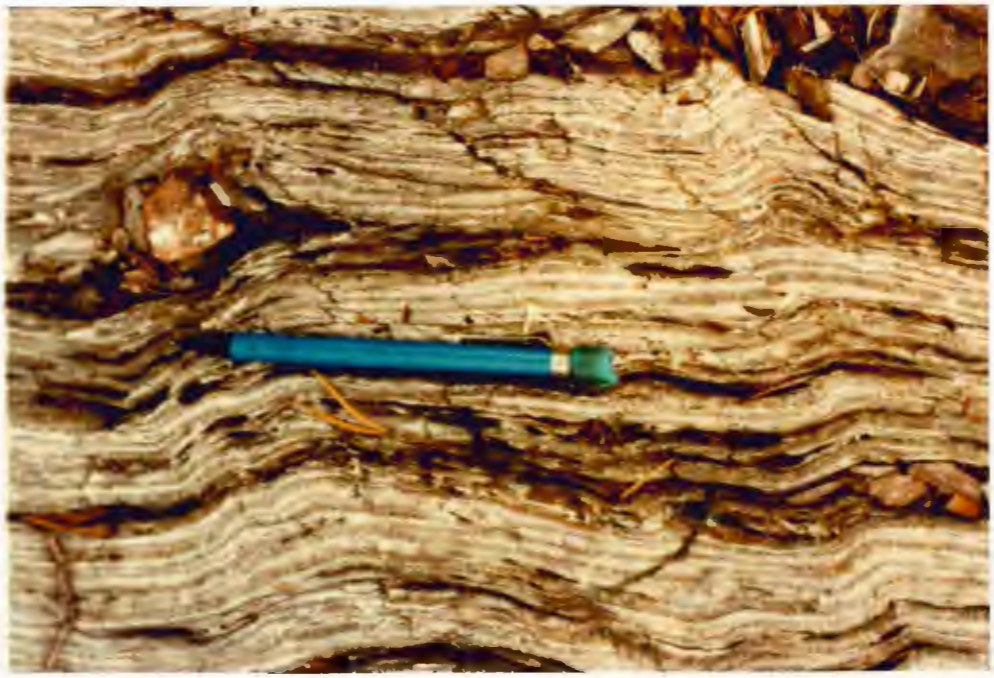

Figure 10. Thickly-laminated tuff, Cycle I felsic volcanic rocks. Pencil is 13 cm in length.

of the tuffs have a thinly-banded appearance caused by the relatively deep weathering of chlorite, chloritoid, and/or sericite-rich zones (1-10 mm) which alternate with relatively resistant quartz-rich zones (1-5 mm). The tuffs typically exhibit a well developed bedding plane cleavage, and shearing locally imparts a lens-shaped appearance to individual beds.

Although most exposures are laminated to thinly-bedded (or thinly-banded), thickly-bedded units do occur. An example of this is found northeast of MacDonald Lake (grid location 49 sw, 3+50 nw) where a 2 m thick section of tuff has been intensely altered and locally appears pale greenish and very cherty. Two cleavages, which intersect at approximately 120 degrees, impart a distinct diamond-shaped appearance to the rock. The rock is traceable along strike for approximately 140 m, and is conformable to the laminated and thinly-bedded tuffs. This cherty rock may represent an originally thickly-bedded ash deposit, or a laminated and/or thinly-bedded ash deposit in which intense alteration has obscured bedding.

Lapilli and block-sized lithic fragments constitute 0-5% of individual ash beds and are typically light greenish-gray in color and appear siliceous (Fig. 11). The fragments are generally subround to subangular, range up to 20 cm in diameter, and appear massive on outcrop. Several exposures contain 1-2% reddish to orange "sulfide burned", limonitic patches which average 5 cm in diameter (Fig. 12). It is believed these are probably weathered massive sulfide fragments.

Petrographically the lapilli and block-sized lithic fragments are composed of very fine-grained (<0.3 mm) recrystallized quartz (85-92%),

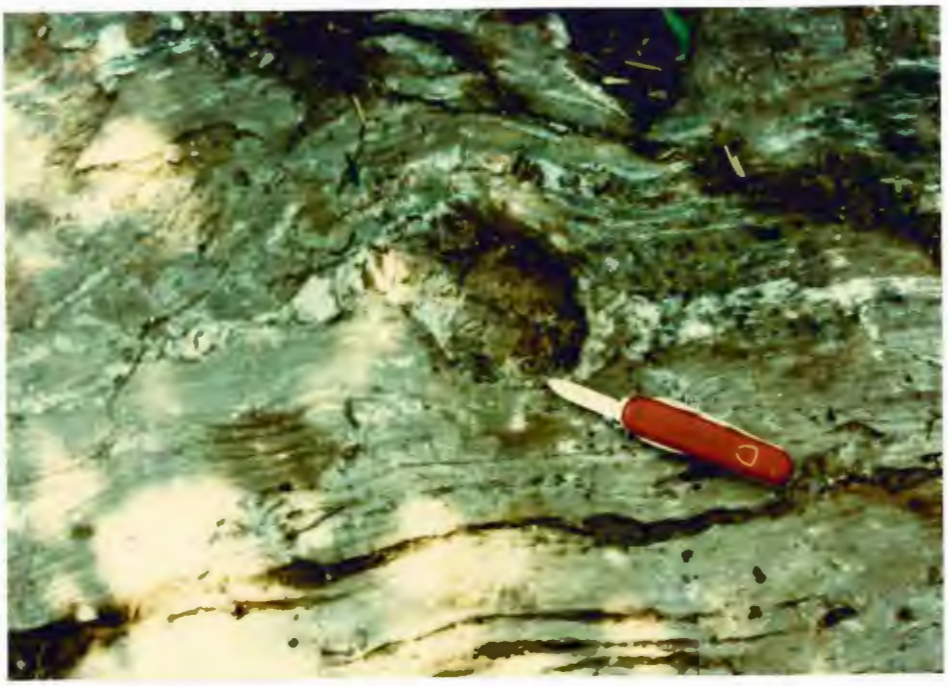

Figure 11. Block-sized lithic fragment within altered ash tuff, Cycle I felsic volcanic rocks. Knife is 15 cm in length.

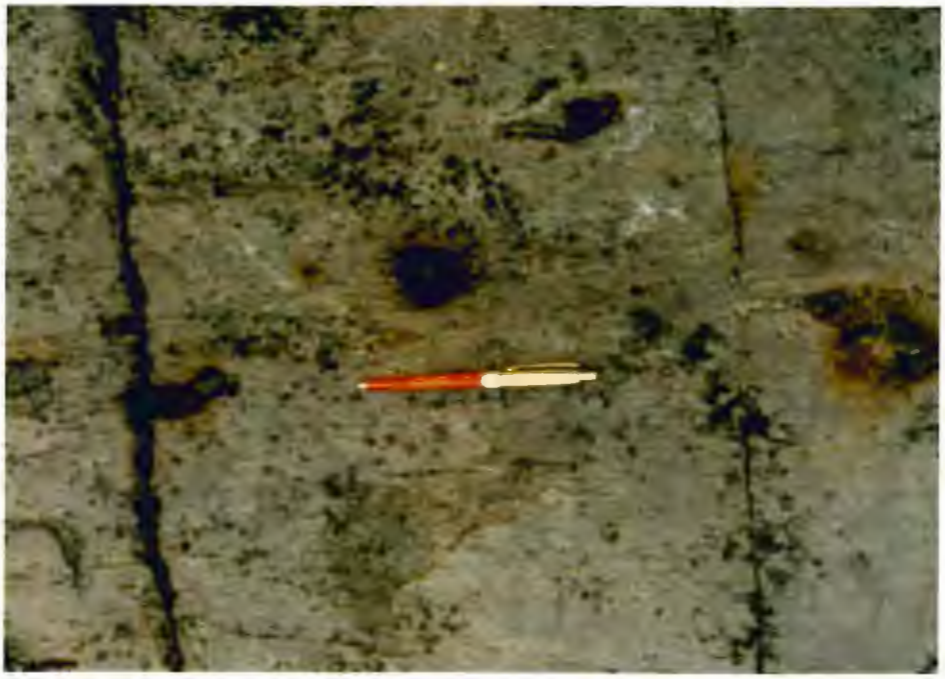

Figure 12. Weathered sulfide fragments(?) within altered ash tuffs, Cycle I. Pen is 13 cm in length.

with accessory sericite (5-8%) and chlorite (3-7%). In addition to lapilli and block-sized lithic fragments, altered ash-sized lithic fragments are also present within the tuffs, and are conspicuous in thin section (Fig. 13). They are similar in mineralogy to, but vary in textural fabric and/or modal mineral abundance from the matrix. They are typically irregular in shape, 1-1.5 mm in diameter, and compose 0-15% of the rock. Juvenile fragments were not recognized in the rock, perhaps due to alteration.

Fine to medium- (0.5-5 mm) grained quartz crystals were also observed under the microscope. The crystals range from angular and broken, to subhedral and embayed (Fig. 14), and constitute 0-5% of the rock. Where the crystals have undergone cataclasis they appear fractured, exhibit strong undulose extinction, and may exhibit incipient development of a mortar texture. Oval pods, 0.5-2 mm in diameter, composed of polygonal-shaped microcrystalline quartz are frequently seen and are believed to represent highly strained and recrystallized quartz crystal fragments.

There is no recognizable change in fragment content, composition, or size either across or along strike throughout the tuff deposits.

The lithic and crystal fragments are set in an extremely fine-grained ($\leq$0.1 mm) altered matrix of granoblastic-polygonal quartz (+ albite?) (25-55%), strongly foliated sericite (10-45%), chlorite (0-25%), and stilpnomelane (0-8%), and anhedral carbonate (0-15%). Fine-grained, untwinned albite may be present in these rocks, but if so is petrographically indistinguishable from microcrystalline quartz. Chloritoid (0-85%) occurs as 0.5-2 mm bow-tie twinned porphyroblasts,

Figure 13. Photomicrograph of ash-sized fragments within laminated-bedded tuffs. Plane polarized light, field of view: 4.8 x 4 mm.

Figure 14. Photomicrograph of resorbed quartz phenocrysts within laminated-bedded tuffs. Crossed polars, field of view: 4.8 x 4 mm.

and pyrite (1-3%) as 0.2-2 mm subhedral-euhedral opaque grains. Other opaques appear as subparallel tabular to blocky or rod-like grains (0.2-3 mm) which are pale red or milky-white in reflected light. These compose 0-2% of the rock and may represent altered ilmenite and/or magnetite grains (Appendix I).

Quartz Crystal Tuffs (Unit 2b on Plate 1)

A thin lens-shaped deposit of quartz-rich crystal tuff overlies mafic lava flows and laminated-bedded tuffs northeast of MacDonald Lake (Plate 1). The unit is approximately 20-30 m in thickness and is inferred to extend along strike for approximately 450 meters.

Intense sericitization imparts a pale green to pale brown color to most outcrop exposures. Bedding is not distinguishable in the tuffs although dark greenish chloritic zones, 5 cm-1 m in thickness, can occasionally be traced across outcrop surfaces. These zones, although now mineralogically reflecting hydrothermal alteration, may also reflect a primary bedding in the rock.

Fragments are difficult to distinguish in outcrop, principally due to intense alteration. Recognized fragments constitute <2% of the rock, range from 1-2 cm in diameter, and are sericite and quartz-rich. Some outcrops contain sericitic lenses which are slightly lighter in color than the surrounding material and these may represent altered rock fragments. The most distinctive feature of this unit is the presence of blue quartz crystals which range from 0.5-6 mm in diameter, and constitute 25-30% of the rock.

Under the microscope, the quartz crystals vary from angular and broken, to subhedral and embayed (Fig. 15). Elsewhere the crystals have

been cataclasized and exhibit a wavy, undulose extinction and incipient development of a mortar texture. The quartz crystals are set in a very fine-grained (<0.1 mm) matrix of granoblastic-polygonal quartz (+albite?)(20-45%), strongly foliated sericite (30-60%), and a purplish-birefringent chlorite (<5%). As in laminated-bedded tuffs described above, untwinned albite may be present but is petrographically indistinguishable from quartz. Chloritoid occurs as 1-2 mm diameter bow-tie twinned porphyroblasts and constitutes up to 25% of the rock (Appendix I). In thin section the sericitic lenses are indistinguishable from the surrounding material.

Sparse, ash-sized altered lithic fragments (0.2-1 mm in diameter) are conspicuous in thin section and constitute 4-8% of the rock. These fragments are generally subrounded-subangular, and are mineralogically identical to the matrix, but vary in mineralogical mode, textural fabric, or grain size relative to the matrix.

Quartz-Porphyritic Lava Flow (Unit 2c on Plate 1)

A quartz-kyanite schist caps the volcanic rocks of Cycle I and is thought to represent an altered felsic lava flow. The unit overlies the quartz-crystal tuffs (unit 2b), ranges up to 50 m in thickness, and can be traced for >200 m along strike. (Plate 1).

On outcrop the rock appears pale greenish and very siliceous (Fig. 16), and is characterized by a well-developed ribbony-appearing cleavage. The flow is porphyritic, with 2-5% blue quartz phenocrysts, which range from 0.2-6 mm in diameter. No flow breccia or flow banding was observed on outcrop.

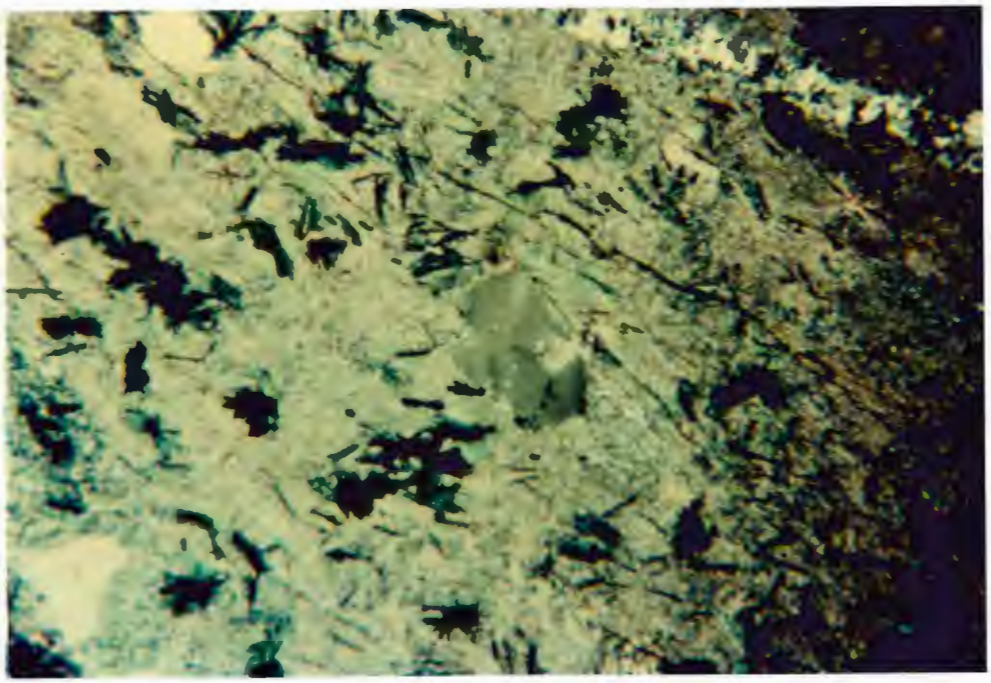

Figure 15. Photomicrograph of quartz crystal tuff. An embayed quartz phenocryst is set in a fine-grained quartz-sericite matrix (bright area); dark areas represent chloritoid porphyroblasts and opaque minerals. Field of view: 5 x 7 mm.

Figure 16. Altered, kyanite-bearing quartz-porphyritic lava flow of Cycle I felsic volcanic rocks. Pencil is 16 cm long.

In thin section quartz phenocrysts appear subhedral and variably resorbed, and are locally cataclasized and recrystallized. They are set in a fine-grained (≤0.5 mm) matrix of recrystallized quartz (35-40%), andalusite poikiloblasts (0-8%), foliated sericite (3-20%), and chlorite (0-4%). Chloritoid (0-15%) porphyroblasts, and kyanite (0-31%) occur locally, but never together. Kyanite occurs as elongate (up to 5-7 mm) poikiloblasts concentrated in 1-5 mm wide bands which are separated by 1-5 mm zones of microcrystalline quartz. Contorted foliation patterns in strained quartz between the kyanite bands, and cataclasis of quartz phenocrysts suggests the rocks have undergone intense shearing. Shearing evidently developed parallel microfaults along which kyanite poikiloblasts nucleated and grew during regional metamorphism (Poulsen, 1985, personal communication).

The presence of resorbed quartz phenocrysts, the lack of lithic and/or crystal fragments or identifiable intrusive relationships, and the relatively thick, but laterally limited nature of the unit suggests it probably is an altered felsic lava flow.

Cycle II Felsic Volcanic Rocks

Rocks of Cycle II occur in the north-central portion of the study area as a linear zone which parallels the Onaman River (Plate 1). Here the felsic volcanic rocks consist dominantly of laminated to bedded tuff deposits; felsic lava flows compose the southwestern portion of this cycle.

Laminated-Bedded Tuffs (Unit 3a on Plate 1)

Laminated to bedded tuff deposits of Cycle II are generally very similar in character to those of Cycle I (unit 2a), and are mostly con-

fined to a strip 100-200 m thick and 2 km in length. The deposit thins rapidly to the northeast to <30 m, and eventually pinches out in the Coulee #2 area (Plate 1). The tuffs are typically dark green or pale brown in color, and are generally laminated to thinly-bedded (or thinly-banded) and are similar in appearance to the tuffs of unit 2a.

Lapilli and block-sized lithic fragments generally constitute 0-5% of the tuffs, although locally near the base of the deposit (grid location 6 sw, 8 nw to 6 ne, 5nw) they range from 10-15% in abundance. Most fragments are light green to pale brown, and appear silicified and sericitized. The fragments are generally subround-subangular and/or flattened, and range up to 20 cm in diameter; most appear massive, although porphyritic and fragmental textures are locally present. Sulfide fragments are rare (<1%), and were observed only in the extreme southwestern portion of the unit.

In thin section, as on outcrop, the tuffs of Cycle II are similar to those of Cycle I. Ash-sized lithic, and quartz crystal fragments constitute 0-15%, and 0-5% of the rock respectively, and are set in an extremely fine-grained (<0.1 mm) matrix dominated by quartz, sericite, and chlorite (Appendix I). As in unit 2a, there is no recognizable change in fragment content, composition, or size either across, or along strike throughout the deposit.

Quartz-Feldspar Porphyritic Lava Flows (Unit 3b on Plate 1)

Two felsic lava flows constitute the southwestern portion of the Cycle II deposits, and directly overlie a polymicitic diamictite deposit (unit 4, page 32) northeast of MacDonald Lake (Plate 1). Although poorly exposed,the lava flows appear to be of only local extent.

In outcrop they are tan to gray and are dominantly massive in morphology, although at one outcrop (grid location 52 sw, 4 nw) a 1-2 m thick brecciated and flow-banded zone underlies the massive flow (Fig. 17). Fragments within the brecciated zone are typically flattened, average 3-5 cm in diameter, and appear similar to the overlying massive rock. The fragments are set in a fine-grained, brownish matrix, and are vaguely concentrated in 4 cm thick bands. Round to oval (0.5-2 mm) spherulites(?) are common (20-25%) in the matrix. On outcrop the spherulites are lighter in color than the surrounding rock.

Blue quartz phenocrysts are easily visible on outcrop within the massive portions of the flows and are typically 0.5-2 mm in diameter; they constitute 7-8% of the rock.

In thin section quartz phenocrysts vary from subhedral to anhedral and are frequently cataclasized and partially recrystallized along their borders. Untwinned, sericitized K-feldspar phenocrysts (0.5-1 mm in diameter) were also observed in thin section and constitute up to 3% of the rock. The phenocrysts are set in a matrix of very fine-grained ($\leq$0.1 mm) recrystallized quartz (+ albite?) (50-60%), strongly foliated sericite (25-30%) and chlorite (2-10%), anhedral carbonate (2-7%), and subhedral pyrite (1-4%) (Appendix I). Flow bottom fragments are petrographically similar to massive flow material, and their matrix is composed of fine-grained foliated sericite and microcrystalline quartz, with accessory chlorite and carbonate.

In thin section the spherulites(?) appear as diffusely bordered, oval structures composed of microcrystalline quartz (40-45%), and very fine-grained ($<<$0.1 mm) sericite (50-60%) (Fig. 18). They tend to be

Figure 17. Brecciated and flow-banded basal portion of quartz-feldspar porphyritic lava flow overlying a polymictic diamictite deposit. Hand lens and neck strap is approximately 40 cm in length.

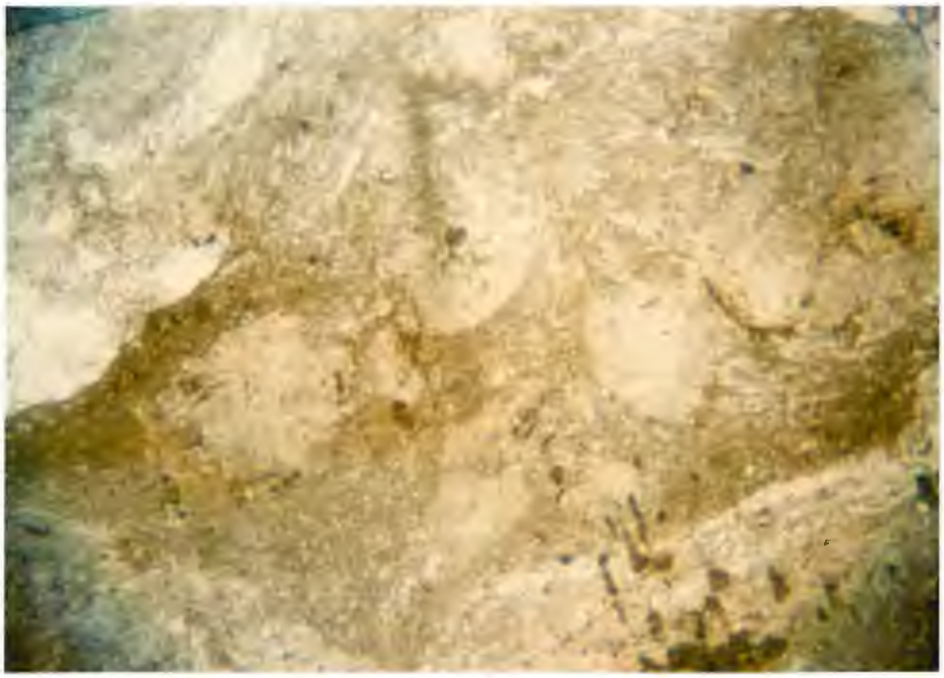

Figure 18. Photomicrograph of spherulites(?) in sericitized felsic lava flow. Plane polarized light. Field of view: 4.8 x 4 mm.

quartz-rich towards their cores, and sericite-rich towards their outer margins, and are distinctly finer-grained and less strongly foliated than the surrounding material. No radial structure was found.

METASEDIMENTARY ROCKS

Sedimentary rocks are a minor lithological constituent of the study area. Iron formation and a polymictic diamictite deposit are the sedimentary lithologies present.

Polymictic Diamictite (Unit 4 on Plate 1)

A polymictic diamictite deposit crops-out in the southwestern portion of the study area where it separates felsic volcanic rocks of Cycles I and II (Plate 1). The term diamictite is used here as defined in the Glossary of Geology (Bates and Jackson, 1980) as a nongenetic term for a nonsorted, or poorly-sorted sedimentary rock that contains a wide range of particle sizes. Where relatively undeformed the deposit is 5-10 m in thickness. Clasts are unsorted, range from <5 cm to 1 m in diameter, and are supported in a well-foliated, nonbedded, fine-grained, greenish-gray matrix. Clast types include well-rounded granitic boulders and cobbles (25-30%), and subrounded-subangular quartz porphyritic volcanic, and/or subvolcanic pebbles and cobbles (10-15%) (Fig. 19). Other less abundant clast types include pebbles and cobbles of cherty and banded iron formation (2-4%), milky quartz (2-3%), and rarely mudstone (1-2%). More resistant granitic or felsic volcanic clasts are in some places impressed into the mudstone clasts showing the latter to have been soft at the time of their incorporation

Figure 19. Rounded granitic, and cherty iron formation clasts within a polymictic diamictite deposit. Hand lens with neck strap is approximately 40 cm in length.

in the deposit. Dark green chloritic lens-shaped patches, up to 10 cm in length, are occasionally seen and may represent stretched-out mafic volcanic clasts.

In thin section the matrix to the clasts appears hydrothermally altered and consists of fine-grained recrystallized quartz (35-40%), strongly foliated chlorite (10-35%) and sericite (10-30%), anhedral carbonate (0-15%), chloritoid porphyroblasts (5-13%), and subhedral pyrite (5-7%) (Appendix I).

Although the origin of this deposit is uncertain, the matrix supported nature of this deposit, lack of recognized sorting of clasts or bedding in the matrix, and evidence stated above indicating the inclusion of unlithified mudstone clasts during deposition suggests this unit was deposited by relatively nonturbulent mass transport and represents a debris flow deposit (Pettijohn, 1975). However, the possibility remains that the deposit may represent a conglomerate of fluvial origin in which much of the well foliated matrix actually represents smeared-out and altered mafic volcanic and/or sediment clasts.

Some of the clasts within the deposit, notably the granitic and iron formation boulders and cobbles, are well-rounded and are not common local lithologic types. This suggests that if the deposit represents a debris flow, the flow engulfed well-worn polymictic cobbles, boulders, and gravels outside the study area before transport into and deposition within the study area. Amuken (1980) mapped and described extensive deposits of conglomeratic rocks to the immediate southwest of the study area.

The clast-bearing deposit locally (grid location 35sw, 11 nw) grades stratigraphically up into a 7 m thick section of fine-grained, intensely altered, greenish-gray rock consisting of recrystallized quartz (40%), anhedral carbonate (37%), well-foliated chlorite (11%) and sericite (8%), with subhedral pyrite and magnetite (4%). This greenish-gray rock may represent a fine-grained, altered graywacke, siltstone, or mudstone as frequently found associated with subaqueous debris flow deposits (Pettijohn, 1975; Williams and McBirney, 1979; Fischer and Schminke, 1984).

Iron Formation (Unit 5 on Plate 1)

Iron formation crops-out in the extreme northeast portion of the study area (Coulee #2 area, grid location 67ne, 1nw) as discontinuously exposed units ranging from 15-75 cm in thickness; these are associated with altered mafic lava flows, tuffs, and quartz-feldspar porphyry sills (Plate 1 and Fig. 20). In outcrop the iron formation has a strong bedding-plane cleavage and typically consists of 1-3 cm thick light-dark gray cherty layers, which alternate with 0.5-3 cm thick dark green-black magnetitic layers.

INTRUSIVE ROCKS

Quartz-Feldspar Porphyry (Unit 6 on Plate 1)

Several quartz-feldspar porphyritic sills and dikes are present within or near the felsic volcanic deposits. The sills and dikes range from <1-120 m in thickness, and are traceable up to 365 m along strike. Cross-cutting contacts and xenoliths were locally observed.

Outcrop appearance varies from massive to well-foliated, and light

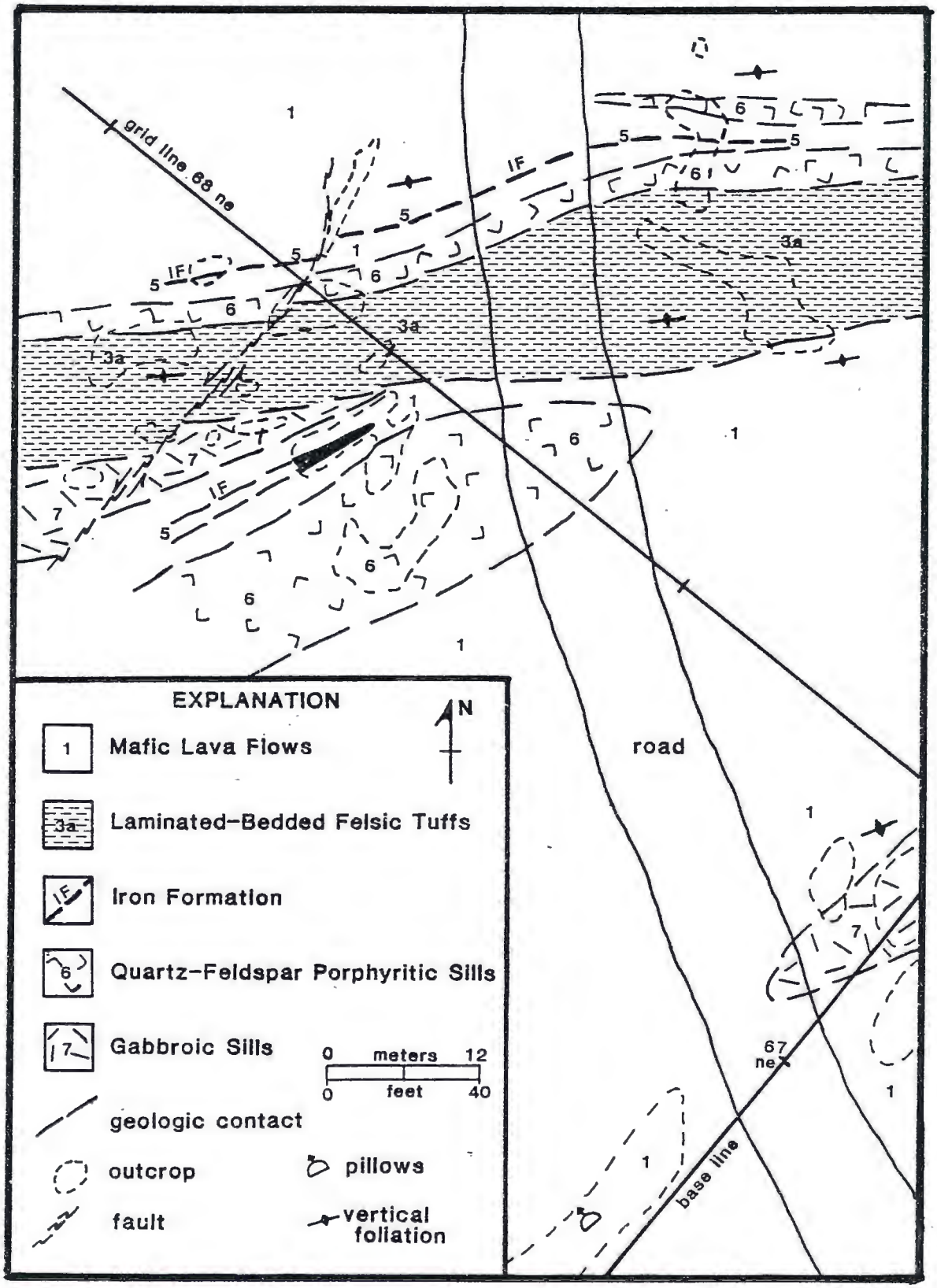

Figure 20. Detailed geologic map of the Coulee #2 area (grid location 67 ne, 1 nw).

to pale green in color. The rocks are typically porphyritic, with 0-10% blue or clear quartz phenocrysts, and 0-7% light green plagioclase phenocrysts, typically 0.2-6 mm in diameter.

Petrographically, quartz phenocrysts appear subhedral and variably resorbed, and are locally cataclasized and partially recrystallized. Plagioclase phenocrysts are twinned, and commonly carbonatized, sericitized, and cataclasized. The phenocrysts are set in a fine-grained (<0.1 mm) matrix of recrystallized quartz (+ albite?)(25-60%), well-foliated sericite (3-50%) and chlorite (0-20%), anhedral carbonate (0-30%), and opaques (1-4%) (Appendix I). Fine-grained, untwinned albite may be present but is not distinguishable in thin section from fine-grained quartz.

Gabbroic Sills (Unit 7 on Plate 1)

Several gabbroic sills are found within the mafic volcanic succession. Although poorly exposed, they generally appear to be lens-shaped and vary from <10 m to 45 m in thickness, and up to 365 m in strike length (Plate 1).

The gabbros are easily recognizable in the field as medium (1-5 mm) to coarse- (>5 mm) grained grayish-green rocks. They generally appear very massive (Fig. 21) and lack the well-developed foliation frequently seen in the volcanic rocks.

In thin section the gabbroic rocks are dominated by actinolite (10-40%), which commonly appears as pseudomorphs of 2-5 mm pyroxene oikocrysts, altered euhedral plagioclase laths (5-10%), fine-grained (<1mm) euhedral epidote (7-30%), foliated chlorite (10-30%), and subhedral pyrite (1-3%). Fine-grained, recrystallized quartz is commonly

Figure 21. Gabbroic sill. Pencil is 13 cm long.

found in irregular-shaped patches and typically composes 2-12% of the rock. Sills in the extreme northeastern portion of the study area (grid location 68 ne, 1nw) (Plates 1 and Fig. 21) contain quartz (5%) which appears micrographically intergrown with feldspar suggesting a primary igneous origin (Appendix I).

Felsic Dikes

Hydrothermally altered quartzo-feldspathic dikes occur locally within the felsic succession, are approximately 1 m in thickness, and appear light brown to reddish-brown on outcrop. The dikes contain 5-10% accessory granitic clasts which are leucocratic, fine to medium-grained (<5 mm), subrounded, and range from 5 cm to 20 cm in diameter (Fig. 22). In thin section the matrix to the clasts is fine to medium-grained (<5 mm), equigranular, and composed of partially recrystallized quartz (50-60%) and plagioclase (5-15%), iron carbonate (25-50%), chlorite (2-10%), pyrite (0-4%), and sericite (5-17%) (Appendix I). Hydrothermal alteration prohibits determination of the primary lithology of the dikes.

Granitic Pluton (Unit 8 on Plate 1)

Ontario Geological Survey geologists (Amuken, 1980; Thurston, 1980) mapped quartz monzonitic-granodioritic rocks to the southeast of the volcanic succession (Plate 1). Although poorly exposed, these are believed to have intruded the volcanic succession. Two outcrops, in the northeastern corner of the study area, were examined during this study. The outcrops consist of massive, medium to coarse-grained (>1mm), pink-white quartz monzonite. In thin section the rock contains quartz (47%), perthitic microcline (25%), and plagioclase (20%) with minor sericite, biotite and opaques (Appendix I).

Figure 22. Altered felsic dike with accessory granitic clasts. Knife is 20 cm in length.

II.3 Volcanological Interpretation

The volcanic stratigraphy in the Headway-Coulee area is dominated by a relatively thick pile of mafic lava flows which, locally, are interrupted by two cycles of felsic volcanic rocks (Plate 1). The presence of pillows, quench textures, and hyaloclastite indicate that the mafic lava flows were deposited in a subaqueous environment (Bryan, 1972; Yeats et al., 1973; Pierce 1974; Gelinas and Brooks, 1974). Field evidence suggests that the felsic volcanic rocks were also deposited in a subaqueous environment. The following discussion is a volcanological model for their formation and deposition.

The felsic rocks of Cycles I and II vary from poorly to well-bedded ash, and crystal tuffs, which are of very limited lateral (<2-3 km) and vertical extent (up to 200 m). The characteristics of these felsic rocks are similar to those described from tuff cone sequences (Womer et al. 1980; Sheridan and Wohletz, 1981, 1983; Wohletz and Sheridan, 1983). Tuff cones are relatively small volcanic landforms that commonly occur in clusters and have relatively thick (100-800 m), but laterally limited (usually <3 km diameter) deposits which may be highly asymmetric in distribution (Wohletz and Sheridan, 1983). Tuff cones are formed as a result of hydrovolcanic eruptions, i.e., eruptions resulting from the interaction, in varying proportions, of magma or magmatic heat with an external source of water, such as a surface body or ground water (Sheridan and Wohletz, 1981). Experimental studies (Sheridan and Wohletz, 1981, 1983; Wohletz and McQueen, 1981,1984) and detailed study of the morphology and evolution of tuff cones (Sheridan and Wohletz, 1983; Wohletz and Sheridan, 1983;

Wohletz, 1983) indicates the style of hydrovolcanic eruptions depends largely upon the explosivity of the water-magma interaction which is controlled mainly by the water/magma ratio. Eruptions under low water/magma ratios (subareal conditions?) are dominantly magmatic in nature and, for felsic magmas, lead to the formation of lava flows and pumice-fall deposits. Increased water/magma ratios (available ground water?) promote highly energetic, rapid, explosive eruptions of superheated, vapor-expanded base surges and ash falls which deposit well-bedded, fine-grained ash. At higher water/magma ratios (shallow surface water?) "wetter" and "denser", less explosive eruptions give rise to water-saturated surges and falls and, more rarely, vent lahars, which deposit dominantly thick, massive ash beds (Sheridan, 1979; Sheridan and Wohletz, 1981; Wohletz and Sheridan, 1983). Where water is abundantly available (very high water/magma ratios, deeper water conditions?) relatively passive volcanism occurs and results in lava flows and hyaloclastite deposits (Wohletz and Sheridan, 1983).

Tuff cones form as a result of hydrovolcanic eruptions under dominantly shallow aqueous conditions, and are constructed of relatively wet, massive and bedded ash (100-800 m thick) deposits which, in many cases, overlie an explosion breccia formed by initial vent breaching (Wohletz and Sheridan, 1983). Locally access of water to the erupting magma may be restricted by a build-up of ash around the vent, and/or by a collapse of the crater deposits into the vent; such conditions may lead to eruptions under low water/magma ratios and the formation of lava flows (Womer et al., 1980; Wohletz and Sheridan, 1983).

In the Headway-Coulee area, the ash tuffs of Cycles I and II form relatively thick, laterally limited deposits which are thought to have formed the submerged flanks of two separate, though adjacent tuff cones (Fig. 23). The felsic lava flows of Cycles I and II may have formed under low water/magma ratio conditions as access of water to the erupting magma was restricted, and/or under high water/magma ratio conditions within a water- flooded vent or on the submerged flanks of the cone.

The vents to the cones were probably located down, or up-dip from the present erosional surface in the map area, rather than along strike outside of the present map area. Several features, when considered together, suggest this. These include: the absence of explosion breccias underlying the ash deposits as frequently observed in and around the vents of tuff cones (Sheridan and Wohletz, 1981; Wohletz and Sheridan, 1983; Groves, 1984; Groves et al., 1985); the absence of localized felsic dikes, commonly interpreted as feeders to overlying volcanic rocks in vent areas (Simmons, 1973; Williams and McBirney, 1979; Wohletz and Sheridan, 1983; Fischer and Schmincke, 1984; Groves, 1984); and the interlayered nature of the ash deposits and subaqueous mafic lava flows, a feature which would be expected in the distal portions of the tuff cone (Heiken, 1971; Wohletz and Sheridan, 1983).

II.4 Stratigraphy and Geologic History

The stratigraphic succession at the Headway-Coulee area is dominated by two distinct styles of volcanism: 1) mafic subaqueous, and 2) felsic hydrovolcanic. Northwest-southeast stratigraphic sections at

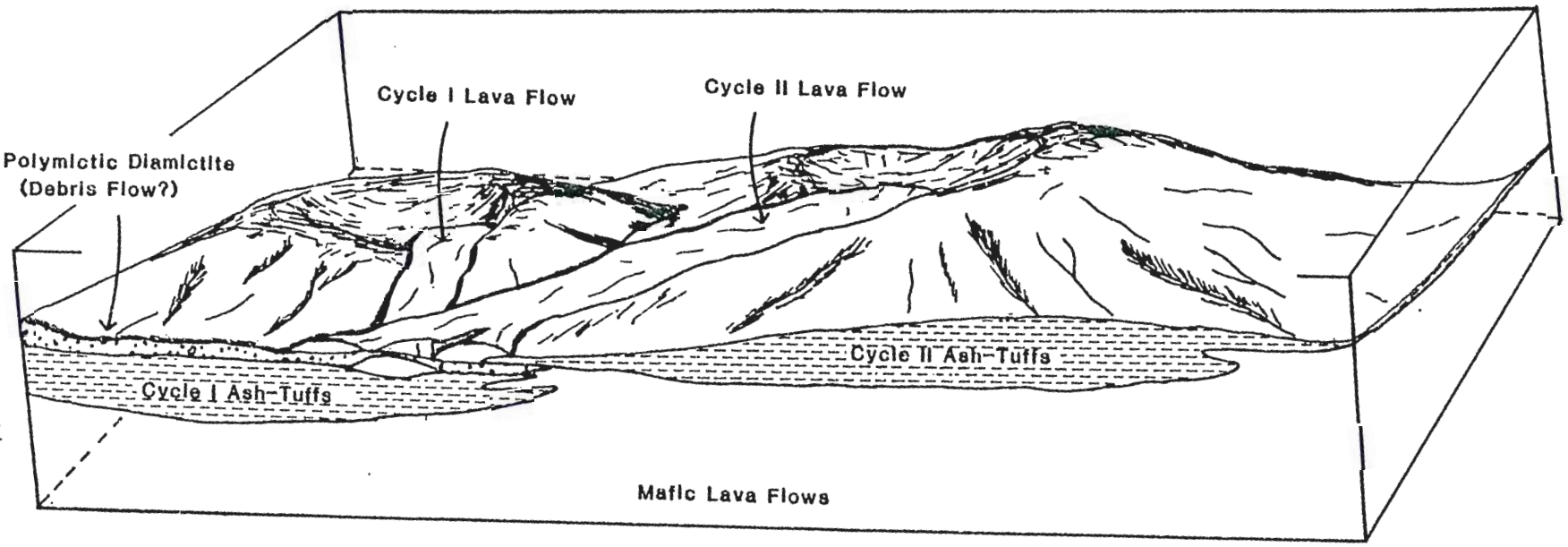

Figure 23. Diagrammatic model of the volcanological environment at the Headway-Coulee prospect showing two adjacent tuff cones. The front face of the block diagram illustrates stratigraphic relationships within the study area.

grid lines 38 sw, and 10 sw are shown on Fig. 24 and along with Plate 1, illustrate the stratigraphic relationships of the mafic and felsic volcanic rocks.

The lower portion of the volcanic succession formed as voluminous outpourings of mafic lava constructed a thick pile of pillowed, massive, and brecciated lava flows on the sea floor. As deposition of mafic lavas continued, the pile gradually shallowed upward and mafic volcanism was eventually interrupted by deposition of iron formation and felsic volcanic material. Deposition of mafic flows was first interrupted in the southwestern portion of the map area by explosive felsic hydrovolcanism, and emplacement of relatively thick, but laterally limited ash deposits of a tuff cone. Deposition of mafic lavas continued northeast of MacDonald Lake, and eventually covered the northeastern end of the ash deposits. Relatively brief episodes of explosive felsic volcanism occurred sporadically and resulted in deposition of four thin lenses of ash which are interlayered with mafic lavas northeast of MacDonald Lake. A final phase of explosive felsic volcanism locally deposited crystal-rich ash and was followed by relatively passive volcanism with deposition of a localized lava flow. Emplacement of the lava flow completed the first cycle of felsic volcanism.

Deposition of Cycle I felsic volcanic rocks was followed in the southwest portion of the area by emplacement of a polymictic diamictite deposit (debris flow?) which had its source to the southwest of the area. Thin lenses of iron formation were deposited locally in the extreme northeast end of the map area.

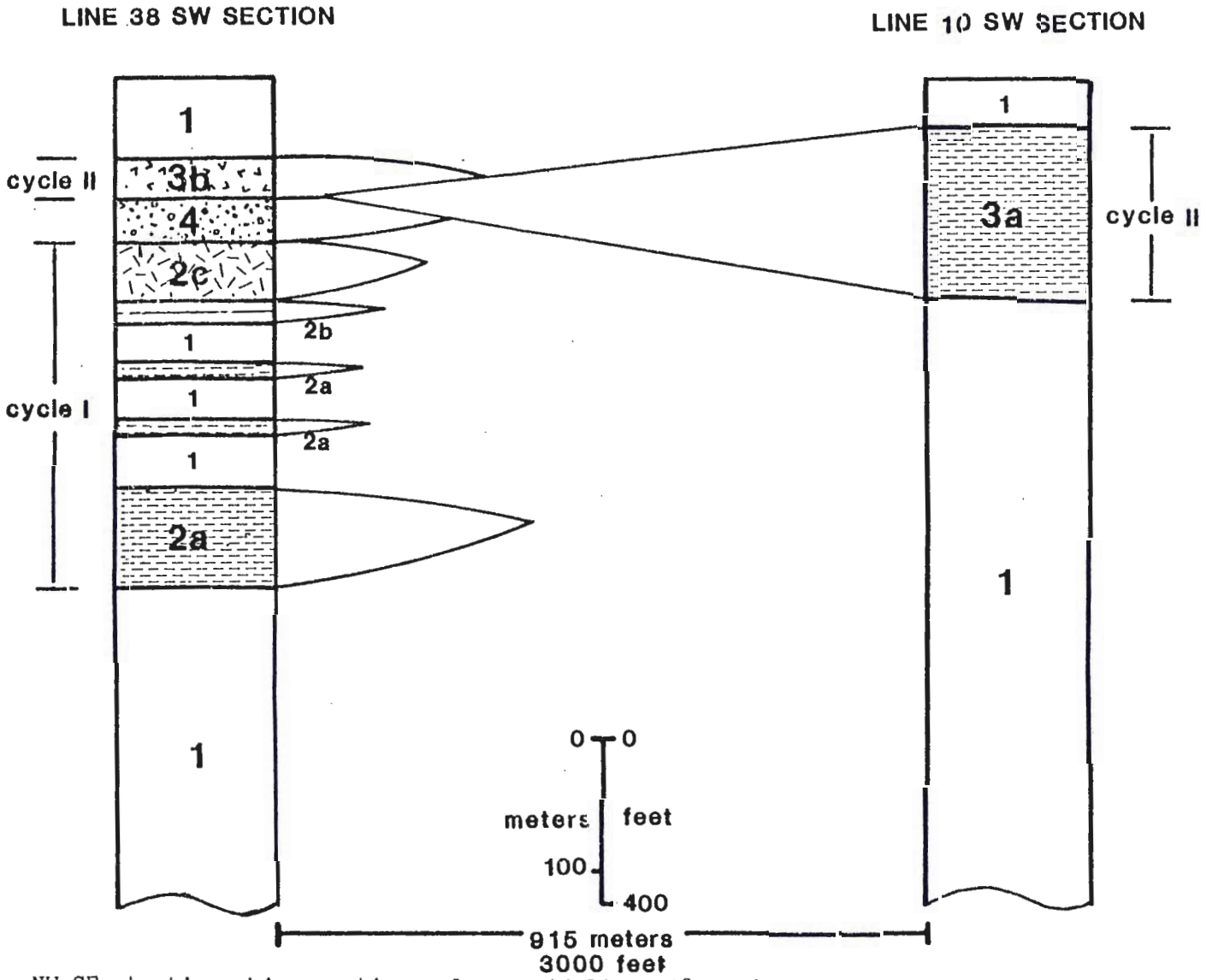

Figure 24. NW-SE stratigraphic sections along grid lines 38 sw (A-A'), and 10 sw (B-B'), respectively (see Plate 1). See the following page for explanation.

Fig. 24. Explanation

3b Quartz-feldspar porphyritic lava flow

3a Laminated-bedded tuff

4 Polymictic diamictite deposit (debris flow?)

2c Quartz porphyritic lava flow

2b Quartz crystal tuff

2a Laminated-bedded tuff

1 Mafic lava flows

A second cycle of felsic hydrovolcanic eruptions deposited ash in the northcentral portion of the map area. Deposition of localized lava flows northeast of MacDonald Lake (Plate 1) concluded this hydrovolcanic cycle.

Deposition of the felsic volcanic rocks was accompanied by intrusion of several quartz-feldspar porphyry sills and dikes. As felsic volcanism eventually ceased an extensive hydrothermal system developed and caused widespread alteration of the rocks.

As hydrothermal activity waned there was a return to subaqueous deposition of mafic lava flows and intrusion of several gabbroic sills which represent late stage igneous activity in the area.

III. ALTERATION AND METAMORPHISM

III.1 Introduction

The rocks exposed at the Headway-Coulee prospect have been variably altered by hydrothermal solutions and all have been subsequently metamorphosed to greenschist facies (Thurston, 1980). One of the purposes of this study is to describe the mineralogical and textural changes in the rocks caused by hydrothermal and metamorphic processes. Definition of these changes will enable geochemical comparison of variably altered rocks derived from individual lithologies (Chapter IV).

III.2 Metamorphism

The mafic lava flows which were unaffected by intense hydrothermal alteration are composed of chlorite, epidote, actinolite and albite, a typical assemblage resulting from lower greenschist facies metamorphism of mafic rocks. Hydrothermally altered mafic, as well as felsic rocks, contain chloritoid, and/or coexisting sericite and chlorite, but lack biotite; these are mineral associations which are also indicative of lower greenschist facies conditions (Winkler, 1976; Turner, 1981; Hyndman, 1985). The chloritoid occurs as porphyroblasts which are believed to result from isochemical mineralogical and textural changes brought on by regional metamorphism.

Metamorphism of the rocks in the Headway-Coulee area was accompanied by deformation. On an outcrop scale, deformation is evident in many forms. Pillows in mafic lava flows commonly appear

flattened in plan view, and in many instances, are elongated in a third dimension thereby forming a strong lineation in the rocks.

Shearing in the tuffs commonly imparts a lens-shaped appearance to individual beds (Fig. 25) and, where extreme (Poulsen, 1983, personal communication), imparts a banded appearance to the rocks. Here 1-10 mm wide sericite, chlorite, and/or chloritoid-rich bands alternate with quartz-rich bands. A well-developed bedding-plane cleavage (050^{o}-075^{o}) accentuates the banding in these rocks. This cleavage is also present in most mafic lava flows, being particularly well-developed in the upper portions of the stratigraphic succession. Other cleavages are locally present including a well-developed, north-south trending (355^{o}-005^{o}), subvertically dipping crenulation cleavage.

Clasts within ash tuff and polymictic diamictite deposits are sheared-out and deformed to varying degrees. Shapes range from spherical to angular (undeformed), to intensely flattened depending on the competence of the clast. Occasional clasts were observed which are flattened and elongate similar to deformed pillows in mafic lava flows. Extremely flattened clasts have length:width ratios (in plan view) up to 20:1. Other outcrop features observed in the tuffs which are indicative of deformation include local, moderately to steeply plunging, upright folds with an S-symmetry, and kink bands.

Textures indicative of deformation are also evident in thin section. Such textures include strong foliation of micaceous minerals, broken, crushed phenocrysts, strong undulose extinction in phenocrysts, development of mortar textures, and recrystallization of quartz.

III.3 Distribution of Alteration Types

The distribution of the hydrothermally altered rocks within the map area is shown on Plate 2. Hydrothermally altered rocks are defined as those rocks containing quartz, sericite, chlorite, carbonate, kyanite, actinolite, epidote or chloritoid in modal abundances which are inconsistent with primary igneous compositions. The altered rocks form relatively broad, subconcordant zones in the southern portion of the area, and extend northeast as relatively narrow, generally conformable zones which parallel the Onaman River (Plate 2).

The original permeability of the volcanic rocks was apparently an important factor in controlling the distribution of alteration. Alteration in the felsic ash deposits along the Onaman River (Plate 2) is laterally extensive. These deposits were probably, upon deposition, highly permeable (relative to sills and lava flows) to hydrothermal fluids. On outcrop, and in thin section, the tuffs commonly display adjacent beds or laminae composed of the same minerals but widely ranging mineralogical modes. This is thought to indicate variable alteration of beds dependent upon differing primary composition, and/or permeability. Massive portions of lava flows typically display less intense alteration than associated brecciated portions, a feature also related to permeability.

On outcrop, and in thin section, irregular veins, and anastomosing veinlets filled with alteration minerals are occasionally observed. These veins and veinlets are believed to represent fractures in the rocks which locally provided fluid channels for the focused movement of hydrothermal solutions.

III.4 Alteration Zones

Detailed field mapping, supplemented by petrographic study, has allowed subdivision of the altered rocks, for descriptive purposes into four zones based on different mineral assemblages. These zones are defined by distinct mineral assemblages identifiable in the map area, and are named generally for the dominant mineral(s) present. The zones are: (1) least-altered, (2) quartz-sericite, (3) iron chlorite, and (4) chloritoid.

On outcrop and in thin section, cross-cutting and replacement textures are occasionally seen between the quartz-sericite and the iron chlorite or chloritoid zones. These textures, along with the relative distribution of the zones, indicates replacement of one zone by another, and thereby implies relative timing of the formation of the zones.

In order to identify variations in composition of certain minerals between alteration zones, rock samples from across the map area were studied by electron microprobe analysis, x-ray diffraction, and/or by thin section staining. A suite of nine polished thin sections were prepared and analyzed at laboratories of the Geological Survey of Canada in Ottawa in order to determine variations in chemical compositions of chlorite, carbonate, sericite, chloritoid, and opaque minerals. Nine additional samples were analyzed by x-ray diffraction to distinguish chlorite species, and to distinguish iron-bearing from non-iron-bearing carbonates. To futher distinguish between different carbonate species, 13 samples were stained with a potassium ferricyanide solution prepared according to Evamy (1963).

The mineralogy, textures, and distribution of the four different alteration zones are summarized below in the general order of increasing alteration intensity.

Least Altered Zone (Actinolite-Chlorite-Epidote-Albite ± Quartz-Calcite)

Only gabbroic sills and some mafic lava flows can be classified as least altered. These compose approximately 50% of the stratigraphic succession and occur dominantly in the northeastern, as well as the extreme northern portions of the map area, and along the Onaman River immediately northeast of MacDonald Lake (Plate 2). On outcrop the rocks appear light to dark green and are generally weakly or non-foliated.

In thin section the mafic volcanic rocks typically display porphyritic and quench textures, and gabbroic sills commonly exhibit poikilitic textures; both volcanic rocks and sills consist of actinolite (15-44%), epidote (15-35%), chlorite (20-35%), and albite (0-20%), with accessory quartz and calcite (Fig. 26). Although such minerals in mafic rocks are indicators of lower greenschist facies metamorphism (Winkler, 1976; Turner, 1981; Hyndman, 1985), they may also be indicative of "spilitic" alteration resulting from the interaction of the mafic rocks and seawater shortly after deposition (MacGeehan, 1977; Parry and Hutchinson, 1981; Gibson, et al., 1983; Seyfried, 1984). It is for this reason that the rocks cannot, with complete certainty, be classified as unaltered.

Figure 25. Sheared, lens-shaped beds within ash tuffs. Knife is 8 cm long.

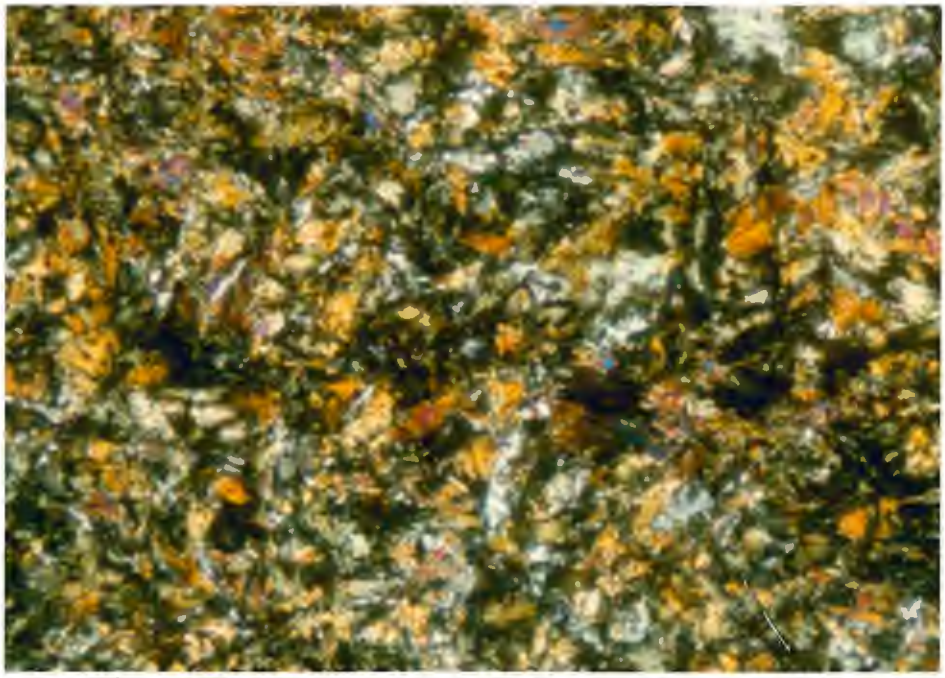

Figure 26. Photomicrograph of least altered mafic lava flow. Crossed polars, field of view: 2 x 1.5 mm.

Quartz-Sericite Zone (Quartz-Sericite ± Mg Chlorite- Calcite-Epidote-Ti-bearing Opaques)

Rocks containing the quartz-sericite assemblage occur as a relatively wide zone dominantly within mafic lava flows, which cross-cuts stratigraphy in the south-central portion of the map area. Quartz-sericite altered rocks extend into the north-central portion of the area as a relatively narrow zone paralleling the Onaman River within mafic lava flows, felsic ash tuffs, and quartz-feldspar porphyritic sills (Plate 2). Lack of outcrop exposure or drill core data prohibit determination of whether rocks of this assemblage occur along the eastern shores of MacDonald Lake. Quartz-sericite altered rocks grade laterally into least-altered rocks, and are usually recognized in the field by their light brown to dark green color, and well-developed foliation.

Altered mafic lava flows, especially those in the south-central portion of the area, tend to be chlorite-rich (15-50%), and relatively sericite-poor (2-15%). The intense alteration in the mafic lava flows has obliterated most primary textures. Amygdaloidal and quench textures are the only primary textures preserved in thin section, and are only rarely observed. Pillows and pillow fragments are commonly discernable on outcrop.

Felsic ash tuff deposits along the Onaman River tend to be sericite-rich (15-65%), and relatively chlorite-poor (0-25%). In thin section preserved textures include quartz phenocrysts and ash-sized lithic fragments. Quartz-feldspar porphyritic sills are also pervasively altered, and tend to be sericite-rich (6-50%).

The rocks within this alteration type are composed of quartz (+albite?)(15-50%), and sericite (2-65%), with or without chlorite (0-50%), carbonate (0-25%), epidote (0-32%), opaques (0-6%), and stilpnomelane (0-5%) (Fig 27). Sericite occurs as well-foliated, fine-grained, plate-like aggregates dispersed throughout the rock and is everywhere associated with fine-grained, recrystallized quartz.

Chlorite in these rocks has a distinct greenish birefringence in thin section and petrographically appears identical to that in least-altered rocks. Microprobe and X-ray analyses (Appendix III) indicates it is a Mg-rich (Fe:Mg = 0.8) ripidolite or clinochlore (Berry, 1974; Deer et al., 1978). Thin section staining, along with microprobe and x-ray analyses, indicate the carbonate is dominantly calcite, with minor dolomite/ankerite present. Qualitative microprobe analyses of randomly selected opaque minerals reveals the opaques are Ti-rich suggesting they are ilmenite and/or titaniferous magnetite. Polished thin sections were also probed for composition of the white mica in the rocks, and confirmed the presence of the K-rich mica sericite (Appendix III).

Iron Chlorite Zone (Quartz-Iron Chlorite ± Sericite-Ankerite-Ti-bearing opaques-Epidote)

Rocks containing iron chlorite occur as a relatively long (2 km), but narrow (25-100m) zone in the north-central portion of the map area. This alteration type is largely restricted to felsic ash deposits with smaller, poorly exposed zones in mafic lava flows adjacent to the Onaman River, and in felsic lava flows northeast of MacDonald Lake (Plate 2). Although contacts with other alteration zones

are not exposed, the general distribution of this zone (Plate 2) suggests that it cross-cuts the quartz-sericite zone, and therefore post-dates development of that alteration type.

The presence of chlorite imparts a dark greenish color to many of the rocks of this zone, although they locally appear light greenish-brown, and/or reddish-brown where sericite and carbonate are also abundant.

In thin section the essential minerals of this assemblage include recrystallized quartz (+ albite?)(25-50%) and well foliated, distinctly purplish-birefringent chlorite (2-30%)(Fig. 28). Accessory minerals range widely in modal abundance and include sericite (0-45%), carbonate (0-30%), opaques (0-10%), and epidote (0-7%). Microprobe and X-ray analyses (Appendix III) indicate that the chlorite is an extremely iron-rich (Fe:Mg ratio = 2.33) ripidolite or chamosite. Microprobe study, along with staining techniques, indicates the dominant carbonate species is ankerite. Qualitative microprobe analyses also detect the presence of Ti-rich opaques (ilmenite and/or titaniferous magnetite?)(Appendix III). As in the quartz-sericite assemblage, alteration was largely pervasive, and primary textures such as phenocrysts and ash fragments are only occasionally observed in thin section.

Chloritoid Zone (Quartz-Chloritoid ± Iron Chlorite-Sericite-Ankerite-Paragonite-Ti-bearing Opaques)

Chloritoid zone rocks dominate the southwestern portion of the study area and occur as a relatively broad, subconcordant zone within mafic and felsic volcanic units. Three other, relatively locallized,

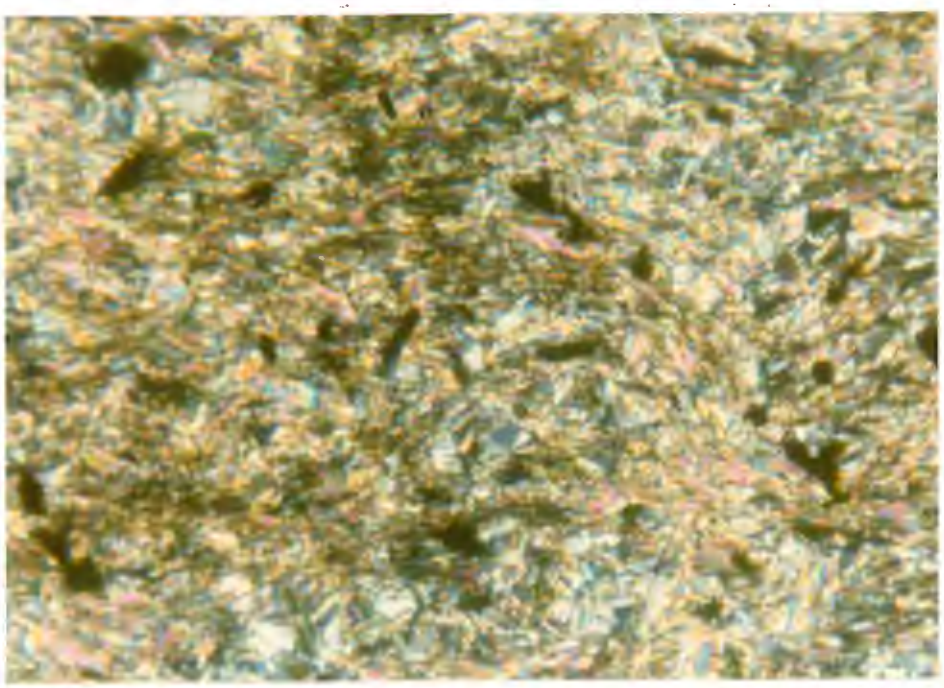

Figure 27. Photomicrograph of quartz-sericite alteration within laminated-bedded ash tuffs. Crossed polars, field of view: 2 x 1.5 mm.

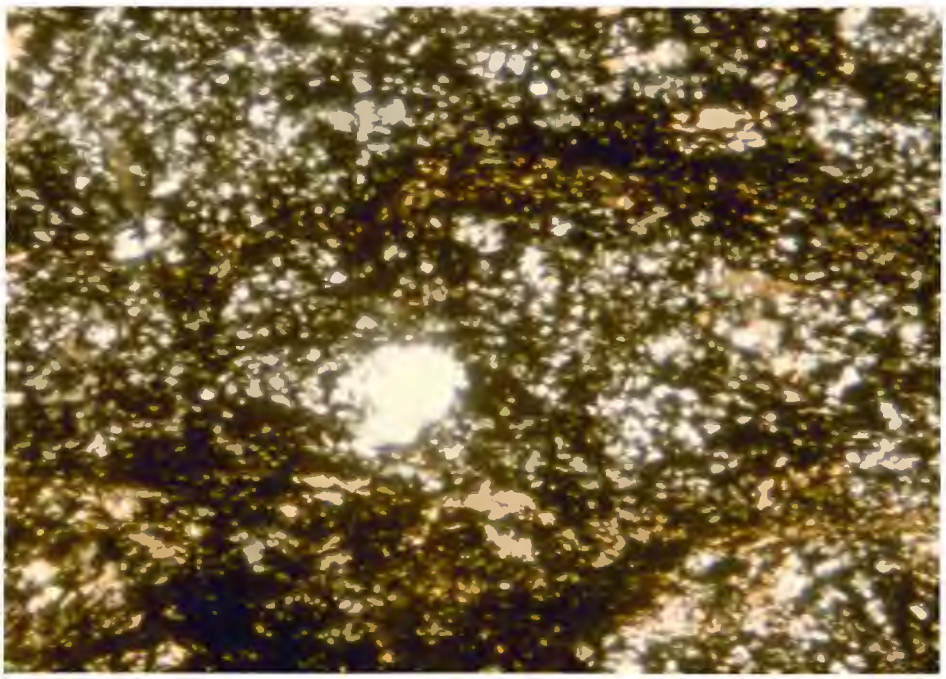

Figure 28. Photomicrograph of iron chlorite alteration within laminated-bedded ash tuffs. Crossed polars, field of view: 2 x 1.5 mm.

poorly exposed domains of chloritoid-bearing rocks occur in the north-central portion of the area where they are found surrounded by iron chlorite and quartz-sericite alteration types (Plate 2). The contacts between rocks of the chloritoid and quartz-sericite zones, where exposed, appear very sharp. This fact, along with the distribution of the chloritoid-bearing rocks (Plate 2), suggests that the chloritoid zone cross-cuts, and therefore post-dates formation of the quartz-sericite zone. Contacts with the iron chlorite zone are not exposed and contact relationships are therefore uncertain.

On outcrop chloritoid-bearing rocks typically appear well-foliated and light brown due to the presence of abundant sericite. Chloritoid is typically visible as dark green, 1-2 mm round to tabular grains which are set in the well-foliated sericitic matrix. Chloritoid composes up to 50% of the altered ash tuffs, and 5-30% of the mafic lava flows.

In thin section chloritoid zone rocks consist mainly of quartz (+albite?)(5-55%), and chloritoid (5-50%)(Fig. 29). Nonessential minerals include sericite (0-60%), chlorite (0-45%), carbonate (0-57%), and opaques (1-5%). Sericite and chlorite occur as fine-grained, well-foliated blades and aggregates dispersed throughout the rock along with recrystallized quartz. Chloritoid appears as 1-2 mm bow-tie twinned porphyroblasts and is commonly found associated with chlorite, but is elsewhere present in total absence of chlorite. Elsewhere chloritoid is associated with abundant ankerite. Numerous thin sections display chlorite patches which cross-cut, and replace sericite aggregates implying the chlorite post-dates formation of sericite in these rocks (Fig. 30).

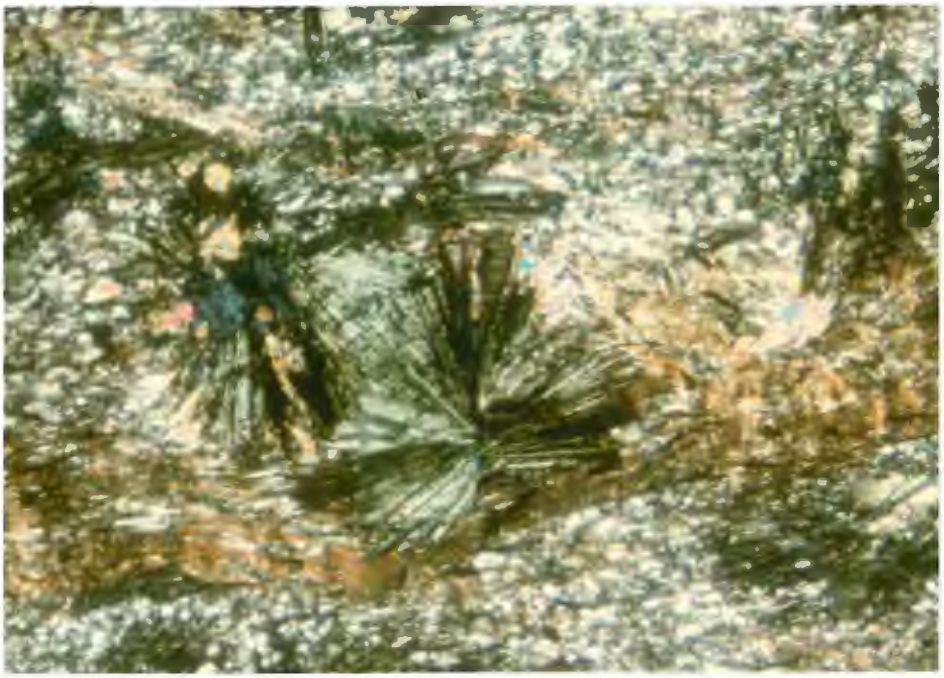

Figure 29. Photomicrograph of chloritoid alteration in quartz-crystal tuffs. Crossed polars, field of view: 2 x 1.5 mm.

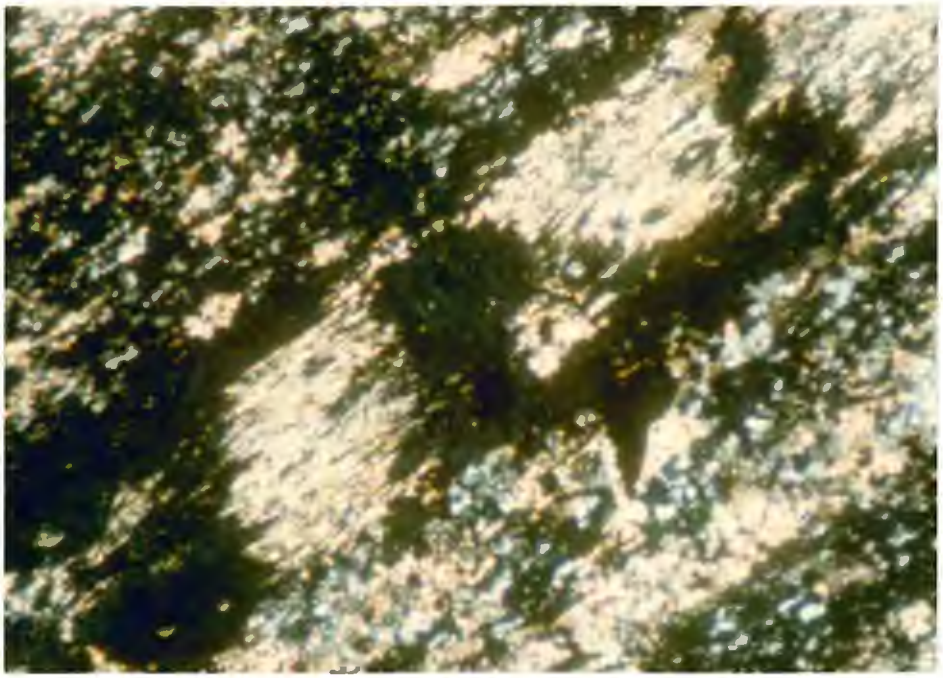

Figure 30. Photomicrograph of iron chlorite alteration (dark areas) replacing sericite alteration (bright areas) in laminated-bedded ash tuffs. Crossed polars, field of view: 2 x 1.5 mm.

As in the iron chlorite zone, microprobe and X-ray analyses (Appendix III) indicate the chlorite and carbonate are iron-rich. The chlorite has a deep purplish birefringence and is iron ripidolite or chamosite (Fe:Mg = 1.33). The carbonate is dominantly ankerite, with minor calcite present. Microprobe analyses of the chloritoid indicates it is also iron-rich (Fe:Mg = 4), and analyses of white mica in three polished thin sections verifies the presence of a K-rich phase (sericite), and indicates the presence of a Na-rich phase (paragonite) (Appendix III). Qualitative microprobe analyses of opaque minerals indicate they are Ti-rich and are probably ilmenite and/or titaniferous magnetite (Appendix III).

Several outcrops of the chloritoid and sericite-bearing ash tuffs contain dark greenish chlorite-chloritoid patches which compose up to 5% of the rock. These patches vary from oval-shaped pods up to 1 m in diameter within the quartz crystal tuffs (unit 2b), to highly irregular-shaped patches up to 2 m across within laminated-bedded tuffs (units 2a, and 3a).

Petrographically the chlorite-chloritoid patches consist of quartz (35-45%), chloritoid (5-50%), chlorite (6-45%), and opaques (3-7%). There is virtually no sericite or carbonate present within the patches. X-ray and microprobe analyses of the chlorite indicates it is similar in composition (iron-rich) to that present in the rock surrounding the patches. The patches commonly contain anhedral-subhedral quartz phenocrysts (3-5%) indicating that the patches are of an alteration origin rather than being deformed mafic fragments. On outcrop the patches appear to cross-cut the surrounding sericitic rock

suggesting that their development post-dates formation of sericitic alteration.

The porphyroblastic habit of the chloritoid indicates that it probably developed during regional metamorphism. Numerous studies (Zen, 1960; Hoschek, 1969; LaTour et al., 1980; Nebel, 1982; Morton and Nebel, 1984; Groves, 1984; Hyndman, 1985) have shown that chloritoid is characteristic of iron-rich, alkali- and Ca-depleted, aluminous rocks. Most of these studies conclude that chloritoid developed from a pre-metamorphic assemblage of chlorite and a hydrous Al-silicate (e.g. kaolinite, pyrophyllite, paragonite, etc.) which became unstable with increased temperatures during metamorphism. The common association of chloritoid with chlorite in rocks of this area suggests that such an origin of chloritoid is plausible, and was, in most cases, probably limited by the amount of hydrous Al-silicate present in the rocks. The chlorite and Al-silicate were presumably of hydrothermal origin. The development of chloritoid in the hydrothermally altered rocks will be further considered in the following chapter.

Al-silicate minerals were rarely observed in coexistence with chloritoid within rocks of the study area. Kyanite (with minor andalusite, but no chloritoid) was found locally northeast of MacDonald Lake (Plate 2). Because of the limited distribution of the kyanite-bearing rocks, and because of their spatial association with the chloritoid-bearing rocks, they are grouped as a subdivision of the chloritoid zone and are described here.

In the field the kyanite-bearing rocks appear pale greenish and very siliceous. In thin section quartz phenocrysts (2-5%) are set in a

matrix (Fig. 31) of foliated kyanite (25-31%), recrystallized quartz (35-60%), and minor andalusite (0-5%) and sericite (2-5%).

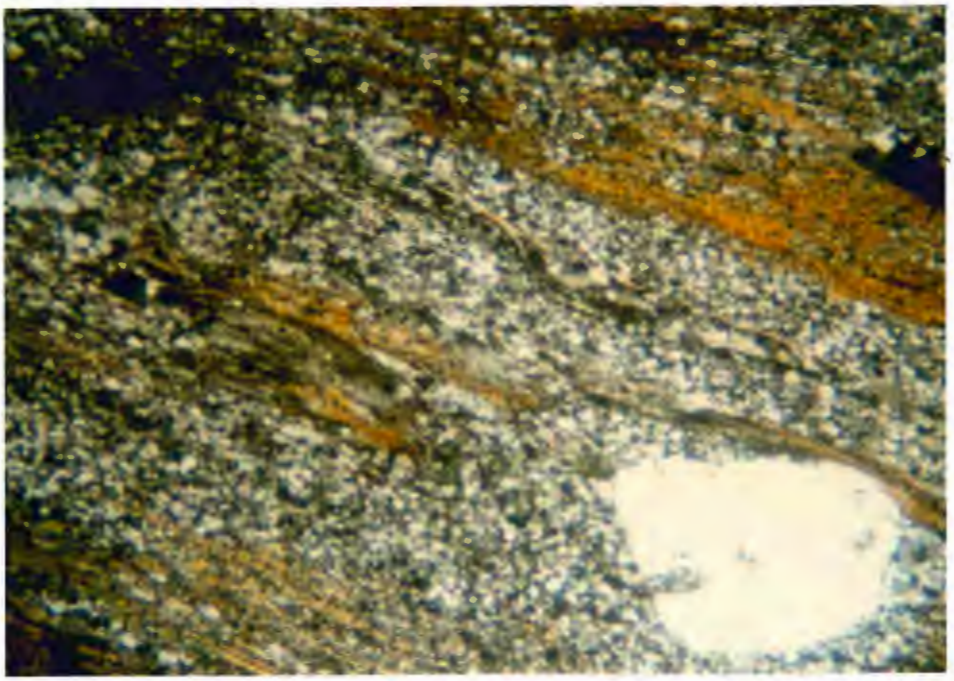

Figure 31. Photomicrograph of a quartz phenocryst enclosed in a matrix of foliated kyanite and recrystallized quartz in the quartz porphyritic lava flow. Crossed polars, field of view: 4.8 x 4 mm.

IV. GEOCHEMISTRY

IV.1 Introduction

Hydrothermal alteration at the Headway-Coulee Prospect has been mineralogically defined in Chapter III; it is the purpose of this chapter to document the geochemical changes in the rocks resulting from hydrothermal alteration and to develop an alteration model.

To determine chemical variations within and between rock units defined in the study area, 117 rock samples were collected and analyzed for major oxides and 16 trace elements. The analyses were done by the Geological Survey of Canada's Analytical Laboratory Section and the results, along with analytical methods used, are listed in Appendix II. Locations of rock samples are shown on Plate 1. Normative mineral calculations were made using the major oxide analyses and are listed in Appendix IV.

An inspection of the major element chemistry indicates that individual original rock types range widely in their chemical composition (Tables 1 and 2). SiO_2 contents in mafic lava flows vary from 37.3% to 57.8% (wt.%). Least-altered lava flows exhibit much less variation, with SiO_2 contents near 50% (46.7-49.9%); this indicates that they are basaltic in composition. Felsic rocks (ash tuffs, lava flows, and sills) have SiO_2 values ranging from 34.9% to 83.7% (Table 2). Such wide variation indicates that SiO_2 was depleted in many of the rocks, and enriched in others. Chemical classification of these rocks based on SiO_2 content alone would thus be invalid and unreliable.

Table 1. Summary of Major and Selected Trace Element Geochemistry of Mafic Rocks

Alteration Zone:	Mafic Lava Flows: Least-Altered		Quartz-Sericite		Iron Chlorite		Chloritoid		Gabbroic Sills: Least-Altered	
Major Element (in wt.%)	(n=11)* Range	Average	(n=19) Range	Average	(n=2) Range	Average	(n=17) Range	Average	(n=3) Range	Average
SiO2	46.70-49.90	48.60	43.20-55.70	48.98	52.30-53.30	52.80	37.30-57.80	50.25	46.60-48.50	47.40
TiO2	0.69- 1.01	0.84	0.65- 1.04	0.87	0.92- 1.07	1.00	0.66- 1.20	0.96	0.58- 0.75	0.65
Al2O3	14.30-15.40	14.80	13.20-15.47	15.47	15.20-16.3	15.75	11.30-24.40	16.70	12.90-15.40	14.60
Fe2O3	1.30- 5.30	2.86	1.00- 4.60	1.93	1.30- 1.90	1.60	1.10- 5.10	1.94	1.40- 2.90	2.20
FeO	5.40- 9.50	8.27	6.30-10.80	8.15	6.20-12.00	8.93	5.20-10.00	7.34	7.30- 8.40	7.80
MnO	0.12- 0.29	0.20	0.08- 0.84	0.24	0.19- 0.20	0.20	0.17- 0.96	0.30	0.18- 0.23	0.20
MgO	5.84- 9.46	7.63	4.13-11.00	6.92	4.59- 6.17	5.38	1.38- 6.61	3.94	8.08-10.10	9.33
CaO	3.20-15.30	9.61	0.50-10.80	4.86	2.23- 7.35	4.79	1.23-10.90	7.45	8.52-12.20	10.13
Na2O	0.60- 2.60	1.77	0.00- 3.20	1.23	0.60- 1.90	1.25	0.00- 2.20	0.50	0.70- 1.40	0.97
K2O	0.00- 1.53	0.24	0.00- 2.52	0.70	0.02- 0.55	0.29	0.12- 2.66	1.02	0.03- 0.17	0.09
CO2	0.20- 4.50	1.55	0.20- 9.90	4.80	0.60- 3.60	2.10	0.40-18.20	6.87	0.50- 6.90	2.73
H2O	2.10- 4.80	3.48	3.10- 6.42	4.58	4.30- 5.00	4.65	1.70- 4.90	3.55	4.10- 5.00	4.43
Selected Trace Elements (in ppm)										
Zr	35-120	56.11	28-170	60.40	53-56	54.50	36-66	52.67	32-36	34.00
Cr	210-340	273.56	8-410	210.65	240-340	290.00	8-430	247.47	310-520	400.00
Nb	0-4	2.11	0-7	2.25	2-3	2.50	0-4	1.67	1-2	1.33
Ni	110-190	133.33	30-200	107.25	130-160	145.00	33-200	119.59	88-210	149.00
Th	0-9	3.67	0-11	3.10	2-5	3.50	0-8	2.00	0-6	2.67

*n = # of analyses

Table 2. Summary of Major and Selected Trace Element Geochemistry of Felsic Rocks

	> Laminated-Bedded Tuffs <				> Quartz-Crystal Tuffs <	
Alteration Zone:	Quartz-Sericite		Iron Chlorite		Chloritoid	
Major Element (in wt. %)	(n=5)* Range	Average	(n=6) Range	Average	(n=27) Range	Average
SiO2	50.80-71.60	63.94	34.90-65.70	53.95	36.50-75.80	55.10
TiO2	0.29- 1.12	0.75	0.57- 2.04	1.00	0.37- 2.09	1.23
Al2O3	13.70-19.60	16.98	11.70-17.60	16.55	12.80-36.60	20.26
Fe2O3	0.30- 1.60	1.00	0.60- 2.40	1.45	0.30-25.60	3.42
FeO	0.20- 8.70	3.20	2.00-14.80	8.35	0.00-19.30	5.76
MnO	0.02- 0.27	0.12	0.08- 0.43	0.22	0.00- 0.54	0.22
MgO	0.40- 5.00	2.31	1.35- 8.82	4.11	0.09- 4.48	1.86
CaO	0.99- 5.58	3.04	0.65- 9.23	4.09	0.14-10.40	1.56
Na2O	0.10- 1.00	0.54	0.00- 1.10	0.57	0.00- 2.50	0.69
K2O	0.79- 3.96	2.54	0.16- 3.09	1.65	0.06- 6.88	2.46
CO2	0.70- 4.50	2.34	0.10-11.90	4.40	0.00- 7.70	0.89
H2O	2.60- 5.20	3.50	0.50- 5.80	3.57	2.50- 6.60	4.13
Selected Trace Elements (in ppm)						
Zr	53-230	133.00	40-220	101.33	45-440	132.81
Cr	3-310	137.20	12-390	218.17	9-860	137.48
Nb	2-8	5.20	1-9	4.00	0-22	5.00
Ni	2-220	76.20	13-160	104.67	7-330	41.67
Th	0-11	5.00	0-13	6.33	0-27	9.15

					150-270	204.00
					30-38	33.10
					8-11	8.60
					7-26	13.26
					10-19	13.00

*n = # of analyses

(continued)

Table 2. (continued)

	QFP > Lava Flow <		QP > Lava Flow <		QFP Sub- >volcanic Sills<	
Alteration Zone:	Iron Chlorite		Chloritoid**		Quartz-Sericite	
Major Element (in wt.%)	(n=2)* Range	Average	(n=4) Range	Average	(n=6) Range	Average
SiO2	66.00-69.80	67.90	69.90-83.70	76.80	49.90-76.00	67.10
TiO2	0.47- 0.62	0.55	0.46- 0.82	0.67	0.24- 0.72	0.45
Al2O3	16.10-17.10	16.60	14.80-28.00	20.85	14.10-16.50	15.40
Fe2O3	0.80- 0.90	0.85	0.00- 0.70	0.18	0.70- 1.70	1.01
FeO	3.00- 3.30	3.15	0.00- 0.30	0.11	0.50- 6.30	2.31
MnO	0.07- 0.08	0.08	0.00- 0.01	0.003	0.03- 0.21	0.20
MgO	0.85- 1.15	1.00	0.00- 0.07	0.04	0.21- 4.49	2.03
CaO	1.24- 2.71	1.98	0.06- 0.36	0.17	0.37-10.40	2.53
Na2O	1.70- 3.90	2.80	0.00- 0.50	0.33	0.30- 4.60	1.91
K2O	1.45- 2.33	1.89	0.11- 0.26	0.17	0.47- 3.04	2.14
CO2	0.70- 0.80	0.75	0.00- 0.10	0.03	0.60- 5.70	2.03
H2O	1.90- 3.00	2.45	0.30- 0.80	0.60	1.50- 3.80	2.73
Selected Trace Elements (in ppm)						
Zr	150-210	180.00	160-310	227.50	61-170	118.45
Cr	16-28	22.00	5-29	15.75	5-28	13.36
Nb	4-8	6.00	7-13	10.50	0-9	4.40
Ni	9-12	10.50	4-8	5.00	7-170	31.34
Th	10-18	14.00	10-20	13.00	4-17	9.22

*n = # of analyses
**Kyanite-bearing rocks

Hydrothermal alteration is also indicated by widely ranging Al_2O_3 contents. In mafic lava flows, Al_2O_3 varies from 11.3-24.4%, and in the felsic rocks, from 11.7-36.6%. Carmichael et al. (1974) give an average Al_2O_3 content for basalts as 14.07%, and for rhyolites as 13.45%. This indicates that, by comparison, some of the Headway-Coulee rocks are anomalously enriched in Al_2O_3. The Al enrichment of the rocks is reflected in normative mineral calculations by the presence of up to 30% corundum (Appendix IV). However, Al-silicate minerals (e.g. kyanite, andalusite) were not recognized in thin section, except for a local occurrence in felsic rocks northeast of MacDonald Lake. All of the Al in the altered rocks is thus assumed to be present in such phases as chloritoid, sericite, paragonite, and chlorite.

TiO_2 values also vary widely and are anomalously high in many of the rocks (Tables 1 and 2). TiO_2 in the mafic rocks ranges from 0.58-1.20%, and in felsic rocks from 0.29-2.70%. According to Carmichael et al. (1974), TiO_2 values in basalts generally range from 0.80% to 3.20%, and in rhyolitic rocks from 0.07% to 0.50%. The highest TiO_2 contents in the felsic rocks generally occur in altered ash tuffs. The presence of quartz phenocrysts in many of these TiO_2-rich tuffs verifies a felsic protolith and implies that TiO_2 was, at least in the felsic tuffs mobilized by the alteration process. However, the possibility remains that some of the altered, TiO_2-rich tuffs (those which contain no quartz phenocrysts) may represent interbeds which had a mafic or intermediate protolith. High normative ilmenite abundances (up to 4%) reflect the TiO_2-rich nature of the felsic rocks (Appendix IV).

Na_2O values are relatively low in the study area indicating Na depletion. In the mafic lava flows, Na ranges from 0.00 to 3.2% (ave. 1.18%), and for all felsic rocks it varies from 0.00% to 4.6% (ave. 0.91%). K_2O contents vary from 0.00% to 2.66% in mafic lava flows, and from 0.00% to 6.55% in the felsic rocks; they are highest where the rocks are most intensely sericitized.

Fe_2O_3, FeO, MnO, and MgO values also vary widely (Tables 1 and 2), and are generally highest in chlorite, ankerite, and/or chloritoid-rich rocks.

Trace element contents, like the major elements, tend to be highly variable. The majority of the trace elements exhibit no consistent relationships to lithologic type, but Zr, Cr, Nb, Ni, and Th are exceptions and have average abundances which are generally distinctive for felsic and mafic rocks (Tables 1 and 2). This group of elements has traditionally been interpreted (Cann, 1970; Davies et al., 1979; Campbell et al., 1984) as being relatively immobile during all but the most intense stages of hydrothermal alteration and this appears to be the case within the study area.

Zr, Nb, and Th are generally most abundant in felsic rocks, whereas Cr, and Ni are typically most abundant in mafic rocks (Tables 1 and 2). Although usually true, there are exceptions to this generalization, especially in intensely altered ash tuffs. Many of these exceptions may represent altered tuffs which had a mafic or intermediate protolith as suggested above to explain some of the anomalously TiO_2-rich tuffs.

Due to intense hydrothermal alteration of the rocks within the

area it is not possible to identify petrogenetic trends, or to classify the rocks using standard petrochemical graphs, such as AFM diagrams, Jensen cation plots, and Harker diagrams. However, Thurston (1980) did a study of the geochemistry of volcanic rocks throughout the entire Onaman Lake region and reported that those rocks which had been least affected by hydrothermal alteration have a tholeiitic affinity, and range from basalts through rhyolites in terms of SiO_2 contents.

Because standard petrochemical techniques do not adequately illustrate the effects of metasomatic alteration, chemical changes in the rocks have been studied by comparison of progressively altered samples using the mass balance techniques of Gresens (1967).

IV.2 Mass Balance

Gresens (1967) demonstrated that quantitative geochemical comparisons of metasomatically altered rocks must consider possible volume changes in the rocks which occurred during the alteration process. Gresens developed a generalized equation, which incorporates volume changes and calculates actual gains and losses of chemical components.

The Gresen equation is written as:

$$Xn = \{Fv[G(b)/G(a)]Cn(B)-Cn(A)\}100, \text{ where,}$$

Xn = actual gain or loss in grams of component n per 100 grams of original rock,

Fv = volume factor, i.e. the ratio between the final and ini-

tial volumes of the rock, such that:

when Fv>1, alteration involves a volume gain;

when Fv=1, alteration is at constant volume;

when Fv<1, alteration involves a volume loss.

G(a),G(b) = specific gravity of unaltered rock (a), and altered rock (b), respectively, and

Cn(a), Cn(b) = weight fraction of component n in unaltered rock (a), and altered rock (b), respectively.

Specific gravities used in mass balance calculations were measured on a modified beam balance calibrated with an Al standard of specific gravity = 2.71. Specific gravities, as measured, are included with chemical data in Appendix II.

Since specific gravities {G(a), G(b)} and chemical compositions {Cn(a), Cn(b)} are measured quantities, the Gresen equation can be simplified to two unknown variables, Fv (volume change), and Xn (compositional change). In order to solve the equation an assumption must be made concerning the value of Fv or Xn. Three possible approaches can be used to obtain a value for Fv or Xn.

(1). Assume alteration has occurred at constant volume (Fv=1).

The Gresen equation is then solved for Xn for each component. This assumption is frequently made in mass balance studies where delicate primary textures (e.g. amygdules, fiamme structures, shards, etc.) are preserved in an undeformed state. Intense alteration and well-developed deformational textures (e.g. foliation) in the rocks of this study makes assumption of constant volume conditions during alteration tenuous.

(2). Assume one or more components have been relatively immobile during alteration. Xn is set = 0 for these components and the Gresen equation is solved for Fv. This value of Fv represents the true volume factor in the rock and is used to calculate gains and losses for the remaining components. There is no recognized evidence for assuming the complete immobility of any component during the alteration of the rocks within the study area.

A graphical approach (after Appleyard, 1980) can be used to determine an Fv value. One altered sample is compared to several unaltered (or least altered) samples by arbitrarily setting Xn = 0 and calculating Fv for each component in each comparison. The resulting Fv values are then plotted on a $\log_{10}$ scale in histogram form (e.g. Fig. 32). The "peak" Fv value (that value with the greatest frequency) represents the true Fv for the rock. Elements which consistently plot within the peak area can be considered to have been relatively immobile; those consistently plotting as a volume decrease (negative $\log_{10}$ Fv) have been added, and those consistently plotting as a volume increase (positive $\log_{10}$ Fv) have been lost. The Fv value so determined can be substituted into the Gresen equation and used to calculate Xn for each component.

For rocks of this study, no evidence is recognized for the valid assumption of constant volume, or immobility of any component. Therefore, the graphical method of comparing on altered sample to several unaltered samples (approach #3) has been used in the following mass balance comparisons. An attempt was made to select samples for the comparisons which are petrographically representative of each alteration type within an individual lithologic unit.

IV.3 Alteration Zones

Quartz-Sericite Zone

To identify chemical trends involved in the development of sericitic alteration, mass balance comparisons were made between mafic lava flows of the least-altered and quartz-sericite zones. Figs. 32 and 33 are two examples of representative volume factor histograms illustrating the chemical component trends and their typical variations; Table 3 summarizes the alteration trends. "Peaks" on the histograms are near $\log_{10}$ Fv values approximately = 0 (Fv = 1), indicating alteration was near volume-for-volume.

As suggested by the mineralogy of sericitically altered rocks, the major chemical feature associated with the alteration is the addition of large amounts of K. Rb was also gained, and is assumed to have substituted readily for K. Na consistently plots as positive $\log_{10}$ Fv values, indicating it was lost during alteration. Al, Ti, Ni, Cr, Si, Fe^{+2}, Y, and Co generally plot within, or near the "peak" area of the histogram suggesting they were relatively immobile components. With the exception of Ca, and C^{+4} (which can be directly related to variations in the modal abundance of calcite in the compared rocks), the other elements exhibit no consistent patterns when comparing different histograms representing the transition from least-altered to quartz-sericite alteration (e.g. Figs. 32 and 33).

Numerous studies (Hemley and Jones, 1964; Riverin and Hodgson, 1980; Nebel, 1982; Morton and Nebel, 1984; Groves, 1984) attribute the process of sericitization to the breakdown of plagioclase feldspar during hydrothermal alteration. Plagioclase would be abundant in the mafic

Table 3. Summary of Mass Balance Comparisons between Alteration Zones

Comparison	Lithology	Volume Change	Elemental Trends		
			Gained	Lost	Immobile
Least-Altered to Quartz-sericite	Mafic Lava Flows	none	K, Rb	Na	Al, Ti, Ni, Cr, Si, Y^{+2}, Co, Fe^{+3}
Quartz-sericite to Iron chlorite	Felsic Tuffs	none	Mn, Fe^{+2} Fe^{+3}, Cr Ti, Y	Na, Ca C^{+4}	Al, Si
Quartz-sericite to Chloritoid	Mafic Lava Flows	-21% to -39%	Fe^{+3}, Cr	Na, Mg, Ca, Sr, C^{+4}	Al, Ti, Zr Si
Quartz-sericite to Chloritoid	Felsic Tuffs	-21% to -50%	Ti, Mn, Y, Zr, Cr, Nb, Fe^{+2} Fe^{+3}, Mn	Si, K, Rb, Na, Ca, Sr, Ni, C^{+4}	Al

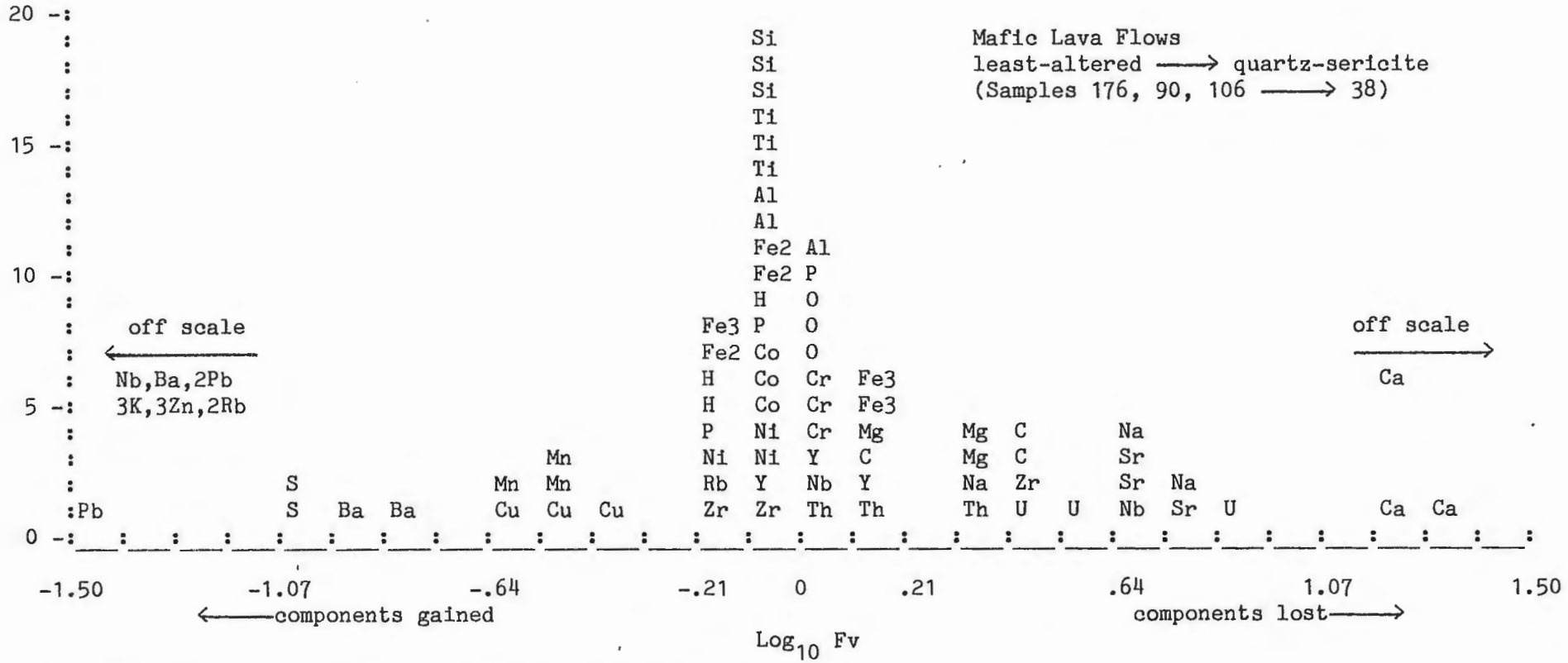

Figure 32. Volume-factor histogram for mafic lava flows: least-altered zone to quartz-sericite zone, example #1.

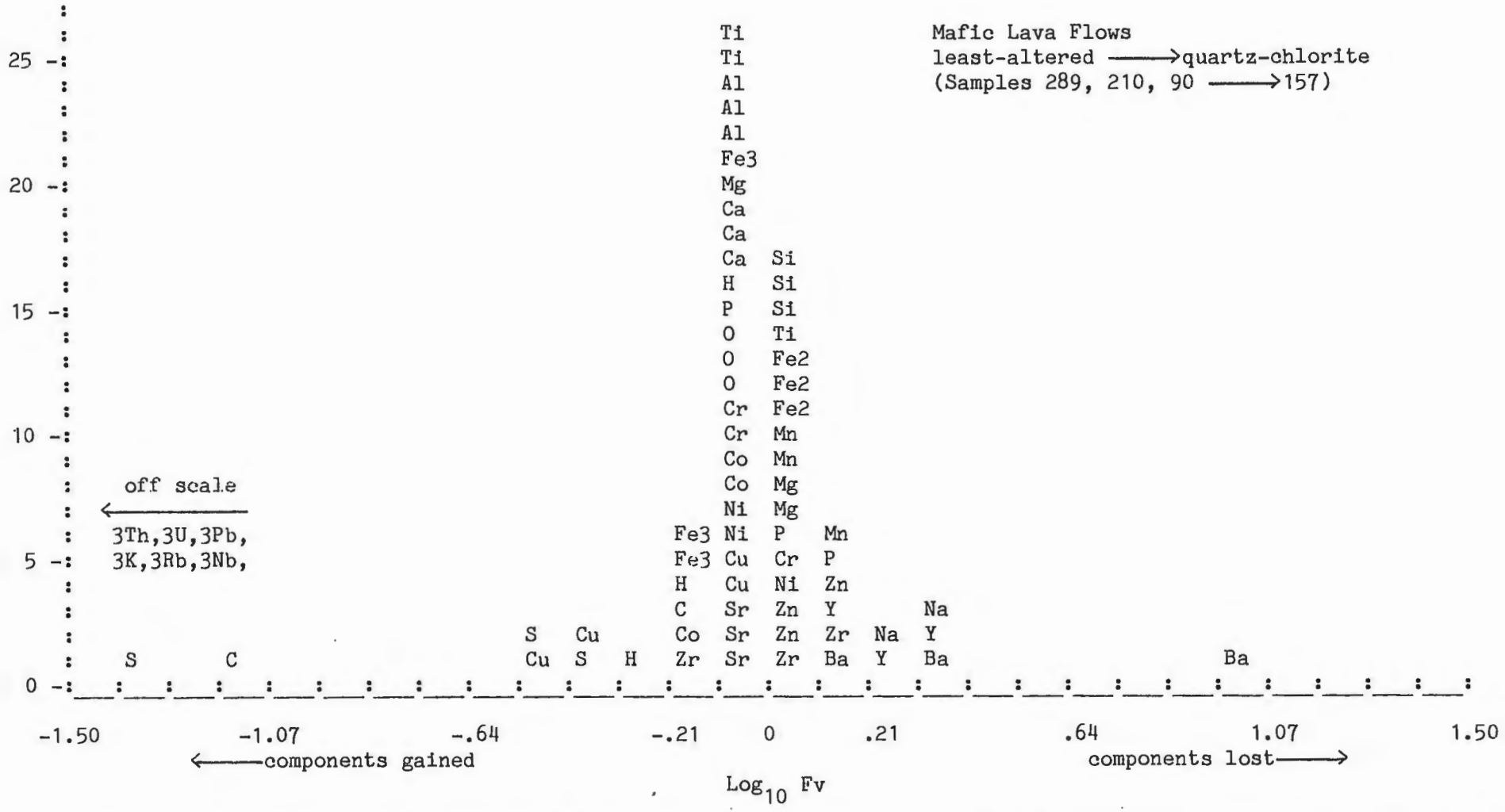

Figure 33. Volume-factor histogram for mafic lava flows: least-altered zone to quartz-sericite zone, example # 2.

mafic rocks prior to sericitization and could conceivably vary in An content between different locations depending upon the intensity of spilitization prior to hydrothermal alteration. The following reactions (reactions 1 and 2) are presented to illustrate the alteration of plagioclase of varying An content in mafic lava flows. The alteration of extremely Ca-rich plagioclase can be represented by reaction (1):

$$\text{(1)}\quad \overset{\text{anorthite}}{3CaAl_2Si_2O_8} + K_2O + 2H_2O + 0.92CO_2 = \overset{\text{sericite}}{2KAl_3Si_3O_{10}(OH)_2} + \overset{\text{calcite}}{0.92CaCO_3} + 2.08CaO.$$

Such a reaction may be responsible for the local sericite and calcite-rich altered rocks.

Sericite, along with quartz, may also form at the expense of sodic plagioclase, as suggested by Morton and Nebel (1984) according to the following reaction:

$$\text{(2)}\quad \overset{\text{albite}}{NaAlSi_3O_8} + 0.33\ K^+ + 0.67H^+ = \overset{\text{sericite}}{0.33KAl_3Si_3O_{10}(OH)_2} + \overset{\text{quartz}}{2SiO_2} + Na^+.$$

Compositions, and molar volumes of minerals in these reactions are included in Table 4.

Mass balance analyses of sericitic alteration of the felsic volcanic rocks is not possible because unaltered equivalents are not ex-

Table 4. Mineral Formulas and Molar Volumes Used for Balancing Alteration Reactions.

Mineral	Formula	Molar Volume (cm^3)
Anorthite	$CaAl_2Si_2O_8$	106.1
Albite	$NaAlSi_3O_8$	100.0
Sericite	$KAl_3Si_3O_{10}(OH)_2$	142.0
Calcite	$CaCO_3$	37.0
Quartz	SiO_2	23.7
Chlorite	$Mg_{2.5}Fe_{2.5}Al_2Si_3O_{10}(OH)_8$	215.0
Pyrophyllite	$Al_2Si_4O_{10}(OH)_2$	125.9
Kaolinite	$Al_2Si_2O_5(OH)_4$	99.5
Chloritoid	$H_2(Fe,Mg)Al_2SiO_7$	96.1

[1] Data from Robie et al., (1967); Helgeson et al., (1978); Deer et al., (1966).

posed. However, it seems reasonable to suggest that sericitization of the felsic rocks may have occurred principally at the expense of Na-rich plagioclase.

Iron Chlorite Zone

Field and petrographic evidence suggests that the iron chlorite alteration zone cross-cuts the quartz-sericite alteration zone. Mass balance comparisons were made between zones of quartz-sericite and iron chlorite alteration within felsic ash tuffs. Two representative volume factor histograms which illustrate typical chemical component trends and their variations are shown in Figs. 34 and 35. Chemical trends illustrated by the histograms and are summarized in Table 3. Fv "peaks" on the histograms are relatively broad. Al and Si consistently cluster tightly within the peaks, and are therefore considered to be relatively immobile components. Log_{10} Fv values represented by the peaks are approximately = 0 (Fv = 0), indicating alteration was generally at constant volume. Other elemental trends indicated by the histograms include the addition of Fe^{+2}, Fe^{+3}, and Mn in most cases, and are attributed to the development of iron chlorite with or without ankerite in the rocks. Na is consistently lost in all comparisons. Ca and C^{+4} are typically lost; Ca loss is thought to be related to a change in carbonate species from calcite to ankerite during iron chlorite alteration, and losses in C^{+4} may reflect CO_2 driven off during regional metamorphism (decarbonitization). K and Mg are variable and generally correspond to variations in the modal abundance of sericite and chlorite in the rocks. Ti, Cr, and Y usually plot slightly to the left of the Fv peaks on the histograms indicating

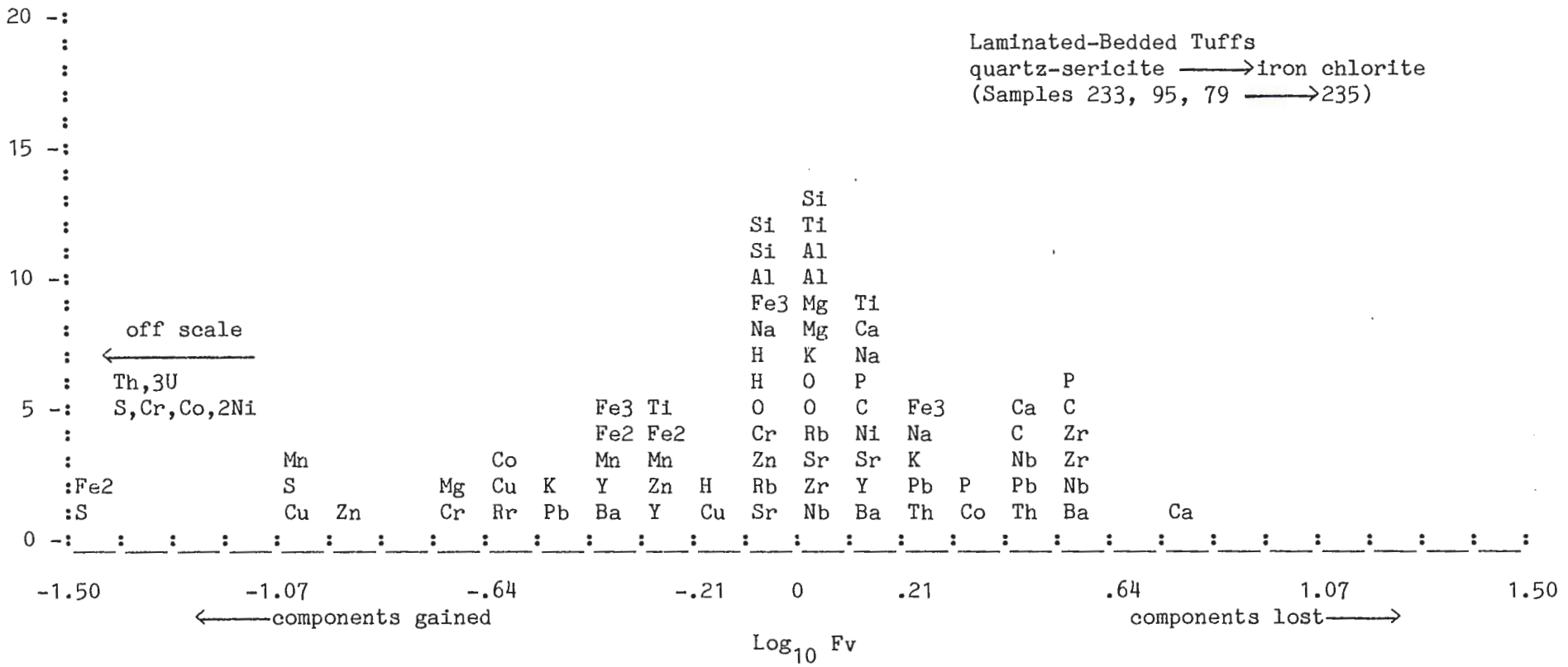

Figure 34. Volume factor histogram for felsic ash tuffs: quartz-sericite zone to iron chlorite zone, example # 1.

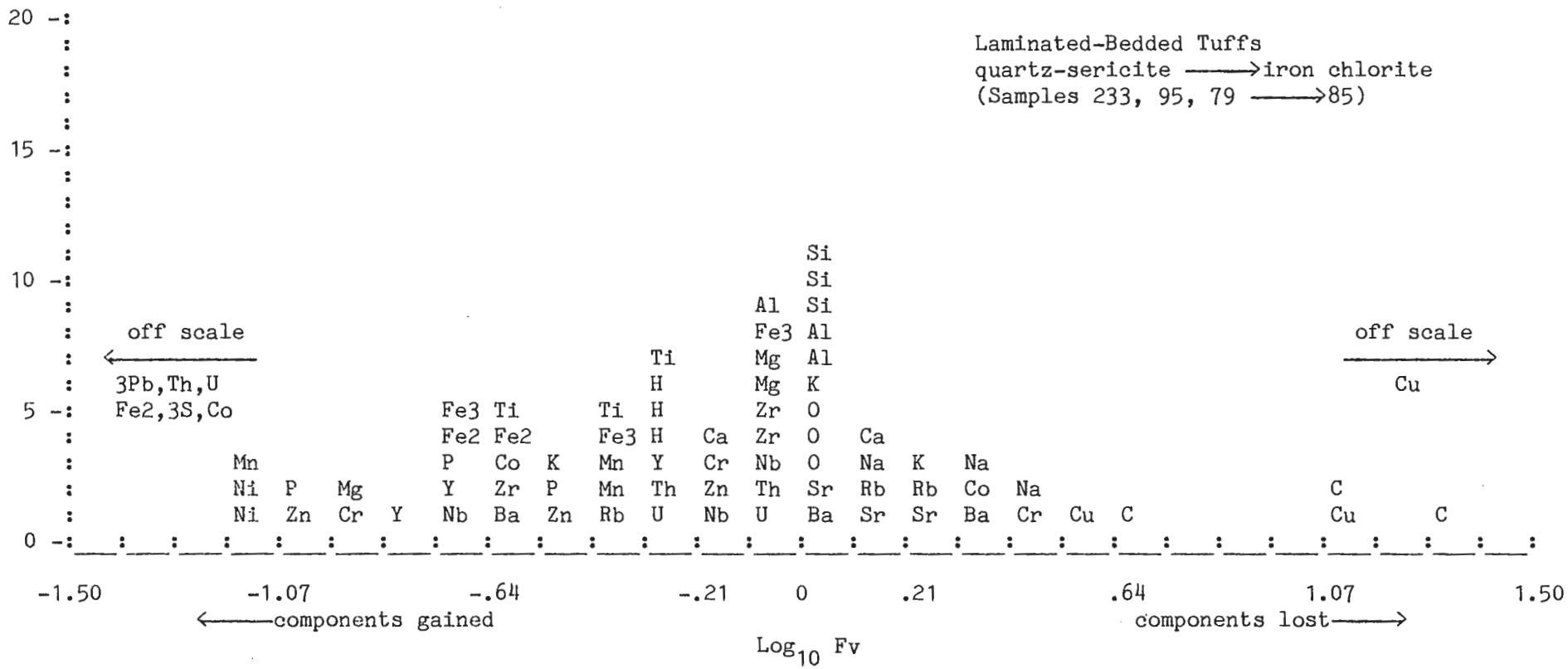

Figure 35. Volume factor histogram for felsic ash tuffs: quartz-sericite zone to iron chlorite zone, example # 2.

minor to moderate gains. The high Ti and Cr contents in many of the ash tuffs is apparently the result of mobility of these elements. However, the possibility exits that the tuffs underwent relatively large volume losses during compaction and accompanying sericitic alteration prior to iron chlorite alteration, thereby resulting in apparent high elemental abundances of Ti and Cr. Williams and McBirney (1979) report that pyroclastic deposits may lose up to 50-60% of their original volume during post-depositional alteration suggesting such a hypothesis is reasonable.

As stated above, the distribution of the iron chlorite-bearing rocks suggests they formed at the expense of the quartz-sericite assemblage. The development of chlorite at the expense of sericite can be represented by the following reaction (at approximately constant molar volume):

$$(3)\quad \overset{\text{sericite}}{3KAl_3Si_3O_{10}(OH)_2} + 10Fe^{+2} + 32H_2O = \overset{\text{chlorite}}{2Fe_5Al_2Si_3O_{10}(OH)_8} + 3Si(OH)_4^- + 5Al(OH)_4^- + 3K^+ + 22H^+$$

Riverin and Hodgson (1980) and Morton and Nebel (1984) similarly concluded that chlorite developed at the expense of sericite at the Millenbach and Helen Mines respectively, and proposed similar reactions. However, microprobe analyses (Appendix III) indicates that chlorite of the iron chlorite zone at the Headway-Coulee prospect is more Fe-rich than that at the Millenbach and Helen Mines.

Chloritization may also occur at the expense of albite which was not converted to sericite during quartz-sericite alteration. Morton and

Nebel (1984) suggest the development of chlorite beneath the Helen Mine may locally have occurred by such a process (at constant molar volume):

$$(4)\quad \underset{\text{albite}}{NaAlSi_3O_8} + 2.5(Fe,Mg)^{+2} + \underset{\text{quartz}}{0.32SiO_2} + 7.63H_2O = \underset{\text{chlorite}}{0.5(Mg,Fe)_5Al_2Si_3O_{10}(OH)_8} + 4H^+ + 1.82H_4SiO_4 + Na^+.$$

Addition of Fe to the rocks, with minor amounts of Mg, could also explain the presence of ankerite as the dominant carbonate species in the iron chlorite-bearing rocks rather than calcite which is found in the quartz-sericite alteration assemblage.

The iron chlorite alteration assemblage was only rarely observed in mafic lava flows and, because stratigraphically equivalent sericitic or least-altered rocks are not exposed, mass balance comparisons were not made.

Chloritoid Zone

Chloritoid-bearing rocks were compared chemically to rocks of the quartz-sericite and, where possible, iron chlorite zone. As with the iron chlorite zone, field and petrographic evidence suggests that the chloritoid-bearing rocks formed at the expense of sericite-bearing rocks. Two representative histograms which illustrate typical variations of the chemical component trends for comparisons of mafic lava flows in the chloritoid and quartz-sericite zones are shown in Figs. 36 and 37. Mass balance trends are generally similar to those described above for comparisons of iron chlorite and sericitically altered ash tuffs and are summarized in Table 3. Volume factor peaks

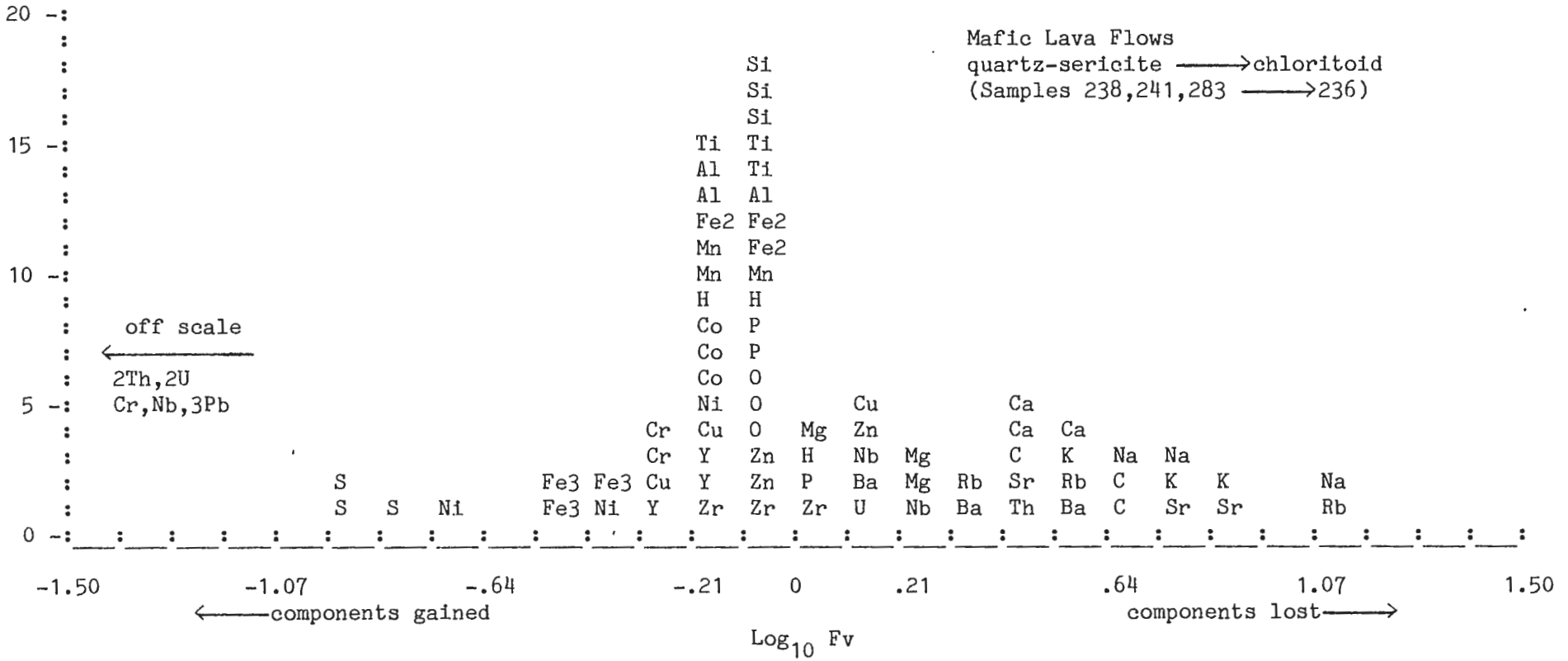

Figure 36. Volume-factor histogram for mafic lava flows: quartz-sericite zone to chloritoid zone, example # 1.

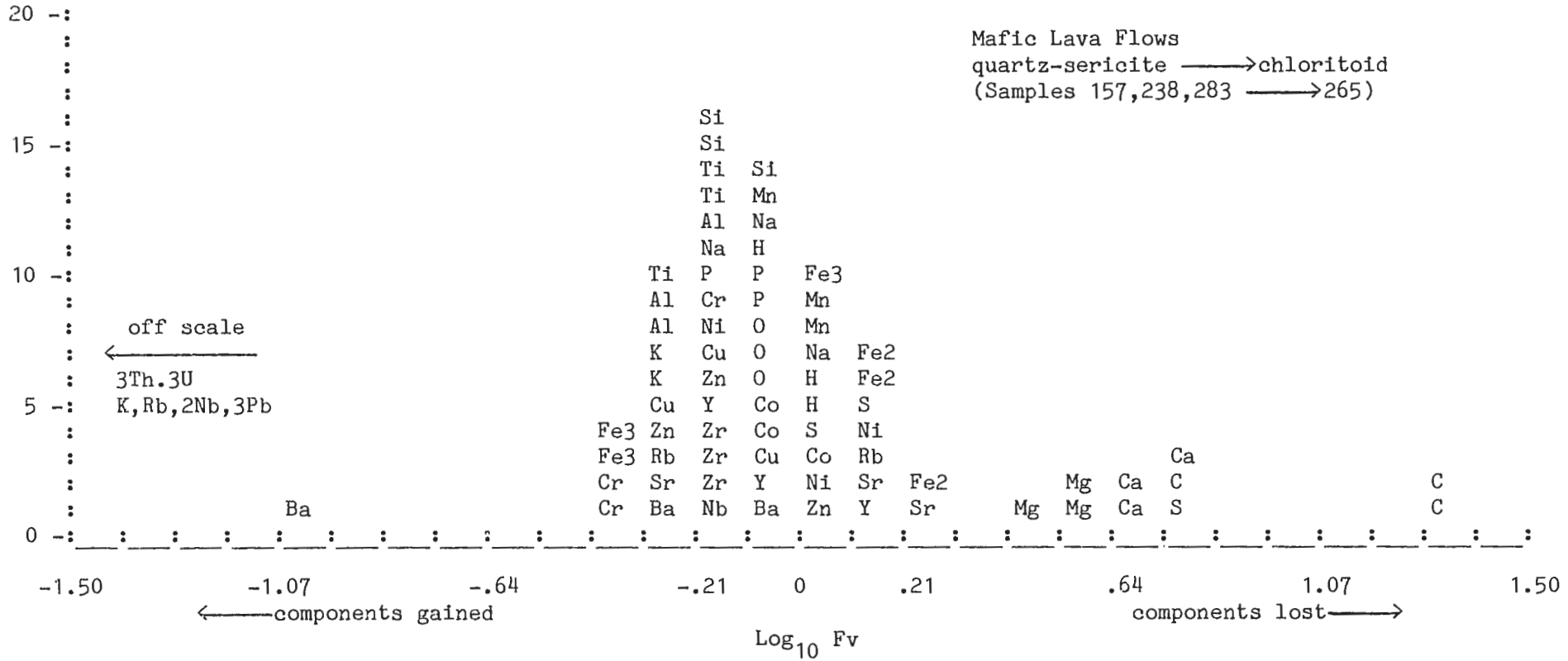

Figure 37. Volume-factor histogram for mafic lava flows: quartz-sericite zone to chloritoid zone, example #2.

are well defined by a clustering of relatively immobile Al, Ti, Zr, and Si, but unlike the iron chlorite to quartz-sericite comparisons, volume losses (21% to 39%) are indicated. Fe^{+3} and Cr typically plot as slight gains, and Na, Mg, C^{+4}, Ca, and Sr commonly as losses. As in the iron chlorite zone, losses in Ca are associated with a change in carbonate species from calcite to ankerite, and C^{+4} losses may reflect CO_2 loss during regional metamorphism. Fe^{+2} is generally immobile, or slightly lost, in which case it is nearly always lost in lower amounts than Mg within individual one-to-one sample comparisons. The histograms exhibit no consistent gains or losses in K, Rb, Ni, Nb, Co, Mn, or Y.

Geochemical trends between chloritoid and quartz-sericite alteration assemblages in the ash tuffs are illustrated in Figs. 38 and 39 and are summarized in Table 3. The trends differ from those in mafic lavas in that Zr, Ti, and Si appear less immobile than in mafic lavas. The histograms generally display gains in Ti, Mn, Y, Zr, Nb, and Cr and slight to moderate losses in Si. Al appears relatively immobile, and when so considered, volume losses (up to approximately 50%) are greater than in mafic lavas. Mg trends are erratic; K, Rb, Na, Ca, C^{+4}, and Sr are usually lost, and Fe^{+2}, Fe^{+3}, and Mn usually gained. The gains in Fe^{+2}, Fe^{+3}, and Mn, and losses in Ca are related to the formation of iron chlorite and, the conversion of calcite to ankerite during alteration.

As discussed in the previous chapter, chloritoid is found in iron- and alumina-rich rocks, and is thought to have developed during region-

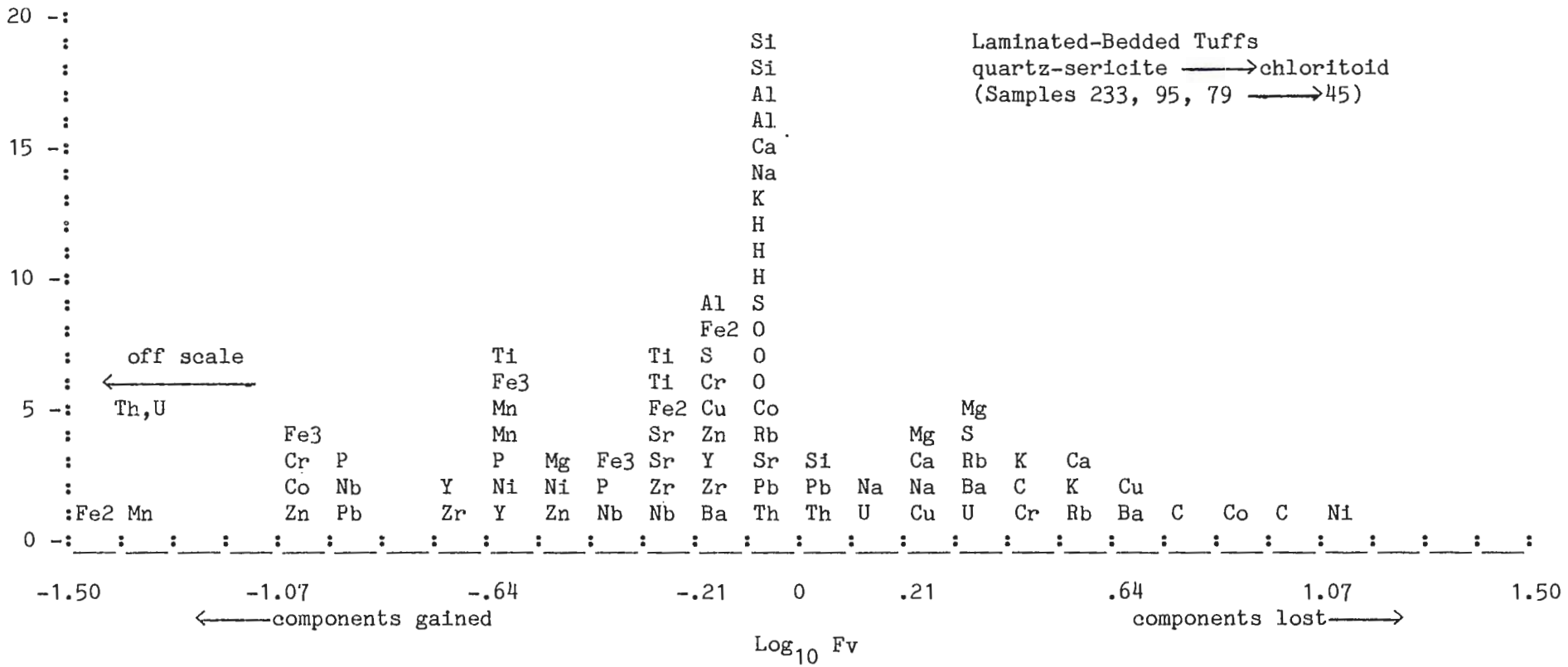

Figure 38. Volume-factor histograms for felsic ash tuffs: quartz-sericite zone to chloritoid zone, example #1.

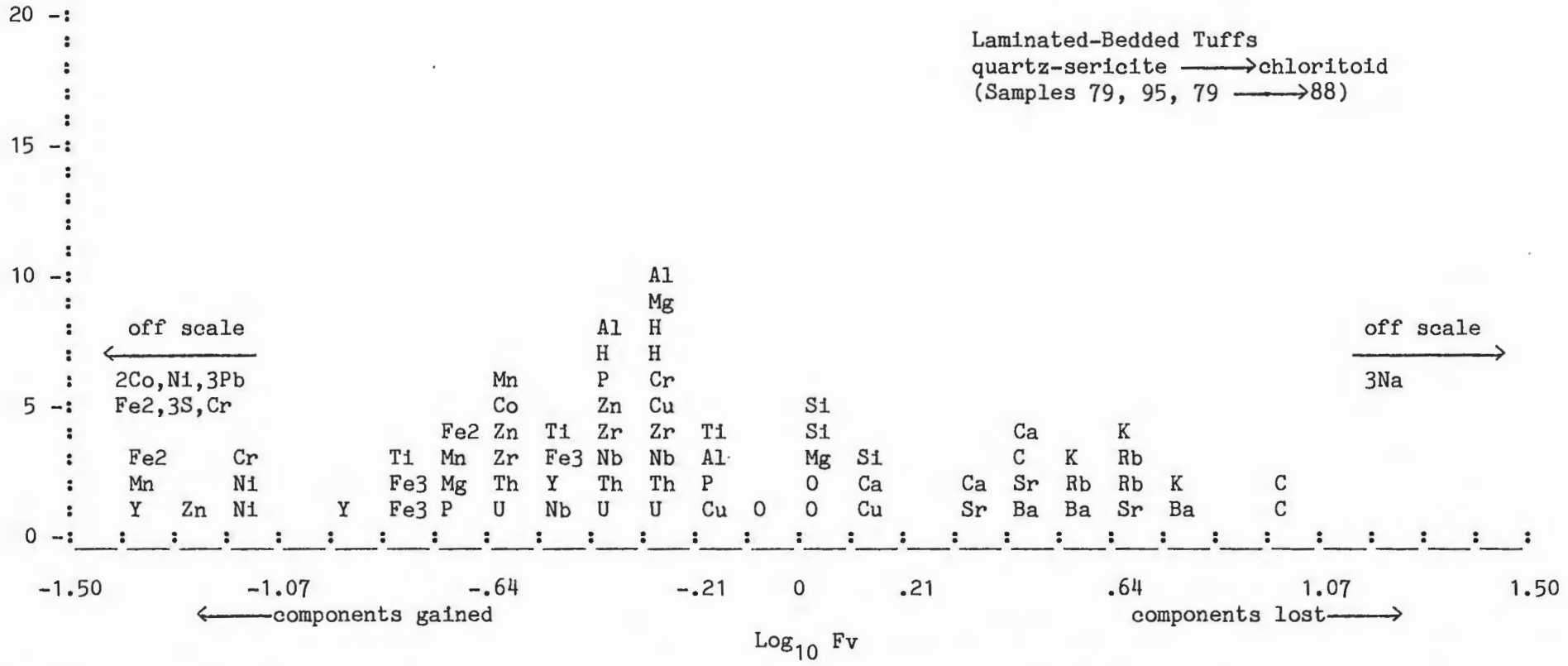

Figure 39. Volume-factor histograms for felsic ash tuffs: quartz-sericite zone to chloritoid zone, example #2.

al metamorphism by reaction of iron chlorite and a hydrous Al-silicate (Zen, 1960; Hoschek, 1969; Hyndman, 1985; LaTour et.al., 1980; Nebel, 1982; Morton and Nebel, 1984; Groves, 1984). The chlorite may have formed at the expense of sericite, at least in part, according to the reaction listed above (reactions 4). The chloritization of sericite can also be written as:

$$\overset{\text{sericite}}{KAl_3Si_3O_{10}(OH)_2} + 1.00Fe^{+2} + \overset{\text{quartz}}{2.80SiO_2} + 0.90H_2O =$$
$$\overset{\text{chlorite}}{0.20Fe_5Al_2Si_3O_{10}(OH)_2} + \overset{\text{pyrophyllite}}{1.30Al_2Si_4O_{10}(OH)_2} + 0.50K_2O + 0.80H^+. \quad (5)$$

This reaction results in the production of iron chlorite and pyrophyllite. Pyrophyllite, so produced, could have represented the hydrous Al- silicate phase necessary for growth of chloritoid during metamorphism. In addition to the formation of a hydrous Al-silicate as a by-product of the chloritization of sericite, Al-silicates may also have developed during hydrothermal alteration, as proposed by Zen (1959), along with dolomite and quartz at the expense of calcite, chlorite, and CO_2 according to the generalized reaction:

$$\text{Calcite} + \text{Mg-Chlorite} + CO_2 =$$
$$\text{Dolomite} + \text{Kaolinite} + \text{Quartz} + H_2O \quad (6)$$

Calcite and Mg-chlorite are present in the quartz-sericite alteration assemblage, whereas ankerite and Fe-chlorite are present in the chloritoid zone. Such a reaction accompanied by addition of iron to the

the rocks may have converted rocks of the quartz-sericite zone to the pre-metamorphic equivalent of the chloritoid zone.

Hemley and Jones (1964) suggested that Al-silicates may form during hydrothermal alteration by the addition of H^+, and removal of K^+ from sericite by the following reactions:

$$\text{(7)}\quad \underset{\text{sericite}}{KAl_3Si_3O_{10}(OH)_2} + H^+ + 1.5H_2O = \underset{\text{kaolinite}}{1.5Al_2Si_2O_5(OH)_4} + K^+$$

$$\text{(8)}\quad \underset{\text{sericite}}{KAl_3Si_3O_{10}(OH)_2} + H^+ + \underset{\text{quartz}}{3SiO_2} = \underset{\text{pyrophyllite}}{1.5Al_2Si_4O_{10}(OH)_2} + K^+$$

However produced, a hydrous Al-silicate is a necessary component in the formation of chloritoid. Chloritoid-forming reactions, as suggested by Frey (1978), Hoschek (1969), and Zen (1960), are of the general form:

(9) Chlorite + hydrous Al-silicate = Chloritoid + Quartz + H_2O.

Hyndman (1985) suggested that chloritoid could also form from chlorite and paragonite by the generalized reaction:

(10) Chlorite + Quartz + Paragonite = Albite + Chloritoid.

Although albite was not observed in thin section in association with chloritoid, fine-grained, untwinned albite which is petrographically indistinguishable from fine-grained quartz may be present. Paragonite was identified by microprobe analyses (Appendix III) of chloritoid-bearing rocks suggesting such a reaction may have occurred. According

to Reed (1984), paragonite may develop by the hydrolysis of albite according to the reaction:

(11) Albite + H^+ = Paragonite + Quartz + Na^+.

Albite remaining in the rocks after sericitic alteration as an excess reactant phase may have formed paragonite by such a reaction.

If chloritoid did develop by reaction of chlorite and a hydrous Al-silicate (reaction 9), chlorite and hydrous Al-silicate (or its metamorphic equivalent) should not coexist in chloritoid-bearing rocks. Petrographic study indicates that this is the case. Chlorite is commonly found associated with chloritoid in this zone, but never with an Al-silicate. This suggests that Al-silicate was the limiting reactant phase in the formation of chloritoid. Similarly, if chloritoid developed by reaction of chlorite and paragonite (reaction 10), chlorite, paragonite, and quartz should not coexist in chloritoid-bearing rocks. This was generally found to be the situation in that chlorite was found in only trace amounts in the sample identified as being quartz and paragonite-rich.

The iron chlorite zone and the pre-metamorphic equivalent of the chloritoid zone probably developed contemporaneously by similar hydrothermal processes. In both assemblages iron chlorite formed at the expense of sericite, but a hydrous Al-silicate apparently developed only in rocks which were later converted to the chloritoid assemblage by metamorphism. Mass balance comparisons were made between ash tuffs of the chloritoid and the iron chlorite assemblages in an attempt to

illustrate chemical differences in the rocks. Figs. 40 and 41 are typical histograms illustrate that chemical trends are generally erratic. Volume factor "peaks" on the histograms are relatively broad and diffuse. Al tends to be the most immobile component, although in some cases even it does not cluster tightly within the center of the "peak".

The lack of chloritoid development in the iron chlorite alteration zone was apparently the result of insufficient hydrous Al-silicate or paragonite present in the rocks prior to metamorphism. If this were the case the rocks should be devoid of hydrous Al-silicates (or their metamorphic equivalents) and paragonite. In fact, no Al-silicates were identified petrographically, and no paragonite was identified in the sample from the iron chlorite zone studied by microprobe, indicating this was probable the case. Additional probe analyses would further support or disprove this hypothesis.

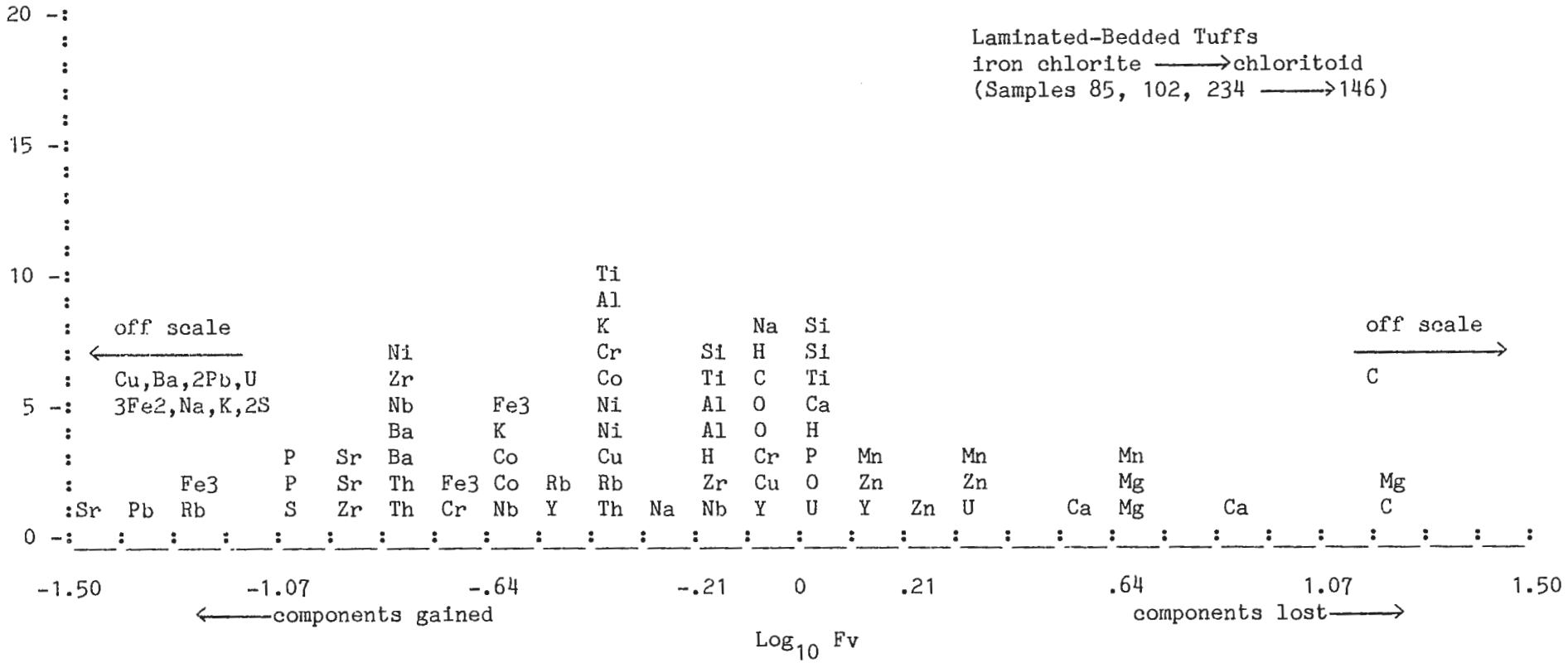

Figure 40. Volume-factor histogram for felsic ash tuffs: iron chlorite zone to chloritoid zone, example #1.

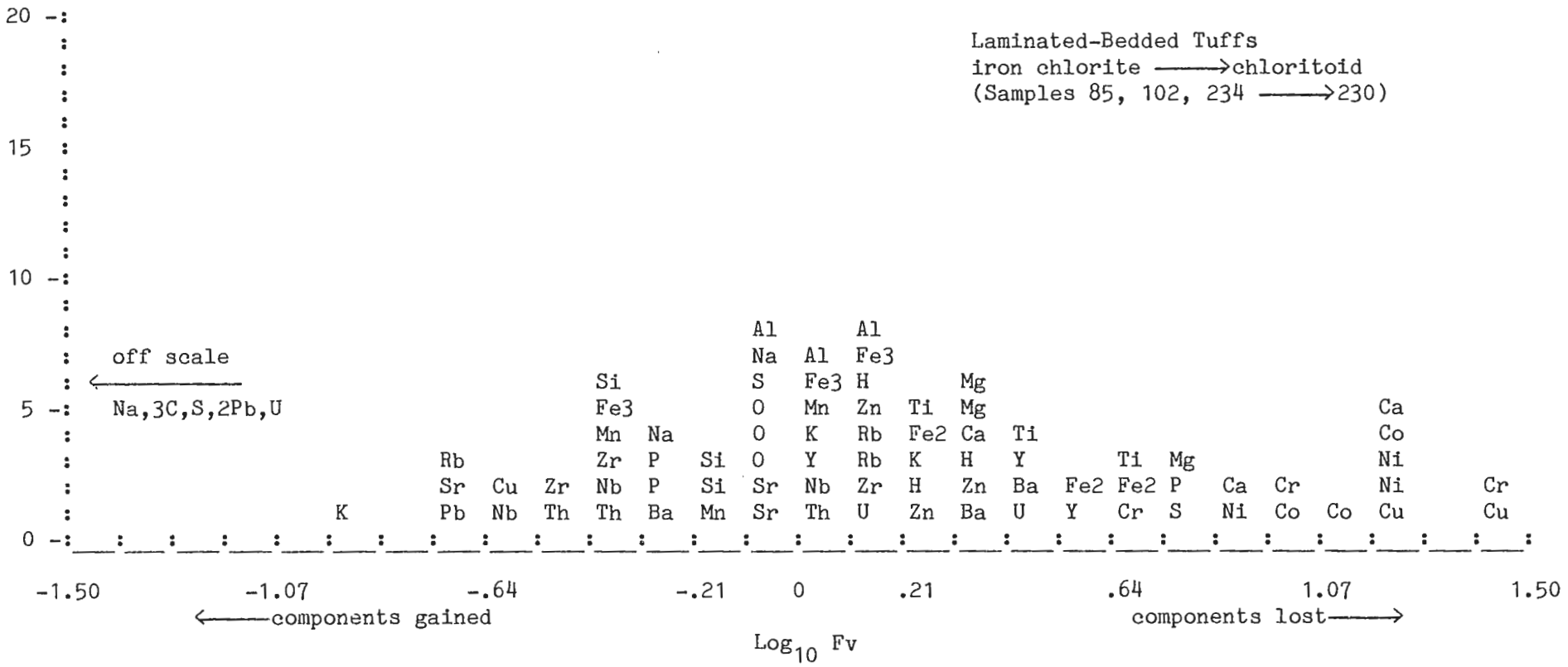

Figure 41. Volume-factor histogram for felsic ash tuffs: iron chlorite zone to chloritoid zone, example #2.

V. ALTERATION MODEL

The zones of hydrothermally altered rocks at the Headway-Coulee prospect are relatively widespread and vary from subconcordant to stratigraphically conformable in distribution. The zones are indicated by anomalous modal abundances of quartz, sericite, iron chlorite, iron carbonate, kyanite, and chloritoid. As such, the alteration differs somewhat from that described at most Archean massive sulfide-type occurrences (Franklin et al., 1981) in that a well-defined, sericite-Mg-chlorite, pipe-like alteration zone is not present; chloritoid, iron-rich chlorite, and carbonate are also rarely described in other deposits. Hydrothermal alteration at most massive sulfide-type occurrences is generally attributed to the movement of hot hydrothermal fluids through the rocks in a geothermal system which developed during the waning stages of volcanism (Franklin et al.,1981).

The essential features of such geothermal systems include a fluid phase, permeable rocks, and a heat source at depth capable of establishing a steep vertical temperature gradient (Reed, 1984; Franklin et al., 1981). This temperature gradient is thought to drive convective circulation of the fluids through the rocks. The association of subaqueous and hydrothermally altered volcanic rocks, coupled with isotopic studies (Hutchinson, 1982) indicate that the hydrothermal fluids are dominantly of seawater origin. They may be either circulated surface water or connate water trapped in the rocks during deposition (Reed, 1984). The heat source is thought to be a cooling, subvolcanic igneous body (Franklin and Thorpe, 1982; Morton

and Nebel, 1984; Mottl, 1983).

Based on the above characteristics of ore-forming geothermal systems, and on the mineralogy and chemistry of the altered rocks in the study area, the following reconstruction of a geothermal system is suggested to explain hydrothermal alteration at the Headway-Coulee prospect. The model is schematically illustrated in Figs. 42 and 43.

A magmatic heat source at depth initiated circulation of an essentially unlimited supply of seawater through porous felsic pyroclastic rocks, and through vesicular and brecciated mafic lava flows (Fig. 42). Resulting chemical exchange between the circulating seawater and the rocks occurred at high seawater/rock ratios. Seyfried and Mottl (1982) have experimentally shown that during high seawater/basalt ratios at 300°C, Mg is lost from seawater in the form of hydrous alteration minerals; resulting solutions have increased H^+ contents and are consequently acidic. However, in the experiments, Mg was never completely removed from solution because there 'is not enough basalt to "titrate" H^+ created by Mg-metasomatism' (Seyfried, 1984). To balance Mg lost from solution, Ca and Na were leached from the basalt and added to the solution, along with lesser amounts of K.

In the proposed model, this downward circulation occurred dominantly outside the study area (perhaps up to several km) and left the rocks Mg-rich. However, the least-altered rocks, within the study area, with their Mg-rich chlorite-quartz-bearing assemblages may reflect early seawater-dominated alteration (Mottl, 1983).

By such a process of reaction of seawater with basalts and felsic

volcanic rocks in the upper portions of the volcanic succession, an acidic, Ca, Na, and K-rich fluid evolved. The acidic fluid, upon continued heating, buoyantly ascended and migrated through the rocks along fractures and porous lithologic units within the study area (Fig. 42). Interaction between the hot fluid and the rocks resulted in widespread sericitization by addition of K to the rocks, and breakdown of plagioclase through base leaching reactions. Mass balance calculations (Chapter IV) indicate that Na $\pm$ Ca was lost from the rocks within the study area during sericitization. This implies that the hydrothermal solution when in the study area was depleted, rather than enriched in Na $\pm$ Ca as discussed above. The Na $\pm$ Ca may have been lost from the evolved fluid in the form of albite $\pm$ epidote prior to sericitization of the rocks (Fig. 42).

Precipitation of alteration minerals decreased the primary permeability of the rocks and eventually formed an impermeable layer near the water-rock interface (Hodgson and Lydon, 1977; Morton and Nebel, 1984).

Circulation of hydrothermal fluids through basalts in the deeper portions of the volcanic succession occurred at relatively low flux rates as much of the original fluid was tapped-off by circulation in the upper portions of the hydrothermal system (Fig. 43). Fluid-rock chemical exchange therefore evolved from seawater-dominated conditions to rock-dominated conditions in these deeper zones, and the fluid was no longer seawater, but was instead an evolved fluid of seawater origin. Experimental work (Seyfried and Bischoff, 1981; Mottl, 1983; Seyfried 1984) has shown that seawater-basalt interaction under rock-

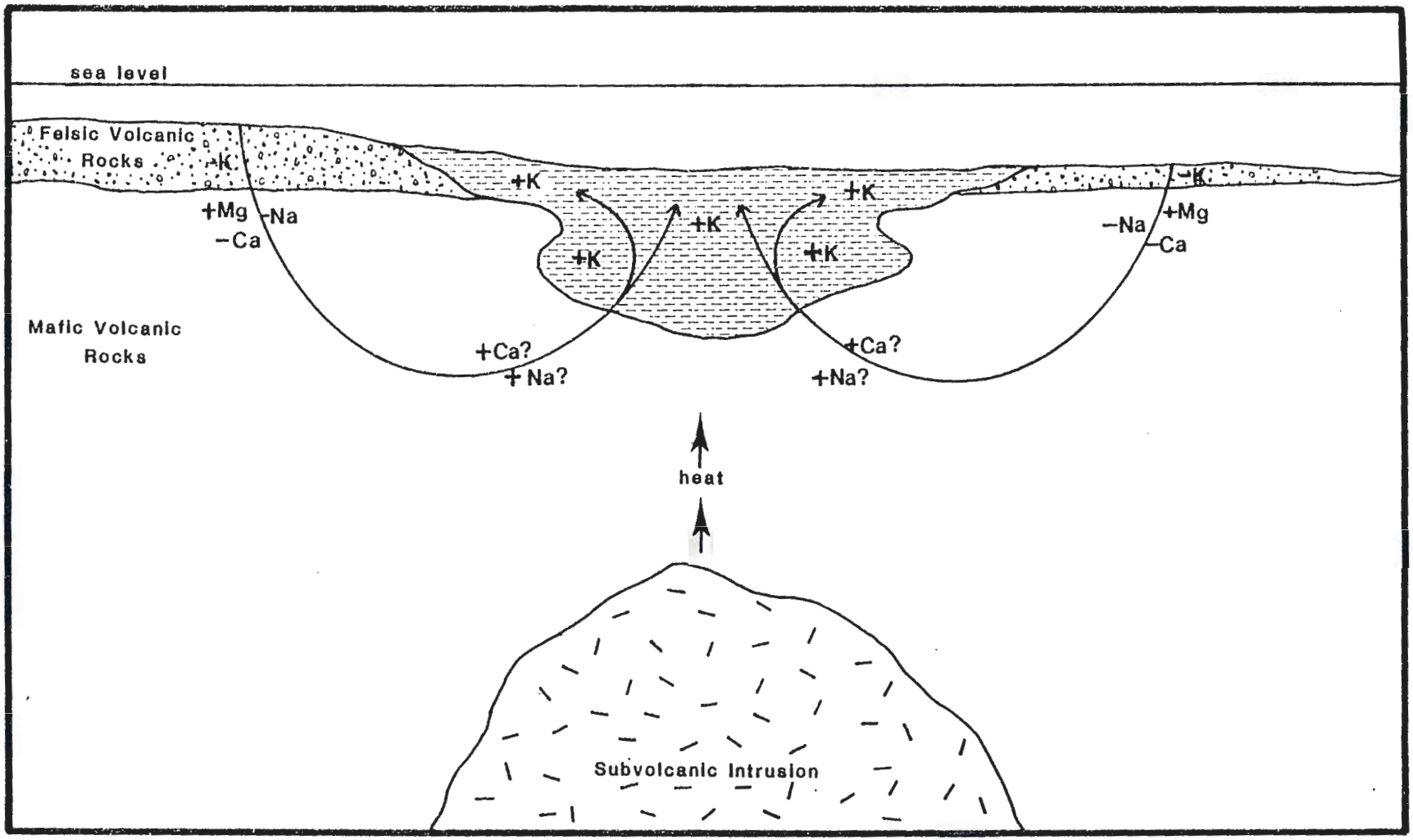

Figure 42. Diagrammatic section through proposed geothermal system during formation of sericitic alteration showing chemical changes in the rocks associated with hydrothermal alteration at the Headway-Coulee prospect (after Morton and Nebel, 1984; Roberts and Reardon, 1978; Mottl, 1983). See text for explanation.

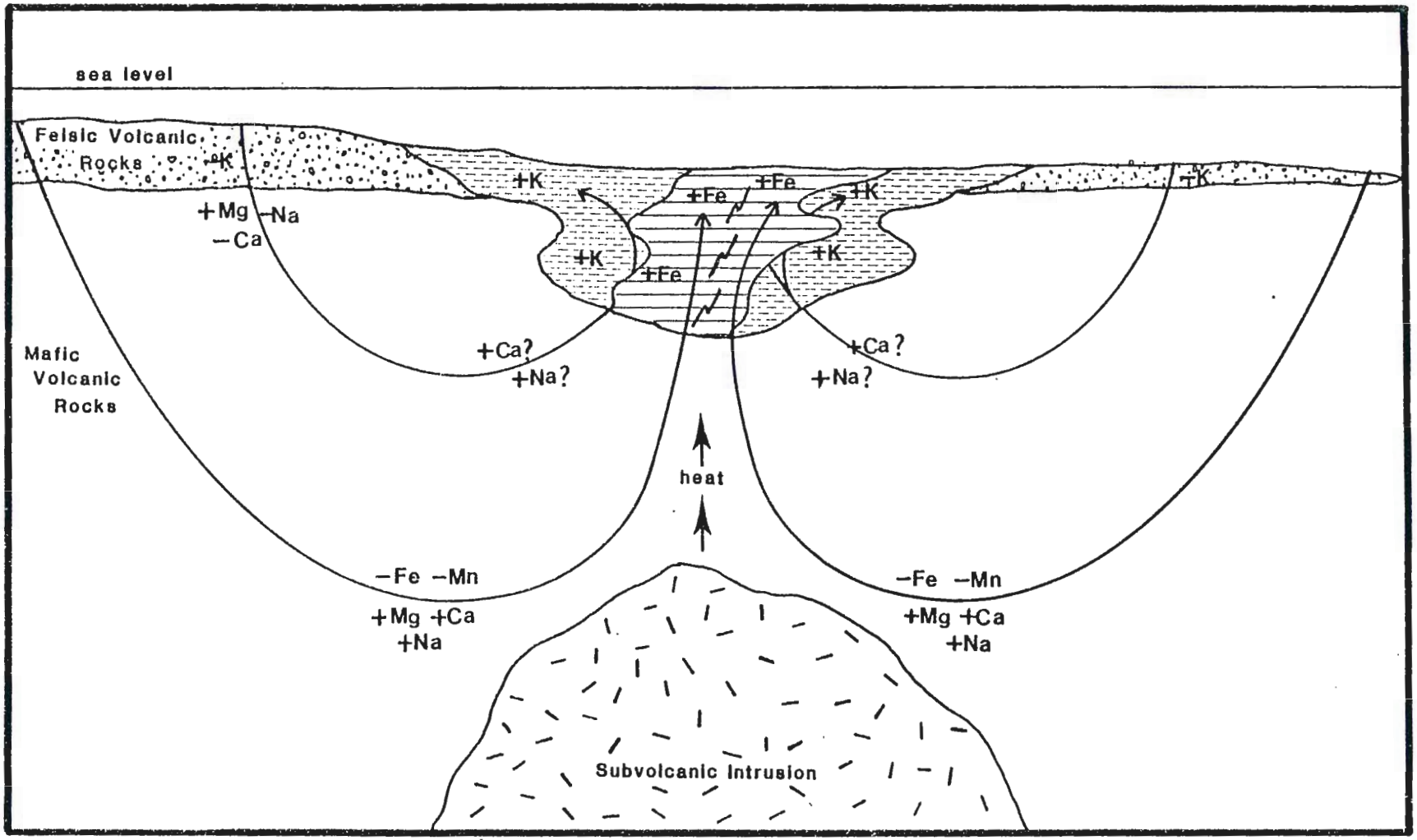

Figure 43. Diagrammatic setction through proposed geothermal system during formation of iron chlorite ± hydrous Al-silicate alteration minerals at the Headway-Coulee prospect (after Morton and Nebel, 1984; Roberts and Reardon, 1978; Mottl, 1983). See text for explanation.

dominated conditions (at 300°C) results in complete removal of Mg, and partial removal of Na and Ca from solution in exchange for Fe, and Mn. The resulting fluids are neutral to slightly alkaline.

By such a process the acidic, Ca and Na-rich fluids evolved into Fe and Mn-rich fluids in deep levels of the hydrothermal system (Fig. 43).

With continued heating the deep-seated fluids were maintained at increasing pressures until tectonically or volcanically induced fractures or faults breached the sericitic cap rock and released the fluids (Fig. 43). The Fe and Mn-rich fluids chemically interacted with the sericitic rocks and, through base-fixing reactions, Fe and Mn were added to, and K removed from the rocks. This resulted in development of iron chlorite ± hydrous aluminosilicate alteration minerals. Addition of iron to the rocks converted pre-existing calcite to ankerite. The decreased pressures and temperatures also caused precipitation of base metal sulfides within the altered rocks during ascent of the fluid, and possibly upon the sea floor.

Two aspects of the alteration at the Headway-Coulee prospect are not explained by this reconstruction. One is the widespread occurrence of carbonate in the altered rocks. As noted above carbonate alteration is relatively rare in massive-sulfide type occurrences. Exceptions include deposits of the Sturgeon Lake and Wawa, Ontario areas. Groves (1984) attributed the presence of dolomite and ferruginous dolomite at the Mattabi Mine in the Sturgeon Lake area to primary diagenetic precipitation. Morton and Nebel (1984) suggest that carbonate in altered footwall rocks at the Helen Mine in the Wawa area may be of a similar

origin. As well, they suggest carbonate may have precipitated from CO_2-rich solutions during hydrothermal alteration. They propose that CO_2 may have been released through decarbonatization reactions during prograde metamorphism at deep levels in the volcanic pile contemporaneously with hydrothermal alteration in the upper portions of the volcanic pile.

The above hypotheses may also have been responsible for carbonate precipitation in rocks of the Headway-Coulee area. However, the present information on the formation of the carbonate is inconclusive.

A second unexplained aspect of alteration at the Headway-Coulee prospect is the localized occurrence of kyanite and quartz-rich rocks northeast of MacDonald Lake. Mass balance calculations indicate that Al was a relatively immobile component during hydrothermal alteration in the study area. However, Al may have been locally mobilized by highly acidic fluids as suggested by Roberts and Reardon (1977). The Al and Si-rich kyanitic rocks may represent an area where highly acidic fluids were vented onto the sea floor. Boiling of the solutions, and mixing with more neutral seawater may have caused massive precipitation of Al and Si in the form of kaolinite or pyrophyllite, and quartz, respectively. It is notable that the kyanite-rich rocks occur near the contact between hydrothermally altered and unaltered rocks indicating they formed at or near the seawater-rock interface. However, the kyanite alteration remains problematic in that it appears to be largely restricted to a felsic lava flow, a deposit which would be expected to

be relatively impermeable to hydrothermal fluids. Further detailed mapping and geochemical study needs to be completed to resolve this problem.

VI. SUMMARY AND CONCLUSIONS

VI.1 Stratigraphy and Volcanology

Detailed geologic mapping along with petrographic studies have allowed the rocks in the Headway-Coulee area to be subdivided into several distinct lithologic types (Plate 1). Preserved primary textures and structures have enabled the environment of deposition of the rocks to be determined.

Mafic volcanic rocks underlie approximately 70% of the study area and form a 1-2 km thick stratigraphic succession. This succession is locally interrupted by a relatively thin, lens-shaped succession (30-200 m x 5 km) of felsic volcanic rocks which interfingers with, and/or is terminated by the mafic lava flows.

The lower portion of the stratigraphic succession formed as mafic lava constructed a relatively thick (>1 km) sequence of pillowed and amygdaloidal to massive and locally brecciated lava flows. The presence of pillows, quench textures, and hyaloclastite indicate the lavas were deposited subaqueously. As deposition of mafic lavas continued, the succession gradually shallowed upward and volcanism changed from mafic and dominantly magmatic, to felsic and dominantly hydrovolcanic in nature.

Felsic volcanic rocks within the study area can be divided into two volcanic cycles on the basis of stratigraphic relationships (Plate 1, Fig. 24). Deposition of the first cycle began in the southwestern portion of the area with the emplacement of a relatively thick (150-200 m) tuff unit, which has an inferred lateral extent of about 2 km (Plate

1). Thin (<10 m), local tuff deposits formed northeast of MacDonald Lake where they are interlayered with mafic lava flows (Plate 1, Fig. 24). The tuffs are dominantly laminated to thinly-bedded, but more rarely may be thickly-bedded, nonbedded, or thinly-banded in appearance. The rocks are extremely fine-grained, and contain only a small percentage of fragments. Lapilli and block-sized lithic fragments typically constitute <5% of the rock. In thin section quartz phenocrysts comprise up to 30%, and altered ash-sized lithic fragments, 0-15% of the rock.

A relatively massive, small (50 m x 200 m) quartz porphyritic lava flow caps the tuffaceous succession northeast of MacDonald Lake, and marks the end of the first cycle of felsic volcanism (Plate 1 and Fig. 24).

A second felsic volcanic cycle deposited ash in the north-central and northeastern portions of the area where it overlies mafic lava flows (Plate 1 and Fig. 24) and a thin, localized iron formation. The ash deposits are similar to those of Cycle I. Two felsic lava flows constitute the southwestern portion of the Cycle II rocks and are underlain by a polymictic diamictite deposit of probable debris flow origin (Plate 1 and Fig. 24). The lava flows vary from massive to brecciated, flow-banded, and spherulitic, and are quartz-feldspar porphyritic. Though poorly exposed they are believed to be of limited extent.

The diamictite deposit pinches out within the volcanic succession northeast of MacDonald Lake (Plate 1) and was deposited after deposition of the Cycle I felsic volcanic rocks. Abundant granitic and

iron formation clasts within the deposit suggest it was transported from outside the study area during a pause between Cycle I and II volcanism. Its source was probably to the southwest of the map area, where extensive deposits of similarly described rocks occur (Amuken, 1980).

The stratigraphic relationships, extreme fine-grain size, laterally limited extent, and the laminated to thickly-bedded nature of the felsic pyroclastic deposits suggest that they formed on the submerged flanks of two separate though adjacent tuff cones (Fig. 23) as a result of explosive hydrovolcanic eruptions. Felsic lava flows were formed during relatively passive eruptions which ended each cycle of felsic volcanism. It is envisioned that the lavas were erupted under low water/magma conditions as access of water to the erupting magma was restricted, and/or under relatively high water/magma conditions within a water flooded vent or on the submerged flanks of the cone.

Intrusion of several quartz-feldspar porphyritic sills and dikes and nonporphyritic felsic dikes accompanied Cycle II volcanism. These sills and dikes vary greatly in size and are locally characterized by cross-cutting contacts and xenoliths.

As felsic volcanism and intrusive activity eventually ceased, an extensive hydrothermal system developed, probably driven by heat from a subvolcanic intrusion, which caused widespread alteration of the rocks. Eventually hydrothermal activity ceased and there was a return to subaqueous deposition of mafic lava flows over the felsic volcanic rocks. Deposition of mafic volcanic rocks was accompanied by intrusion of several gabbroic sills.

VI.2 Alteration and Metamorphism

The rocks exposed at the Headway-Coulee Prospect have been variably altered by hydrothermal solutions and subsequently metamorphosed to greenschist facies. Detailed field mapping, supplemented by petrographic study, has allowed subdivision of the rocks for descriptive purposes into four main alteration zones (Plate 2). The zones, characterized by distinctive mineral assemblages, are:

(1). Least-altered zone (actinolite-chlorite-epidote-ablite ± quartz-calcite). Only gabbroic sills and mafic lava flows in the northeastern and extreme northern portions of the map area, and immediately northeast of MacDonald Lake can be classified as least-altered (Plate 2).

(2). Quartz-sericite zone (quartz-sericite ± Mg-chlorite-calcite-Ti-bearing-opaques). Quartz-sericite assemblage rocks occur in mafic lava flows in the south-central portion of the map area, and within felsic volcanic rocks along the Onaman River in the north-central part of the map area (Plate 2).

(3). Iron chlorite zone (quartz-iron chlorite ± sericite-ankerite-Ti-bearing-opaques-epidote). Iron chlorite alteration occurs dominantly as a relatively long (2 km) but narrow (25-100 m) zone which appears to cross-cut and replace quartz-sericite alteration in felsic tuff deposits along the Onaman River (Plate 2).

(4). Chloritoid zone (quartz-chloritoid ± iron chlorite-sericite-ankerite-paragonite-Ti-bearing opaques). Chloritoid-bearing rocks dominate the southwestern portion of the study area and occur as a subconcordant zone in mafic and felsic rocks and have replaced quartz-

sericite-bearing rocks. Quartz-kyanite-rich rocks are locally found northeast of MacDonald Lake where they are associated with, but separate from chloritoid-rich rocks. These have been included as a subdivision of the chloritoid zone (Plate 2).

In general, hydrothermal alteration has greatly changed the primary geochemistry of the rocks. Tables 1 and 2 summarize the major and trace element geochemistry of the individual lithologies, and illustrate that most elements exhibit relatively wide variation.

To identify chemical trends in the progressive alteration of the volcanic rocks, mass balance comparisons were made utilizing chemical analyses and specific gravities. Table 3 is a summary of the chemical trends identified by mass balance comparisons between samples from the different alteration zones. Estimated volume changes range from 0 to approximately -50%. Al is the only consistently immobile element; all other elements exhibit variations between individual comparisons.

Based on the general characteristics of an ore-forming geothermal system, and on the mineralogy and chemistry of the altered rocks in the study area, the following model is suggested to explain hydrothermal alteration at the Headway-Coulee prospect. A heat source at depth initiated convective circulation of seawater through porous volcanic rocks (Fig. 42). Interaction of the seawater and the rocks in the upper portions of the volcanic succession occurred at high seawater/rock ratios and resulted in evolution of an acidic, Ca, Na, and K-rich fluid. This solution, upon continued heating, buoyantly ascended, and migrated laterally through the rocks. Through base-leaching reactions the solution caused widespread sericitization of both felsic and mafic

rocks to produce the quartz-sericite zone (Fig. 42).

Fluids circulating at deeper levels in the volcanic succession reacted with mafic rocks at lower fluid/rock ratios and evolved into Fe and Mn-rich solutions relative to the fluids circulating at shallower depths (Fig. 43). These evolved fluids were maintained in a pressurized reservoir at depth until synvolcanic or syntectonic faults breached the sericitic cap rock. The fluids ascended and through base-fixing reactions, removed K and Na from, and added Fe and Mn to the rocks, resulting in development of iron chlorite $\pm$ hydrous Al-silicate (e.g. pyrophyllite, kaolinite) alteration minerals (Fig. 43). Base-metal sulfides were deposited within the rocks during ascent of the fluid, and possibly upon the sea floor.

Rocks of the study area later underwent greenschist facies metamorphism as indicated by chlorite-epidote-actinolite-albite mineral assemblages in mafic rocks which were apparently unaffected by intense hydrothermal alteration, and by coexisting sericite and chlorite in intensely altered rocks. Coexisting chlorite and hydrous Al-silicate minerals in hydrothermally altered rocks became unstable during regional metamorphism and reacted to produce chloritoid-bearing assemblages.

Metamorphism was accompanied by deformation, including shearing of the rocks, flattening of pillows in mafic lava flows and fragments in felsic pyroclastic rocks. Foliation of micaceous minerals, development of local minor folds, and recrystallization of quartz in the rocks also reflect deformation during metamorphism.

REFERENCES

Allen, C.C., 1980a. Volcano-ice interactions on Earth and Mars. Advances in Planetary Geology (NASA TM-81979), 161-264.

_____, Jercinovic, J., and Allen, J.S.B., 1982. Subglacial volcanism in north-central British Columbia and Iceland. J. Geol., 90: 699-715.

Amuken, S.E., 1980. Geology of the Conglomerate Lake Area, District of Thunder Bay; Ontario Geological Survey Report 197, 101 p. Accompanied by Map 2429, scale 1:31680 (1 inch to 1/2 mile).

Appleyard, E.C., 1980. Mass balance computations in metasomatism: Metagabbro/nepheline syenite pegmatite interaction in northern Norway. Contrib. Mineral. Petrol. 73, 131-144 (1980).

Bates, R.L., and Jackson, J.A., editors, 1980. Glossary of Geology, Second Edition. American Geological Institute, Falls Church, Virginia.

Berry, L.G., ed., 1974. Selected Powder Diffraction Data for Minerals. Joint Committee on Powder Diffraction Standards.

Bryan, W.B., 1972. Morphology of quench crystals in submarine basalts. J. Geophys. Res., 77: 5812-5819.

Campbell, I.H., Lesher, C.M., Coad, P., Franklin, J.M., Gorton, M.P., and Thurston, P.C., 1984. Rare-earth element mobility in alteration pipes below massive Cu-Zn sulfide deposits. Chem. Geol. 45: 181-202.

Cann, J.R., 1970. Rb, Sr, Y, Zr, and Nb in some ocean floor basaltic rocks. Earth Planet. Sci. Lett. 10: 7-11.

Carmichael, I.S.E., Turner, F.J., and Verhoogen, J., 1974. Igneous Petrology. McGraw-Hill Book Co., 739 p.

Condie, K.C., 1981. Archean Greenstone Belts. Elsevier Scientific Publishing Co., 434 p.

Davies, J.F., Grant, R.W.E., and White, R.E.S., 1979. Immobile trace elements and Archean volcanic stratigraphy in the Timmins mining area, Ontario. Can. Jour. Earth Sci., 16, 305-311.

Deer, W.A., Howie, R.A. and Zussman, J., 1966. An Introduction to the Rock Forming Minerals. Longman Group Ltd., London. 528 p.

DiLabio, R.N.W., 1982. Drift prospecting near gold occurrences at Onaman River, Ontario, and Oldham, Nova Scotia, In Hodder, R.W., ed., Geology of Canadian Gold Deposits, Proceedings of the CIM Gold Symposium, Sept. 1980, CIM Special Volume 24, 286 p.

Evamy, B.D., 1963. The application of a chemical staining technique to a study of dedolomitization. Sedimentology, 2: 164-170.

Fischer, R.V. and Schminke, H.V., 1984. Pyroclastic Rocks. Springer-Verlag, New York, N.Y., 472 p.

Flaherty, G.F., 1936. Mechanics of Structure at Tashota Goldfields Mine, Tashota, Ontario; Canadian Institute Mining and Metallurgy, Trans., Volume 39, 723-738.

Franklin, J.M., 1983. Personal Communication. Geol. Sur. Can.

_____, and Thorpe, R.I., 1982. Comparative Metallogeny of the Superior, Slave and Churchill Provinces. In Precambrian Sulphide Deposits, edited by R.W. Hutchinson, C.D. Spence, and J.M. Franklin. Geological Association of Canada Special Paper 25..

_____, Sangster, D.M. and Lydon, J.W. 1981. Volcanic-associated massive sulfide deposits, In Skinner, B.J., ed., Economic Geology 75th Anniversary Volume. Economic Publishing Co., 964 p.

Frey, M. 1978. Progressive low-grade metamorphism of a black shale formation, central Swiss Alps, with special reference to pyrophyllite and margarite bearing assemblages. J. Petrol., 19: 95-135.

Gelinas, L. and Brooks, C., 1974. Archean quench-texture tholeiites. Can. Jour. Earth Sci., 11: 324-340.

Gibson, H.L., Watkinson, D.H., and Comba, C.D.A., 1983. Silicification: Hydrothermal alteration in an Archean geothermal system within the Amulet Rhyolite Formation, Noranda, Quebec. Econ. Geol., 78, p. 954-971.

Gledhill, T.L., 1925. Tashota-Onaman Gold Area, District of Thunder Bay; Ontario Dept. Mines, Volume 34, pt. 6, 65-85. Accompanied by Map 35g, scale 1 inch to 2 miles.

Gresens, R.L., 1967. Composition-volume relationships of metasomatism. Chem. Geol., 2: 47-65.

Groves, D.A., 1984. Stratigraphy and alteration of the footwall volcanic rocks beneath the Archean Mattabi massive sulfide deposit, Sturgeon Lake, Ontario. unpubl. M.Sc. thesis, Univer. Minnesota-Duluth, Duluth, MN, 115 p.

_____, Morton, R.L., and Franklin, J.M., in preparation. Physical Volcanology of the footwall rocks beneath the Mattabi massive sulfide deposit.

Heiken, G.H., 1971. Tuff rings: Examples from the Fort Rock-Christmas Lake valley basin, south-central Oregon. Jour. Geophys. Res., 76, no. 23:, 5615-5626.

Helgeson, H.C., Delaney, J.M., Nesbitt, H.W., and Bird, D.K., 1978. Summary and critique of the thermodynamic properties of rock-forming minerals. Am. J. Sci. 278-A, 1-227.

Hemley, J.J. and Jones, W.R., 1964. Chemical aspects of hydrothermal alteration with emphasis on hydrogen metasomatism. Econ. Geol., 59, 538-569.

Hodgson, C.J., and Lydon, J.W., 1977. The geological setting of volcanogenic massive sulfide deposits and active hydrothermal systems: some implications for exploration: Canadian Mining Metallurgy Bull., 70, 95-106.

Hopkins, P.E., 1917. The Kowkash gold area (second report); Ontario Bureau of Mines, Vol. 26, 190-226. Accompanied by Map 26a, scale 1 inch to 2 miles.

Hoschek, G., 1969. The stability of staurolite and chloritoid and their significance in metamorphism of pelitic rocks. Contr. Mineral. Petrol., 22, 208-232.

Hutchinson, R.W., 1982. Syn-Depositional Hydrothermal Processes and Precambrian Sulphide Deposits. In Precambrian Sulphide Deposits, edited by R.W. Hutchinson, C.D. Spence, and J.M. Franklin. Geological Association of Canada Special Paper 25.

Hyndman, D.W., 1985. Petrology of Igneous and Metamorphic Rocks. McGraw-Hill Book Co., 533 pp.

Irvine, T.N. and Baragar, W.R.A., 1971. A guide to the chemical classification of the common volcanic rocks. Can. Jour. Earth Sci., 8: 523-548.

LaTour, T.E., Kerrich, R., Hodder, R.W. and Barnett, R.L., 1980. Chloritoid stability in very iron-rich altered pillow lavas. Contrib. Mineral. Petrol., 74: 165-173.

MacGeehan, P.J., 1977. The geochemistry of altered volcanic rocks at Matagami, Quebec: a geothermal model for massive sulphide genesis. Can. Jour. Earth Sci., 15, 551-570.

Morton, R.L. and Nebel, M., 1984. Hydrothermal alteration of felsic volcanic rocks at the Helen siderite deposit, Wawa, Ontario. Econ. Geol., 79, 1319-1333.

Mottl, M.J., 1983. Metabasalts, axial hot springs, and the structure of hydrothermal systems at mid-ocean ridges. Geol. Soc. Amer. Bull., 94, 161-180.

Nebel, M., 1982. Stratigraphy, depositional environment and alteration of Archean felsic volcanics, Wawa, Ontario. Unpubl. M.Sc. thesis, Univ. Minnesota-Duluth, Duluth MN, 114 pp.

Parry, S. and Hutchinson, R.W., 1981. Origin of a complex alteration assemblage, Four Corners Cu-Zn prospect, Quebec, Canada. Econ. Geol., 76, 1186-1201.

Pettijohn, F.J., 1975. Sedimentary Rocks; Third Edition, Harper and Row Publishers, Inc., New York. 628p.

Pierce, T.M., 1974. Quench plagioclase from some Archean basalts. Can. Jour. Earth Sci., 11: 715-719.

Poulsen, K.H., 1983. Personal Communication. Geol. Sur. Can.

_____, 1985. Personal Communication. Geol. Sur. Can.

Pye, E.G., Harris, F.R., Fenwick, K. G. and Bailie, J., 1966. Tashota-Geraldton Sheet, Thunder Bay and Cochrane Districts; Ontario Dept. of Mines, Map 2102, Geological Series, Scale 1 inch to 4 miles. Geological compilation 1964-1965.

Reed, M.H., 1983. Seawater-basalt reaction and the origin of greenstones and related ore deposits. Econ. Geol., 78, 466-485.

Reed, M.H., 1984. Geology, wall-rock alteration, and massive sulfide mineralization in a portion of the West Shasta district, California. Econ. Geol., 79, pp 1299-1318.

Riverin, G., and Hodgson, C.J., 1980. Wall-rock alteration at the Millenbach Cu-Zn mine, Noranda, Quebec. Econ. Geol., 75, 424-444.

Roberts, R.G. and Reardon, E.J., 1978. Alteration and ore-forming processes at Mattagami Lake mine, Quebec: Can. Jour. Earth Sci., 15: 1-21.

Robie, R.A., Bethke, P.M., and Berdsley, K.M., 1967. Selected X-ray crystallographic data, molar volumes and densities of minerals and related substances. U.S.G.S. Bull. 1248, 87p.

Seyfried, W.E., Jr., 1984. Experimental basalt-solution interaction: alteration, heavy metal mobility and implications for the chemistry of ridge crest hydrothermal fluid. In Volcanic Rocks, Hydrothermal Alteration, and Associated Massive Sulfide and Gold Deposits. Edited by R.L. Morton and D.A. Groves. Short course notes, Univ. of Minnesota-Duluth, 74-91.

_____, and Bischoff, J.L. (1981). Experimental seawater-basalt interaction at 300°C and 500 bars: chemical exchange, secondary mineral formation and implications for the transport of heavy metals. Geochim. Cosmochim. Acta, 45, 135-147.

_____, and Mottl, M.J., 1982. Hydrothermal alteration of basalt by seawater under seawater dominated conditions. Geochim. Cosmochim. Acta, 46, 985-1002.

Sheridan, M.F., 1979. Emplacement of pyroclastic flows: a review. In Ash-Flow Tuffs. Edited by C.E. Chapin and W.E. Elston. Geological Society of America, Special Paper 180, 125-134.

_____ , and Wohletz, K.H., 1981. Hydrovolcanic explosions: the systematics of water-pyroclast equilibration. Science, 212: 1387-1389.

_____, and Wohletz, K.H., 1983. Hydrovolcanism: basic considerations and review. J. Volcanol. Geotherm. Res. 17: 1-30.

Simmons, B.D., 1973. Geology of the Millenbach massive sulphide deposit, Noranda, Quebec: Canadian Mining Metallurgy Bull., 166, no. 739, 67-78.

Snyder, G.L. and Fraser, G.D., 1963. Pillowed lavas, I: intrusive layered lava pods and pillowed lavas, Unalaska Island, Alaska. A review of selected recent literature. In Shorter Contributions to General Geology, U.S.G.S. Professional Paper 454-B, 23 p.

Thorsteinson, D., and Cox, N., 1983. Personal Communication, Beardmore, Ontario.

Thurston, P.C., 1980. Geology of the Northern Onaman Lake Area, District of Thunder Bay; Ontario Geological Survey Report 208, 81p. Accompanied by Map 2411, scale 1:31680, and Chart A.

Turner, F.S., 1981. Metamorphic Petrology. Second Edition. McGraw-Hill Book Co., 524 p.

Williams, H. and McBirney, A.R., 1979. Volcanology; Freeman, Cooper and Co., San Francisco. 397 p.

Winkler, H.G.F., 1976. Petrogenesis of Metamorphic Rocks. Fourth Edition, Springer-Verlag New York Inc., 334 p.

Wohletz, K.H., 1983. Mechanisms of hydrovolcanic pyroclast formation: grain size, scanning electron microscopy and experimental studies. J. Volcanol. Geotherm. Res. 17, 31-64.

_____, and McQueen, R.G., 1981. Experimental hydromagmatic volcanism. Eos, 62, no. 45, p. 1085.

_____, and McQueen, R.G., 1984. Experimental studies of hydromagmatic volcanism, In, Studies in Geothermal Series, Explosive Volcanism Inception, Evolution, and Hazards. Studies in Geophysics, National Research Council. 4th ed., National Academy Press, Washington D.C.

_____, and Sheridan, M.F., 1983. Hydrovolcanic explosions II. Evolution of basaltic tuff rings and tuff cones. Am. J. Sci., 283: 385-413.

Womer, M.B., Greeley, R., and King, K.S., 1980. The geology of Split Butte--a maar of south-central Snake River Plain, Idaho. Bull. Volcanol., 43: 453-471.

Yeats, R. S., Forbes, W.C., Scheidegger, K.F., Ross Heart, G., Van Andel, TI.H., 1973. Core from Cretaceous basalts, central equitorial Pacific, Leg 16, deep-sea drilling project. Geol. Soc. Amer. Bull, 84, p. 871-882.

Zen, E-an, 1959. Clay mineral-carbonate relations in sedimentary rocks. Am. J. Sci., 257: 29-43.

_____, 1960. Metamorphism of lower Paleozoic rocks in the vicinity of the Taconic Range in west-central Vermont. Amer. Miner., 45: 129-175.

Zoltai, S.C., 1965. Glacial features of the Quetico-Nipigon Area, Ontario; Can. Jour. Earth Sci., 2, 247-269.

Appendix I. Textures and Modes of Rock Units

The following tables are a summary of modal compositions and textures of lithologic units as observed in thin section.

Minerals	Abbreviations
Quartz	QTZ
Sericite	SER
Chlorite	CHL
Carbonate	CARB
Chloritoid	CHLT
Epidote	EPI
Actinolite	ACT
Opaques	OPA
Stilpnomelane	STILP
Zircon	ZIR
Kyanite	KYN
Biotite	BIO
Andalusite	AND
Plagioclase (albite)	PL
K-feldspar	KSP
Paragonite	PAR
Microcline	MIC

Textures	
Amygdaloidal	A
Quench	Q
Ophitic	O
Micrographic	M
Glomeroporphyritic	G
Porphyroblastic	P
Fragmental	F
Spherulitic	S
Poikiloblastic	PK
Vein	V

All sericite, chlorite, and/or kyanite-bearing rocks are foliated.

Modal values are listed in percent (%).

Table 5. Modal Composition of Mafic Volcanic Rocks

T.S.#	TEXTURES	QTZ	SER	CHL	CARB	CHLT	EPI	ACT	OPA	OTHER
3		45	15	20	12	?			8	
6	P,F,A	27	30	16	3	17			7	
9	A?,P	45	6	30	9	2			8	
10	A	35	4	20	26		8?		7	
14		40	8	20	15				7	20PL?
15	A?	41	15	30	10				4	
19	A,P	40	10	20	25	1			4	
29		30	10	25	25				5	
32		35	9	45	10				1	
33		25	3	35	10		25		2	
37		25	35	25	7				3	5PL?
38		45	40	8	15	10	2		5	
41	P	35	13	4	45				3	
42	P	40	20	8	15	10	2?		5	
47		40	7	10	40				3	
54	A	40	30	20	7				3	
56	P	15	25	10	40	8			2	
61		61		35	5		1		4	
63		15		37	30		1		2	15PL
71	A?	43		35	8		7		7	
90	A	5		5	1		42	45	1	1PL
91		3	34	tr	60				3	
94		10		32	25				3	3PL*
96	40	1	36	20					3	
103	A?	25	13	25	35				2	

*PL phenocrysts

Table 5. (continued)

T.S.#	TEXTURES	QTZ	SER	CHL	CARB	CHLT	EPI	ACT	OPA	OTHER
105	A?	32	1	33	30		1?		3	
106	A,G	3		22	18		35	20	2	
109		30	4	30	10		2		4	20PL
111	A?,V	10	30	25	25				2	
130		12	33	40	13				2	
131	A?	14	20	30	30				6	
132		48	tr	50					2	
135		35	8	40	15					2
141		20	15	35	25				5	
144		30	25	10					10	trPL
150		10	7	45	30				8	
157		8	10	35	12		32		3	
159	P	15	35	3	30	16			1	
161	A?	5	33	10	45				7	
163	P,A?	20	20	5	40	10			5	
165	V,P	10	5	15	65	4			1	
167	P	20	15	3	40	20			2	
171	A	55	22	22					1	
176	A?	5		25			20	30	2	
177	P	30	2	8		26			4	
182	V,A?	5	tr	20	2		45	10	13PL	
187		12	2	44	40				2	
188	V,A?	10	tr	10	4		35	40	1	
189		20	tr	36	40				4	
194		1		26	27			45	1	
195	A?	5		23	22		20	19	3	8PL
200		5		10	77		3?		5	

Table 5. (continued)

T.S.#	TEXTURES	QTZ	SER	CHL	CARB	CHLT	EPI	ACT	OPA	OTHER
205		21	25	30	20				4	
210	Q	7		22			22	50	1	8PL
211	V	13	12	30	18		25		2	
236	P	35	20	15	tr	30			1	
237		36	tr	15	2		2		5	40PL
238		15	7	20	55				3	
239	P	8	30		35	25			2	
240	P,A	6	32	10	20	30			2	
241		13	6	15	62				4	
242	Q,P	6	6	7	55	25			1	
247		10	10?	30	30				7	13PL*
249	V	25	7	8	57				3	
250		15	25	20	33				7	
256		8		40	tr		41	1	10PL	
257		40	tr	50	2				8	
258		20		30	37				3	10PL*
260		10		10			17	50**	5	8PL
265	P	30	25	7		35			3	
279	P	5	32	1	50	10			2	
281	V,A?	17	15	30	38				3	
282		25	3	30	38				4	
283	A	25	8	34	30				3	
284		45	25	20	5				5	
287	Q,V	5		15	4		30	31	1	15PL
289	V	2		30			36	30	1	1PL
290	V	7		10	3		10	60	2	8PL

*PL phenocrysts
**some as phenocrysts

Table 6. Modal Composition of Felsic Tuffs

T.S.#	TEXTURES	PHENOCRYSTS QTZ	QTZ	SER	CHL	CARB	CHLT	OPA	OTHER
Cycle I: Laminated-Bedded Tuffs (unit 2a).									
7	P	1	58	30	2		8	2	
8	P		40	25	5	2	20	8	
11	P		30	13	15	25	10	7	trSTILP?
13	P		45	15	10		28	2	
20	P	tr*	35	28			35	2	
48	P		30	23	12		30	3	2STILP?
51	P		35	25	10		28	2	
146	P		15	60			17	8	
148	P	7	30	33	7	1	15	2	7STILP?
149	P		12	75			8	5	
151	P	3*	37		6		50	7	
152	P,F?		35	12	30	5	8	10	
155	P	2*	40	4	3		47	6	
156	P	4*	54	30	6		5	5	8STILP?
271	F	1*	27	38	30	2		3	
273	V		45	30	8	10		7	
274			13	40		37		10	
299	P,F		60	15	15		8	2	
300	P		50	35	10		3	2	
301	P		40	30	10		15	5	
303	P	1*	30		23		45	3	
Cycle I: Quartz-Crystal Tuffs (unit 2b).									
17	P,F	7	32	60	tr		4	4	trZIR
18	P,F	6	35	56	tr		3	6	
218	P	8	28	60	tr		3	7	2STILP?
219	P	8	35	30			32	3	
220	P	12	45		42		8	5	
251	P	13	28	45			25	2	

*recrystallized phenocryst

Table 6. (continued)

T.S.#	TEXTURES	PHENOCRYSTS QTZ	QTZ	SER	CHL	CARB	CHLT	OPA	OTHER
Cycle II: Laminated-Bedded Tuffs (unit 3a).									
16	P,F		45	15	22	15	tr	3	
23	P	1*	35	25	3		31	1	5PAR
35	P,V		10	55	6		27	2	
43	P		55	10			31	4	
44	P		55	40			4	1	
45	P		35	15	4		26	5	15PAR
46			55	7	7		27	2	
50	P	2	45	30	3		21	1	
52	P,F?	2?*	30	25	10		28	2	
53	P	1	54	35	3		7	1	
58	F	tr*	50	25	15	8		2	
59			30	38	25	5		2	
65			50	25	21			4	
66	F	1*	35	35	28	1		1	
68	P		35	25	18		20	2	
72			40	20	15	13		2	
73	F	1*	45	45	9			1	
74	P		35	33	27?	3		2	
75			10?	80				10	
76			58	20	10?	10		2	
77				99				1	
78			55	20	10	5		2	
79			47	45	4	2		2	
80			50	38	4	7		1	
81			30	65		2		3	
82			32	30	30	5		3	
83			45	37	10	7		1	
84			50	15	20	13		2	
85			55	10	25	7		3	

*recrystallized phenocrysts

Table 6. (continued)

T.S.#	TEXTURES	PHENOCRYSTS QTZ	QTZ	SER	CHL	CARB	CHLT	OPA	OTHER
86			30	14	35	20		1	
87			44	30	15	10		1	
88	P	5*	34	tr	30		35	1	
89	P		45		45	2	5	3	
92		2*	58	40				2	
93			45	5	4	45		1	
95	F	2	15	40	6	35		4	
99		8	35	45		8		4	
102	F		25	1	36	36		2	
104			30	8	30	30		2	trZIR
108	P		33	30	10		25	1	
134		5	50	28	10	7		2	
181		5	27	15	27	25		6	
221a,b	PK	13	46	5				1	40KYN
226**			55		39	tr	2	4	
227			40	40	16			4	
229	P	3*	30	tr	30		30	7	1ZIR
230	P	tr?*	65	20	4		10	1	
231			45	30	8	10		7	
233	F?	2*	50	38	30	2		3	
235			40	40	16			4	
291	P	tr*	40	20	30		6	4	
292	F		50	18	30			2	
293	F	5	40	10	25	22		3	
295**	F	tr*	7	16	10	65		2	
296	P	1	42	tr	45		10	3	

*recrystallized phenocrysts
**Rock Fragment

Table 7. Modal Composition of Intrusive Rocks

Quartz-Feldspar Porphyritic Sills (unit 6)

	PHENOCRYSTS									
T.S.#	QTZ	FSP	PL	QTZ	SER	CHL	CARB	EPI	OPA	OTHER
12			40	80	12	2	3		3	
97	10			40	30	20	9		1	
112				65	6	7	20		2	
113	3*			33	33	4	13		3	
118	8			38	22	16	22		2	
119	5			45	35	4	13		3	
123	3			65	33	tr			2	
124				28	50	7	13		2	
125	24	16		55	30	10			5	
126	40			43	50	3	tr		5	
129	18	27		65	27	tr	4		4	
137	3			50	32	10	5		3	
138	6			40	26	18	15		1	
142	3			38	30	5	25		2	
153	7		5	40	30	25	3	1?	1	
154	4*	3*		46	26	25			3	4CHLT?
207	4			50	25	9	15		1	
255			30	75	16	3	3		3	
263				47	5, plus 25 MIC, 20PL, 2BI				1	

Gabbroic Sills (unit 7)

T.S.#	TEXTURES	QTZ	SER	CHL	CARB	EPI	ACT	OPA	OTHER
55	0	5		28		30	35	2	
110		7		15		35	40	3	
116	0	5		3		45	45	2	
128		7		10		35	45	3	
133		10		7		35	45	3	
139		26	1	30	30			3	10PL
199		15		6		7	55	7	
Felsic Dikes									
69		60	17	10	25			4	5PL
254		43	5	2	50			tr	15PL

*recrystallized phenocrysts

Table 8. Modal Composition of Felsic Lava Flows

T.S.#	TEXTURES	PHENOCRYSTS QTZ	PHENOCRYSTS KSP	QTZ	SER	CHL	CARB	CHLT	KYN	OPA	OTHER
Cycle I Lava Flows (unit 2c)											
21	PK	5		58	5				25	2	10AND
22	PK	1		60	3				35	2	
25	PK	2		55	5				38	2	
253	PK	4		62	2				35	1	
Cycle II Lava Flows (unit 3b)											
1a		5	5	35	43	2	15			5	
1b	S			30	48	tr	22			tr	
27		2	3	60	25	10	2			3	

Table 9. Modal Composition of Polymictic Diamictite Matrix

T.S.#	QTZ	SER	CHL	CARB	CHLT	OPA
2	35	10	35	15		5
24	40	30	20		7	3
26	40	30	10		13	7
224	40	30	20			4

Appendix II. Whole Rock and Trace Element Analyses

The following tables are a compilation of the major and trace element analyses and the analytical accuracy as determined by the Geological Survey of Canada's Analytical Chemistry Section, Ottawa, Ontario.

Whole rock components (Table 12) were determined by X-Ray Fluoresence Wavelength Dispersive Analyses (XRF), except FeO, H_2O, CO_2, and S which were analyzed by rapid chemical methods. All whole rock components are reported in weight per cent (wt.%). Cr_2O_3, Ni, and Zn are reported only when >0.1%. Fe_2O_3 = Fe_2O_3 (XRF) - 1.11134 FeO (volumetric). Volatiles represent all constituents lost on ignition other than CO_2, H_2O, and S.

Trace elements (Table 13) are reported in parts per million (ppm). As, Br, Mo, Nb, Rb, Sr, Th, U, Y, and Zr were analysed by Energy Dispersive XRF. Co, Cr, Cu, Ni, Pb, and Zn were determined by Atomic Absorption (AA) spectrometry.

Blank spaces represent values below detection limits.

The last column on Tables 12 and 13, designated Alt Type, represents a classification of each sample according to the sample's mineral assemblage (see Appendix I). The alteration types coincide with those described in the text (Ch. III, Alteration) and with the Alteration Zones shown on Plate 2. The alteration types include: (1) Least Altered, (2) Quartz-Sericite, (3) Iron Chlorite, and (4) Chloritoid. Type (4) includes quartz-kyanite-bearing rocks locally found associated with chloritoid-bearing rocks. Most of the rocks

with a particular alteration type are located within a zone shown on Plate 2 with the same mineral assemblage. However, some samples are not located within a zone with the same assemblage; these represent isolated occurrences of an alteration type which are indistinguishable at the scale of Plate 2.

Table 10. Accuracy of Whole Rock Analyses as reported by the Geological Survey of Canada

ELEMENT	CALIBRATION RANGE %	ESTIMATE OF ERROR ABSOLUTE +	RELATIVE %	DETERMINATION LIMIT
SiO_2	0 - 100	0.40	1	0.40
TiO_2	0 - 3	0.02	1	0.02
Al_2O_3	0 - 60	0.40	1	0.40
Cr_2O_3	0 - 4	0.02	1	0.02
Fe_2O_3	0 - 90	0.10	1	0.10
FeO	0 - 30	0.20	2	0.20
MnO	0 - 1	0.01	2	0.01
MgO	0 - 50	0.10	1	0.10
CaO	0 - 35	0.10	1	0.10
Na_2O	0 - 10	0.50	1	1.50
K_2O	0 - 15	0.05	1	0.05
H_2O	0 - 5	0.10	5	0.10
CO_2	0 - 20	0.05	3	0.05
P_2O_5	0 - 1	0.02	1	0.02
S	0 - 3	0.04	5	0.04
Ba	0 - 0.3000	0.002	2	0.002
Zn	0 - 0.0200	0.002	10	0.002

Table 11. Accuracy of Trace Element Analyses as reported by the Geological Survey of Canada*

	ESTIMATE OF VALIDITY OF RESULTS		
ELEMENT	ABSOLUTE	+	RELATIVE (% OF CONC.)
As	30		10
Br	10		10
Mo	10		10
Nb	10		10
Pb	30		10
Rb	10		10
Sr	10		10
Th	30		10
U	30		10
Y	10		10
Zr	10		10
Co	10		10
Cr	10		10
Cu	7		10
Ni	15		10
Pb	20		10
Zn	7		10

* As, Br, Mo, Nb, Rb, Sr, Th, U, Y, Zr analyzed by X-Ray Flouresence, and Co, Cr, Cu, Ni, Pb, Zn analyzed by Atomic Absorption.

Table 12. Whole Rock Chemical Analyses of Major Oxides (wt.%)

SPL #	SiO2	TiO2	Al2O3	Fe2O3	FeO	MnO	MgO	CaO	Na2O	K2O	H2O	CO2	P2O5	S	Ba	Total	S.G.[1]	ALT[2] TYPE
1	69.8	.47	16.1	.9	3.0	.07	1.15	1.24	1.7	2.33	3.0	.8	.21	.04	.059	100.9	2.34	III
2	49.9	.75	15.6	1.7	6.2	.20	4.28	10.10	1.8	.50	3.5	6.1	.09	.03	.023	100.8	2.83	IV
3	53.0	.98	16.7	1.3	9.3	.34	3.46	5.26	1.6	.64	4.9	3.0	.17	.03	.017	100.9	2.76	III
10	48.1	.95	14.6	1.1	6.5	.17	5.55	9.86	2.2	.09	4.2	7.1	.11	.09	.006	100.7	2.78	III
11	49.6	.80	12.8	4.0	9.9	.52	4.48	6.03	.1	.21	3.8	7.7	.11	.24	.005	100.4	2.83	IV
12	70.5	.33	16.4	.7	.5	.05	.21	1.84	4.6	1.64	1.5	1.6	.11	.06	.074	100.1	2.66	I
18	74.0	.62	16.6	.9	.7	.02	.24	.44	1.4	2.07	2.9	.1	.25		.035	100.4	2.60	IV
21	76.9	.64	20.2		.3		.07	.12	.5	.20	.8		.14	.03	.009	100.0	2.89	IV**
25	83.7	.46	14.8		.1			.15	.5	.26	.7		.11	.03	.022	100.9	2.74	IV**
26*	54.5	1.15	20.8	4.6	9.0	.29	1.51	.24	.7	1.29	5.4		.15	.57	.035	100.0	2.89	IV
27	66.0	.62	17.1	.8	3.3	.08	.85	2.71	3.9	1.45	1.9	.7	.20		.042	99.8	2.69	III
29	46.7	.65	13.4	2.7	7.4	.84	6.87	6.61	.1	1.34	4.6	9.5	.07	.06	.010	100.9	2.84	II
30	43.2	.77	16.7	1.3	9.1	.25	8.83	5.89	.9	.67	4.7	8.3	.08	.03	.013	100.8	2.87	II
31	50.4	.73	15.1	1.8	6.3	.20	4.15	10.40	1.6	.46	3.4	6.8	.07	.05	.022	100.5	2.64	II
32	53.6	.83	15.8	1.2	10.0	.08	11.30	.72	.1	.35	6.0	.7	.10	.06	.007	100.9	2.79	II
33	48.1	.76	15.1	4.6	6.8	.18	8.00	10.10	.2	.01	4.4	2.0	.07		.003	100.5	2.95	II
35	57.3	1.34	24.8	3.0	3.5	.16	1.18	.75	.9	3.23	4.4	.1	.16	.03	.069	100.9	2.82	IV
38*	55.7	.87	16.2	3.7	8.7	.69	4.25	.50	.3	2.52	5.4	.6	.09	.74	.019	100.5	2.74	III
45	62.5	1.87	19.6	3.2	4.9	.37	1.11	.98	.5	.92	3.3	.2	.65	.03	.009	100.2	2.92	IV
49	64.4	1.17	15.8	1.8	7.4	.23	2.02	.75	.2	1.94	3.6	.3	.36	.07	.015	100.2	2.88	IV
50	72.4	.42	17.1	1.2	1.7	.14	.33	.22	.2	3.53	2.6	.2	.16		.018	100.3	2.76	IV
51	63.0	1.01	17.6	3.2	8.1	.32	2.00	.20		.68	4.4	.2	.09	.03	.008	100.9	2.68	IV
54	48.5	1.04	19.6	1.2	7.0	.12	4.67	5.96	2.0	1.00	4.4	4.2	.10	.12	.014	100.0	2.81	II
55	46.6	.61	15.3	2.9	7.3	.18	9.87	12.20	.8	.03	4.2	.5	.06	.11	.003	100.9	3.06	I
56	45.0	.91	15.9	1.9	8.4	.22	3.53	9.76		1.36	3.1	10.1	.09	.03	.020	100.4	2.77	IV

[1] Specific gravity

[2] Alteration Type: (I) Least Altered, (II) Quartz-Sericite, (III) Iron Chlorite, (IV) Chloritoid

*Also,
SPL #26 reported .21% volatile.
SPL #38 reported .28% volatile, and .476% Zn.

**Quartz-Kyanite-bearing rocks associated with Chloritoid-type alteration.

25

Table 12 (continued)

SPL #	SiO2	TiO2	Al2O3	Fe2O3	FeO	MnO	MgO	CaO	Na2O	K2O	H2OT	CO2T	P2O5	S	Ba	Total	S.G.[1]	ALT[2] TYPE
57	50.7	.73	15.5	1.7	6.3	.19	4.13	10.2	1.8	.49	2.7	6.0	.10	.04	.024	100.8	2.74	II
61	51.4	.93	16.0	1.8	9.2	.14	7.54	3.17	3.1		8.9	2.6	.07		.002	100.9	2.56	II
63	47.5	.80	14.1	1.8	9.0	.17	7.92	6.49	2.1		4.6	5.0	.07	.04	.003	99.7	2.77	II
71	52.3	1.07	15.2	1.6	8.6	.19	4.59	7.35	1.9	.02	4.3	3.6	.09	.03	.008	100.9	2.72	III
79	67.8	1.12	19.4	.8	.2	.02	.40	.99	1.0	3.96	3.4	.7	.31	.03	.053	100.3	2.73	II
80	65.2	.57	17.6	2.4	2.0	.08	1.35	1.71	.9	3.09	3.1	1.0	.30		.030	99.4	2.68	III
85	53.5	2.04	17.3	1.6	13.1	.23	2.77	1.24	.3	2.13	5.7	.1	.81		.021	100.9	2.98	III
86	50.8	.88	16.4	1.4	8.7	.27	5.00	5.58	.3	1.63	5.2	4.5	.10	.04	.013	100.9	2.75	II
88	45.9	1.42	25.2	4.9	12.7	.39	1.87	.64		.60	5.1	.2	.41		.008	99.5	3.20	IV
89	36.5	1.97	30.5	6.5	13.5	.45	2.13	.44	.2	1.81	6.0	.1	.14		.023	100.4	3.08	IV
90	48.1	.69	14.3	2.5	7.8	.18	9.46	10.70	1.3		3.7	1.8	.07	.07	.003	100.7	2.96	I
95	66.3	.51	15.8	1.6	2.8	.10	2.54	2.08	.8	2.78	3.0	2.2	.18	.08	.025	100.9	2.68	II
96	50.7	.76	15.3	1.7	6.3	.19	4.39	10.50	1.7	.47	2.7	6.0	.09	.06	.022	100.9	2.75	II
97	65.1	.47	15.0	1.1	2.9	.08	3.00	2.92	1.6	2.93	3.1	2.2	.21	.04	.060	100.9	2.75	II
99	71.6	.29	13.7	.9	.7	.09	1.20	2.06	.1	3.54	2.6	2.9	.10	.03	.039	100.0	2.60	III
102	34.9	.67	11.7	2.1	14.8	.43	8.82	9.23		.16	4.4	11.9	.08	.24	.004	99.4	2.84	III
104	45.8	.78	16.6	1.2	8.4	.19	7.08	7.35	1.1	.82	5.8	5.5	.07	.05	.011	100.9	2.80	II
106	46.7	.70	15.3	5.3	5.4	.19	5.84	15.3	.6	.01	3.4	1.8	.06	.07		100.8	3.04	II
112	69.3	.53	14.6	.8	2.8	.10	3.03	1.41	.3	2.55	3.8	1.1	.18	.04	.040	100.6	3.00	II
116	48.5	.75	15.5	2.3	7.7	.18	10.10	9.67	.7	.08	4.1	.8	.06	.02	.004	100.6	3.00	II
117	50.1	1.04	15.6	1.7	7.1	.27	7.27	5.00	.5	1.68	5.3	4.4	.51	.23	.053	100.8	2.79	I
118	68.5	.46	14.8	.9	2.7	.07	3.37	1.29	.9	1.92	3.5	1.2	.15	.02	.047	99.9	2.72	II
126	76.0	.24	14.1	1.2	1.3	.06	1.10	.37	.4	2.44	2.9	.7	.04	.02	.030	100.9	2.62	II
127	49.9	.77	15.4	1.7	6.3	.21	4.49	10.40	1.4	.47	3.0	5.7	.10	.11	.023	99.9	2.62	II
129	70.9	.26	16.5	.9	.5	.03	.48	1.05	3.7	2.63	1.6	.8	.07		.045	99.6	2.65	II
132	51.1	.93	16.6	1.5	9.3	.17	6.80	4.38	1.9	.14	5.0	2.5	.08	.06	.008	100.6	2.80	II
139	47.1	.58	12.9	1.4	8.4	.23	8.03	8.52	1.4	.17	5.0	6.9	.08	.02	.006	100.8	2.77	I
144	53.3	.92	16.3	1.3	12.0	.20	6.17	2.23	.6	.55	5.0	.6	.07	.05	.011	99.5	2.67	III
146*	48.5	1.56	26.3	8.7		.09	.50	1.12	.6	5.28	5.3	.1	.77	2.33	.144	100.6	3.00	IV

*Also,
SPL # 146 reported .87% volatile.

Table 12 (continued)

SPL #	SiO2	TiO2	Al2O3	Fe2O3	FeO	MnO	MgO	CaO	Na2O	K2O	H2OT	CO2T	P2O5	S	Ba	Total	S.G.[1]	ALT[2] TYPE
148	61.3	1.28	21.6	1.4	3.5	.14	1.10	2.00	.5	2.99	3.6	.7	.26	.01	.046	100.5	2.84	IV
149	63.4	2.09	23.5	1.0	1.3	.08	.12	.24	.8	3.91	3.3	.2	.10		.059	100.4	2.80	IV
153	70.0	.51	16.5	1.0	1.5	.04	.54	.96	2.4	3.04	2.0	.6	.18	.01	.070	99.4	2.72	II
156*	71.2	.92	16.0	1.0	2.3	.19	.51	.45		3.86	2.9	.5	.25	.31	.041	100.8	2.73	IV
157	45.2	.85	16.0	3.5	7.1	.17	7.60	11.90	.7		4.4	2.7	.08	.24	.002	100.6	2.96	III
159	56.0	1.11	20.2	5.1	6.1	.18	1.38	1.23	.1	2.55	4.3	2.1	.08	.10	.038	100.7	2.87	IV
161	50.6	.76	15.6	1.5	6.5	.19	4.30	10.30	1.6	.49	3.1	5.8	.10	.05	.022	100.9	2.87	III
163*	52.5	.68	14.9	2.9	10.0	.06	4.11	3.84		.90	4.0	4.7	.07	.51	.008	100.0	2.93	IV
167	57.8	.89	17.5	1.9	6.8	.19	2.63	2.52	.5	2.66	3.5	3.7	.08	.04	.021	100.9	2.90	IV
171	54.8	1.12	16.0	1.0	8.5	.13	10.4	.64		1.09	6.0	.2	.47		.022	100.5	2.78	II
176	48.6	.78	14.9	4.9	7.9	.22	8.74	7.74	1.9		4.1	.8	.09	.03	.022	100.8	2.93	I
182	49.9	.98	15.4	2.0	9.5	.23	8.47	7.44	2.4	.09	3.6	.7	.09		.006	100.9	2.81	I
187	48.8	.89	17.1	1.3	9.2	.20	6.81	4.50	2.2	1.08	5.1	3.2	.08	.11	.018	100.6	2.80	II
193	48.9	.85	15.2	2.4	8.4	.19	7.22	11.40	2.4	.18	2.1	1.2	.06	.12	.006	100.8	3.05	I
195	47.7	.83	14.3	1.3	8.4	.18	8.37	6.41	2.6	.03	4.8	4.5	.07		.004	99.6	2.79	I
210	49.8	1.01	15.1	2.7	8.6	.18	7.33	11.20	1.8	.40	2.3	.2	.11	.01	.005	100.9	3.02	I
211*	44.1	.58	13.2	2.1	10.8	.24	11.00	7.24		.42	6.4	4.2	.07	.54	.005	100.7	2.85	II
218	44.1	.66	13.3	.8	1.8	.04	.35	.44	.8	2.70	2.4		.29	.14	.036	100.3	2.77	IV
219	64.9	.78	21.3	2.2	1.9	.09	.54	.76	1.5	1.71	3.1		.38	.01	.029	99.3	2.81	IV
220	43.0	.57	15.5	10.6	16.6	.27	6.57	.53			5.9	.1	.27			100.0	3.17	IV
221	76.7	.74	20.4	7		.01	.03	.36	.3	.12	.3		.28	.26	.007	100.3	2.94	IV**
222	50.6	.79	15.3	1.6	6.3	.19	4.24	10.20	1.2	.48	3.0	6.4	.09	.08	.023	100.5	2.91	IV
224	57.7	1.99	16.9	1.3	5.7	.15	1.50	4.69	1.3	2.46	2.9	2.4	.58	.01	.062	99.8	2.53	III
226*	50.1	.65	13.3	22.4		.18	6.15	.33	.2	.02	6.9	.2	.07	4.08	.008	103.2	2.95	IV
227	63.8	1.95	19.1	.3	2.0	.11	1.15	4.36	.9	1.71	2.7	1.6	.50		.011	100.3	2.79	III

*Also,
SPL # 156 reported .12% volatile, and .248% Zn.
SPL # 163 reported .19% volatile.
SPL # 211 reported .19% volatile.
SPL # 226 reported 1.50% volatile.

**Quartz-Kyanite-bearing rocks associated with Chloritoid-type alteration.

Table 12 (continued)

SPL #	SiO2	TiO2	Al2O3	Fe2O3	FeO	MnO	MgO	CaO	Na2O	K2O	H2OT	CO2T	P2O5	S	Ba	Total	S.G.[1]	ALT[2] TYPE
229*	37.7	2.70	21.1	27.7		.54	3.97	.60	.3		7.1	.1	.30	2.04	.003	103.3	3.19	IV
230	75.8	.37	13.2	1.3	3.2	.35	1.22	.55	.5	1.20	2.5		.13	.04	.008	100.4	2.84	IV
231	55.3	1.64	17.5	1.6	8.6	.32	3.25	4.67	.3	.91	4.5	1.0	.63		.015	100.5	2.90	III
232*	56.6	.80	16.5	12.4		.16	3.93	1.36	.7	1.22	5.0	.5	.03	2.31	.018	100.7	2.86	IV
233	63.2	.99	19.6	.3	3.6	.11	2.41	4.49	.5	.79	3.3	1.4	.09	.02	.006	100.9	2.80	II
234	58.6	1.05	19.7	.6	5.7	.15	2.67	4.36	.5	1.35	4.0	1.9	.07	.04	.022	100.8	2.84	III
235*	65.7	.86	16.4	.8	6.1	.22	1.97	.65	.6	2.35	3.9	.5	.07	.88	.015	100.9	2.76	III
236*	55.8	.93	17.8	3.5	9.1	.24	3.41	2.99	.1	.12	4.4	2.0	.08	.38	.006	100.8	2.85	IV
237	52.4	.90	16.6	1.7	8.9	.12	6.47	3.20	3.2	.15	4.6	1.9	.07		.008	100.2	2.73	I
238	44.1	.73	13.5	1.3	8.7	.16	6.62	10.00	.7	.85	3.8	9.9	.08	.06	.008	100.5	2.82	II
239	43.1	.87	15.8	1.9	8.3	.24	4.99	8.28	.6	.96	3.5	12.2	.09		.012	100.9	2.93	IV
240	51.0	.83	15.6	2.6	6.9	.20	4.15	6.40	.3	1.01	3.7	8.7	.06		.012	100.6	2.92	IV
241	50.4	.79	15.8	1.4	6.3	.19	4.25	10.10	1.4	.53	3.1	6.0	.08	.05	.024	100.4	2.78	II
242	42.6	.66	13.3	1.2	8.3	.32	5.01	10.90	.6	.98	2.6	13.2	.07	.10	.016	99.8	2.90	IV
246	78.3	.23	12.4	.4	1.7	.05	.30	.62	2.5	1.37	1.2	.2	.06	.03	.029	99.5	2.69	I
247	53.3	.92	16.3	1.1	8.9	.22	3.16	6.47	1.6	.71	4.0	3.7	.09	.06	.025	100.7	2.83	III
248	47.8	.98	16.3	1.4	8.2	.30	2.94	10.70	1.5	.27	3.5	6.8	.11	.04	.012	100.9	2.79	IV
249	44.6	.84	14.8	1.1	8.5	.17	5.27	10.30	1.4	.69	3.8	9.0	.09	.21	.008	100.8	2.83	III
250	50.2	.74	15.2	1.9	6.2	.20	4.16	10.30	1.4	.46	3.1	6.1	.09	.08	.023	100.1	2.84	III
251	70.1	.59	17.7	1.1	2.5	.05	1.07	.52	1.0	2.90	2.7	.1	.30	.01	.042	100.9	2.76	IV
253	69.9	.82	28.0		.2		.05	.06		.11	.6	.1	.09		.003	100.0	2.88	IV**
263	76.5	.12	12.8	.7	.6	.04	.32	.82	2.8	4.06	.8	.4	.06	.13	.029	100.2	2.63	I
265	55.9	1.20	24.4	2.9	5.2	.17	1.78	1.98	.7	1.57	4.0	.4	.10	.04	.014	100.5	2.93	IV

*Also,
SPL # 229 reported .76% volatile.
SPL # 232 reported .80% volatile.
SPL # 235 reported .33% volatile.
SPL # 236 reported .14% volatile.

**Quartz-Kyanite-bearing rocks associated with Chloritoid-type alteration.

Table 12 (continued)

SPL #	SiO2	TiO2	Al2O3	Fe2O3	FeO	MnO	MgO	CaO	Na2O	K2O	H2OT	CO2T	P2O5	S	Ba	Total	S.G.[1]	ALT[2] TYPE
273*	39.4	.77	15.2	25.6		.54	1.94	.53	2.1	1.70	4.7	1.7	.08	7.72	.014	99.1	3.03	III
279	37.3	.86	11.3	1.5	7.8	.83	6.61	13.30		1.14	1.7	18.2	.10	.24	.009	100.9	2.92	IV
283	44.3	.92	12.7	1.2	9.2	.20	6.34	10.80	.5	.97	4.5	9.1	.10	.05	.015	100.9	2.81	II
289	48.5	.80	14.5	2.4	8.6	.24	7.86	10.50	1.9	1.53	2.9	1.2	.08	.09	.022	100.9	2.97	I
290	48.9	.95	15.6	3.0	9.1	.29	6.52	10.00	1.1	.06	3.3	1.4	.08	.01	.003	99.5	2.96	I
291	50.9	1.03	18.3	2.3	15.2	.21	3.83	.58		1.42	5.8		.41		.018	100.2	2.77	IV
292	63.6	1.05	17.2	1.1	7.8	.09	2.34	.39	.5	2.26	4.1	.1	.11		.030	100.7	2.84	III
293	48.9	1.01	17.5	2.2	14.1	.26	3.59	2.87	.6	1.61	5.5	1.8	.36		.027	100.5	2.90	III
294	52.7	1.90	31.9	.6	.1		.20	.14	1.5	6.55	4.1	.1	.05	.01	.110	100.2	2.70	IV
295	66.2	.81	17.2	.7	5.4	.07	1.55	.41	.9	2.83	3.4	.2	.12	.19	.029	100.0	2.78	III
296*	46.2	.93	16.6	3.3	19.3	.29	4.90	.85	.2	.06	6.6	.1	.32	.62	.001	100.0	3.01	IV
297*	45.1	1.95	36.6	.7	.1		.19	.50	3.5	6.45	4.8	.1	.22		.072	99.6	2.86	III
298*	52.3	1.64	30.6	.9	1.2	.10	.11	.32	1.7	6.88	4.0	.1	.16		.095	100.3	2.84	IV
299	50.4	.75	15.4	1.8	6.3	.20	3.95	10.40	1.9	.47	3.0	6.1	.10	.02	.023	100.8	2.86	IV
300	75.1	.77	13.4	.9	3.5	.11	.94	.19	.3	2.27	2.6	.1	.10	.20	.018	100.6	2.77	IV

*Also,
SPL # 273 reported 2.89% volatile.
SPL # 296 reported .001% volatile.
SPL # 297 reported .15% Cr2O3.
SPL # 298 reported .13% Cr2O3.

Table 13. Trace Element Analyses

SPL #	As	Br	Mo	Nb	Rb	Sr	Th	U	Y	Zr	Co	Cr	Cu	Ni	Pb	Zn	ALT[1] TYPE
1	6	3	0	4	68	260	10	5	6	150	6	16	9	12	12	83	III
2	3	7	1	4	14	150	8	7	15	60	40	9	80	30	1	93	IV
3	0	1	0	1	23	110	2	1	20	57	45	210	140	97	1	180	III
10	11	4	1	4	5	160	6	4	18	62	44	170	160	110	5	92	III
11	13	7	0	1	9	15	3	9	26	51	49	160	100	140	0	120	IV
12	8	8	0	3	49	330	13	8	0	140	2	5	55	7	15	16	I
18	5	2	0	11	56	380	19	7	14	190	2	30	13	11	12	19	IV
21	26	1	0	11	170	20	8	17	190	1	9	26	4	10	3	0	IV*
25	6	1	0	7	9	290	12	2	3	160	2	5	17	4	20	2	IV
26	6	3	0	6	36	170	15	8	24	120	37	230	52	91	7	160	IV
27	7	7	0	8	40	420	18	5	17	210	9	28	12	9	10	58	III
29	64	2	0	0	47	43	0	0	10	33	39	230	200	180	330	1000	II
30	23	0	0	0	24	160	1	0	10	36	40	330	53	120	26	310	II
31	4	3	2	3	24	160	7	1	16	63	41	9	83	33	0	92	II
32	0	1	1	2	14	10	0	2	12	49	43	280	140	140	5	220	II
33	19	0	0	2	1	190	2	2	17	43	46	250	14	140	3	90	II
35	52	6	0	1	130	490	4	0	19	78	9	420	81	75	10	49	IV
38	36	5	0	1	84	27	3	1	16	49	55	310	370	170	330	5700	III
45	3	0	0	15	32	160	9	3	33	300	10	100	15	15	7	110	IV
49	5	9	1	11	79	51	7	6	36	200	25	46	21	63	0	110	IV
50	5	6	0	7	160	100	15	8	7	190	4	10	0	9	9	42	IV
51	63	0	0	2	28	28	3	0	22	61	53	260	120	110	0	130	IV
54	16	3	2	3	35	170	4	1	19	61	77	410	140	200	0	88	II
55	13	8	3	2	2	150	6	3	15	36	53	520	75	150	0	74	I
56	17	3	0	0	51	150	0	1	17	49	48	350	130	150	0	87	IV
57	5	4	2	4	15	160	5	4	16	62	44	9	78	34	0	93	II
61	8	0	1	2	0	75	3	1	19	52	51	390	39	130	0	120	II
63	2	0	0	1	1	89	1	1	14	41	46	300	96	110	1	140	II
71	9	0	0	2	2	63	2	1	16	56	50	240	85	130	0	85	III
79	2	7	0	8	120	140	11	8	23	230	1	72	30	5	9	12	II
80	22	3	0	7	99	95	13	6	8	190	8	12	5	13	11	100	III

[1] Alteration Type: (I) Least Altered, (II) Quartz-Sericite, (III) Iron Chlorite, (IV) Chloritoid.

*Quartz-Kyanite-bearing rocks associated with Chloritoid-type alteration.

Table 13 (continued)

SPL #	As	Br	Mo	Nb	Rb	Sr	Th	U	Y	Zr	Co	Cr	Cu	Ni	Pb	Zn	ALT[1] TYPE
85	0	6	0	9	64	65	12	9	42	220	33	87	2	55	0	120	III
86	3	0	1	3	64	73	0	4	21	63	53	310	140	150	0	120	II
88	19	7	0	14	22	27	17	12	53	370	33	120	18	52	0	190	IV
89	15	3	0	17	53	87	13	10	37	370	29	160	6	60	0	200	IV
90	24	9	0	1	0	110	3	7	15	35	49	340	120	140	0	76	I
95	6	3	0	7	91	87	8	4	7	190	10	11	12	4	6	87	II
96	1	1	0	3	15	160	5	4	16	61	43	11	76	30	0	98	II
97	1	2	0	7	97	140	8	0	7	170	9	14	5	9	3	97	III
99	6	3	0	60	120	86	6	4	3	130	1	3	12	2	10	59	III
102	11	4	0	2	8	18	5	5	28	43	53	140	110	140	0	170	III
104	0	1	0	1	27	77	0	0	13	40	47	330	100	130	0	82	II
106	9	5	0	4	51	140	4	3	12	120	44	320	130	140	1	68	II
112	2	6	0	4	51	140	4	3	12	120	44	320	130	140	1	68	II
116	8	1	4	1	2	100	2	2	12	34	49	370	99	210	0	75	I
117	4	1	0	6	54	67	8	6	23	150	30	53	19	35	15	130	II
118	11	4	0	6	60	140	9	5	5	150	10	15	5	8	13	130	II
126	1	2	310	9	82	120	17	5	16	98	7	31	18	14	90	200	II
127	10	2	2	3	15	160	4	4	17	61	49	13	81	37	0	97	II
129	10	6	0	0	93	220	5	5	0	81	5	14	23	8	17	93	II
132	0	0	0	1	5	51	0	0	14	51	59	320	130	170	0	97	II
139	0	1	0	1	5	70	0	0	12	32	42	310	130	88	0	130	I
144	0	5	0	3	21	46	5	5	10	53	46	340	59	160	0	130	III
146	75	11	0	12	140	510	27	4	32	340	130	380	230	330	40	60	IV
148	21	9	0	7	120	180	13	3	30	260	16	87	500	26	72	150	IV
149	15	11	0	18	100	520	14	4	22	340	5	120	7	13	30	32	IV
153	9	7	0	6	84	370	11	3	6	160	5	21	16	7	8	39	II
156	14	8	0	7	170	160	7	2	25	200	5	60	46	16	460	3100	IV
157	0	0	0	0	0	140	0	0	10	45	54	280	150	140	0	76	III
159	0	0	0	1	110	44	0	0	10	62	46	400	63	160	15	240	IV
161	9	0	3	3	15	160	8	2	16	62	44	8	79	33	1	97	III
163	12	4	2	2	36	21	7	2	13	37	41	310	99	130	6	230	IV

Table 13 (continued)

SPL #	As	Br	Mo	Nb	Rb	Sr	Th	U	Y	Zr	Co	Cr	Cu	Ni	Pb	Zn	ALT[1] TYPE
167	93	0	2	2	100	25	0	4	17	52	43	310	73	130	8	190	IV
171	0	8	0	7	36	16	11	6	24	170	28	53	2	35	0	330	II
176	13	4	0	0	2	140	6	4	20	44	48	300	92	120	11	110	I
182	12	3	1	2	2	73	5	4	19	53	64	300	65	190	0	120	I
187	0	0	0	0	30	40	0	0	16	48	45	260	180	100	0	90	II
193	5	1	0	2	3	130	3	4	17	46	48	250	140	140	0	80	I
195	0	2	0	1	3	100	0	1	13	44	45	300	26	110	0	88	I
210	9	9	4	4	33	130	9	4	23	65	41	220	44	120	0	110	I
211	7	0	1	1	38	27	5	1	9	28	54	210	120	160	0	330	II
218	14	0	0	8	70	350	10	0	15	200	17	31	14	14	16	16	IV
219	9	5	0	9	43	430	14	0	17	270	5	38	6	7	14	49	IV
220	4	0	0	7	3	4	14	11	11	150	35	32	17	26	0	360	IV
221	10	0	0	11	5	43	10	6	20	250	3	29	21	8	12	24	IV*
222	6	1	0	3	15	150	2	4	16	63	43	12	88	31	1	99	IV
224	34	11	3	13	62	480	7	0	31	240	33	93	39	62	5	63	III
226	38	5	3	2	3	3	5	4	21	38	150	150	190	180	0	210	IV
227	10	2	0	7	63	230	9	0	28	220	18	110	36	36	5	30	III
229	13	0	2	14	4	8	10	3	39	170	95	14	270	100	0	250	IV
230	5	0	0	7	40	80	11	3	10	140	3	15	7	7	10	62	IV
231	0	1	0	7	30	210	3	0	36	210	35	85	14	41	8	120	III
232	13	0	0	0	42	80	0	0	11	45	87	360	320	140	2	140	IV
233	56	0	1	2	27	92	0	0	10	62	89	290	87	220	1	42	II
234	4	3	0	3	53	73	4	0	12	63	39	390	220	130	2	86	III
235	12	2	0	2	100	89	4	0	17	52	42	340	120	260	3	88	III
236	3	5	2	3	7	18	2	3	23	60	64	350	140	200	0	110	IV
237	8	4	2	2	6	74	1	3	16	52	53	320	130	150	0	94	I
238	0	0	0	0	28	110	0	0	13	43	42	200	110	130	0	110	II
239	3	0	0	0	34	54	0	0	3	49	47	310	130	130	0	84	IV
240	0	0	0	2	36	30	1	0	11	46	38	290	110	140	0	70	IV
241	3	2	3	4	17	60	6	4	16	65	43	8	79	38	0	75	II

*Quartz-Kyanite-bearing rocks associated with Chloritoid-type alteration.

Table 13 (continued)

SPL #	As	Br	Mo	Nb	Rb	Sr	Th	U	Y	Zr	Co	Cr	Cu	Ni	Pb	Zn	ALT[1] TYPE
242	0	0	0	0	41	73	0	0	12	36	39	280	120	110	9	92	IV
246	6	1	0	10	41	190	17	1	17	110	4	0	8	5	14	30	I
247	0	4	0	2	27	78	0	0	26	53	44	130	150	160	0	110	III
248	0	0	0	0	11	90	0	0	24	52	44	210	140	140	0	100	IV
249	1	0	0	0	23	180	0	0	17	45	47	290	110	150	0	75	III
250	9	1	3	4	16	160	1	2	16	63	46	9	77	34	0	97	III
251	0	1	0	8	72	190	10	0	11	210	2	32	1	7	13	49	IV
253	9	3	0	13	5	20	10	5	13	310	3	20	4	4	6	12	IV
263	15	3	0	11	170	85	25	2	29	87	3	5	190	2	18	21	I
265	25	3	5	4	54	82	4	2	13	66	47	430	210	110	11	140	IV
273	3	3	0	3	45	59	4	4	12	51	19	190	170	38	0	110	IV
279	34	1	1	3	38	28	5	0	19	52	29	150	210	49	31	160	IV
283	18	5	4	3	86	50	0	0	18	51	41	210	210	79	0	180	II
289	11	10	1	2	130	120	1	0	17	46	48	240	140	110	0	78	I
290	1	7	2	3	2	110	2	1	22	52	49	210	150	130	0	100	I
291	170	3	0	3	41	81	10	3	23	120	75	400	10	280	0	270	IV
292	22	6	4	9	65	180	8	0	20	200	30	88	8	40	180	160	III
293	28	5	0	4	50	100	9	5	15	120	74	210	8	170	10	120	III
294	35	12	0	22	180	550	17	0	48	440	4	160	5	10	31	6	IV
295	14	7	0	5	81	110	5	1	18	120	30	71	72	70	3	58	III
296	66	3	0	3	4	13	13	3	18	100	180	410	170	220	0	300	IV
297	6	9	0	7	170	500	12	0	36	270	9	860	6	31	31	6	III
298	20	5	0	5	200	290	12	0	20	220	8	660	4	19	18	18	IV
299	3	4	3	2	15	160	2	3	16	63	41	9	87	33	0	95	IV
300	24	0	0	2	96	64	1	0	5	53	44	150	60	97	3	72	IV

*Quartz-Kyanite-bearing rocks associated with Chloritoid-type alteration.

Appendix III. Electron Microprobe, X-Ray Diffraction and Thin Section Staining Analyses

Table 14. Electron Microprobe Analyses

The electron microprobe at the Geological Survey of Canada was used to quantitatively analyze the composition of chlorite, chloritoid, and the white micas from throughout the study area. As well, carbonate and opaque minerals were qualitatively analyzed to aid in identification of the mineral species. An accelerated voltage of 15 kV and a beam current of 0.5 A were used for all analyses. Each component was counted for 100 seconds. The analyses presented in the following table represent averages of several spot determinations for each polished thin section.

Table 14. Electron Microprobe Analyses

SPL # 6, Chloritoid Alteration Zone

wt.(%)	Chlorite	Chloritoid	Ankerite[1]
N[2]	(13)[2]	(6)	(7)
SiO2	23.60	24.74	0.01
TiO2	0.17	0.11	0.00
Al2O3	23.12	39.69	0.00
Cr2O3	0.14	0.15	0.00
FeO	30.82	25.47	14.62
MnO	0.12	0.33	0.70
MgO	0.72	2.09	13.84
CaO	0.07	0.04	26.73
Na2O	0.00	0.00	0.00
K2O	0.04	0.03	0.00
Totals	88.78	92.64	55.90
# of ions on the basis of:			
	28(O)	12(O)	6(O)
Si	5.070	2.051	0.001
Ti	0.029	0.007	0.000
Al	5.840	3.878	0.000
Cr	0.022	0.010	0.000
Fe	5.530	1.766	1.181
Mn	0.023	0.023	0.057
Mg	3.412	0.258	1.993
Ca	0.021	0.003	2.767
Na	0.000	0.000	0.000
K	0.009	0.003	0.000
Totals	19.968	7.999	5.999
Proportions			
Fe	61.72	87.11	19.88
Mg	38.04	12.72	33.54
Ca	0.24	0.17	46.58
FM Ratio	0.62	0.86	0.37

[1]Carbonate and opaque analyses used for qualitative interpretation only.

[2]Data represent an average of N spot determinations per polished thin section.

Table 14 (continued)

SPL #: 11, Chloritoid Alteration Zone

wt.(%)	Chlorite	Chloritoid	Ankerite[1]	Opaques[1]
N[2]	(9)	(6)	(5)	(2)
SiO2	23.69	24.65	0.01	0.55
TiO2	0.11	0.11	0.00	44.18
Al2O3	22.85	41.06	0.00	0.16
Cr2O3	0.10	0.12	0.00	0.04
FeO	29.20	23.63	13.99	24.92
MnO	0.17	0.50	1.43	0.90
MgO	11.64	3.17	13.73	0.04
CaO	0.07	0.03	26.30	0.02
Na2O	0.00	0.00	0.00	0.00
K2O	0.02	0.00	0.00	0.00
Totals	87.83	93.26	55.45	71.29
# of ions on the basis of:				
	28(O)	12(O)	6(O)	6(O)
Si	5.100	2.010	0.001	0.040
Ti	0.016	0.006	0.000	2.210
Al	5.796	3.947	0.000	0.014
Cr	0.017	0.008	0.000	0.003
Fe	5.252	1.612	1.140	1.410
Mn	0.031	0.035	0.118	0.051
Mg	3.735	0.385	1.995	0.005
Ca	0.017	0.003	2.746	0.001
Na	0.000	0.000	0.000	0.000
K	0.005	0.001	0.000	0.000
Totals	19.969	8.006	5.999	3.738
Proportions				
Fe	58.36	80.59	19.39	99.59
Mg	41.44	19.25	33.92	0.32
Ca	0.19	0.79	0.35	0.96
FM Ratio	0.58	0.79	0.35	0.96

Table 14 (continued)

SPL #: 45, Chloritoid Alteration Zone

wt.(%)	Chlorite	Chloritoid	Sericite	Paragonite
N^2	(3)	(3)	(2)	(3)
SiO2	24.38	24.81	48.82	47.21
TiO2	0.12	0.10	0.22	0.13
Al2O3	23.10	41.24	36.61	37.41
Cr2O3	0.06	0.08	0.04	0.07
FeO	27.20	22.83	1.01	0.44
MnO	0.28	0.95	0.02	0.04
MgO	12.12	3.15	0.79	0.41
CaO	0.02	0.01	0.05	0.89
Na2O	0.00	0.00	1.93	5.95
K2O	0.04	0.04	6.15	1.78
Totals	87.32	93.21	95.62	94.32
# of ions on the basis of:				
	28(O)	12(O)	22(O)	22(O)
Si	5.213	2.020	6.294	6.111
Ti	0.019	0.006	0.021	0.013
Al	5.821	3.957	5.567	5.728
Cr	0.011	0.005	0.004	0.006
Fe	4.864	1.555	0.109	0.048
Mn	0.050	0.066	0.002	0.004
Mg	3.864	0.382	0.152	0.078
Ca	0.004	0.001	0.007	0.124
Na	0.000	0.000	0.482	1.497
K	0.012	0.004	1.012	0.292
Totals	19.858	7.995	13.648	13.903
Proportions				
Fe	55.70	80.23	40.59	19.06
Mg	44.25	19.73	56.98	33.42
Ca	0.04	0.05	2.44	47.34
FM Ratio	0.55	0.78	0.41	0.37

Table 14 (continued)

SPL #: 265, Chloritoid Alteration Zone

wt.(%)	Chlorite	Chloritoid	Calcite[1]	Opaques[1]
N[2]	(7)	(6)	(2)	(2)
SiO2	24.39	25.25	0.02	1.85
TiO2	0.12	0.07	0.00	63.90
Al2O3	23.78	40.18	0.00	0.14
Cr2O3	0.12	0.20	0.00	0.06
FeO	27.06	23.55	1.62	2.95
MnO	0.17	0.50	1.04	0.00
MgO	12.99	2.92	1.14	0.03
CaO	0.17	0.01	52.43	0.01
Na2O	0.00	0.00	0.00	0.00
K2O	0.03	0.03	0.00	0.00
Totals	88.82	92.72	56.25	68.94
# of ions on the basis of:				
	28(O)	12(O)	6(O)	6(O)
Si	5.116	4.830	0.002	0.126
Ti	0.020	0.010	0.000	2.801
Al	5.879	9.058	0.000	0.010
Cr	0.020	0.030	0.000	0.004
Fe	4.747	3.767	0.135	0.125
Mn	0.030	0.082	0.087	0.000
Mg	4.062	0.833	0.169	0.002
Ca	0.038	0.001	5.603	0.001
Na	0.000	0.000	0.000	0.000
K	0.008	0.007	0.000	0.000
Totals	19.919	18.619	5.998	3.067
Proportions				
Fe	53.66	81.88	2.28	95.40
Mg	45.91	18.09	2.87	2.64
Ca	0.43	0.03	94.85	1.97
FM Ratio	0.54	0.80	0.34	0.97

Table 14 (continued)

SPL #: 47, Quartz-Sericite Alteration Zone

wt.(%)	Chlorite	Calcite[1]	Opaques[1]
N[2]	(6)	(6)	(2)
SiO2	25.11	0.03	1.19
TiO2	0.11	0.00	0.14
Al2O3	23.96	0.00	0.14
Cr2O3	0.16	0.00	0.01
FeO	22.61	2.99	0.42
MnO	0.13	0.45	0.00
MgO	17.16	3.11	0.05
CaO	0.06	49.19	0.02
Na2O	0.00	0.00	0.01
K2O	0.04	0.00	0.00
Totals	89.34	55.78	79.68
# of ions on the basis of:			
	28(O)	6(O)	6(O)
Si	5.109	0.002	0.079
Ti	0.017	0.000	2.902
Al	5.746	0.000	0.011
Cr	0.025	0.000	0.005
Fe	3.847	0.249	0.020
Mn	0.022	0.038	0.000
Mg	5.205	0.462	0.000
Ca	0.013	5.245	0.001
Na	0.000	0.000	0.001
K	0.011	0.000	0.000
Totals	10.005	5.997	3.014
Proportions			
Fe	42.44	4.18	93.32
Mg	57.42	7.75	2.18
Ca	0.14	88.07	4.50
FM Ratio	0.42	0.33	0.98

Table 14 (continued)

SPL #: 63, Quartz-Sericite Alteration Zone

wt.(%)	Chlorite	Calcite[1]
N[2]	(28)	(6)
SiO2	25.74	0.01
TiO2	0.12	0.00
Al2O3	21.30	0.00
Cr2O3	0.18	0.00
FeO	22.20	1.11
MnO	0.15	0.60
MgO	18.30	1.50
CaO	0.26	51.96
Na2O	0.00	0.00
K2O	0.02	0.00
Totals	88.27	55.18
# of ions on the basis of:		
	28(O)	6(O)
Si	5.308	0.001
Ti	0.019	0.000
Al	5.177	0.000
Cr	0.029	0.000
Fe	3.828	0.094
Mn	0.026	0.051
Mg	5.624	0.226
Ca	0.057	5.626
Na	0.000	0.000
K	0.004	0.000
Totals	20.072	5.999
Proportions		
Fe	40.26	1.58
Mg	59.14	3.81
Ca	0.60	94.61
FM Ratio	0.40	0.25

Table 14 (continued)

SPL #: 86, Quartz-Sericite Alteration Zone

wt.(%)	Chlorite	Calcite[1]	Sericite	Opaques[1]
N[2]	(9)	(6)	(4)	(3)
SiO2	25.00	0.01	49.25	1.44
TiO2	0.13	0.00	0.30	47.15
Al2O3	22.93	0.00	33.76	0.40
Cr2O3	0.16	0.00	0.09	0.11
FeO	25.70	1.24	2.11	1.15
MnO	0.20	0.73	0.01	0.00
MgO	14.51	1.18	1.31	0.01
CaO	0.06	52.04	0.24	0.00
Na2O	0.00	0.00	1.84	0.00
K2O	0.05	0.00	6.31	0.02
Totals	88.74	55.20	95.21	50.28
# of ions on the basis of:				
	28(O)	6(O)	22(O)	6(O)
Si	5.211	0.001	6.429	0.114
Ti	0.021	0.000	0.029	2.813
Al	5.635	0.000	5.196	0.037
Cr	0.027	0.000	0.009	0.007
Fe	4.481	0.105	0.231	0.076
Mn	0.036	0.063	0.001	0.001
Mg	4.508	0.179	0.254	0.001
Ca	0.013	5.651	0.033	0.000
Na	0.000	0.000	0.465	0.000
K	0.013	0.000	1.051	0.002
Totals	19.94	5.999	13.697	3.050
Proportions				
Fe	49.78	1.77	44.54	97.97
Mg	50.07	3.02	49.04	1.72
Ca	0.15	0.30	0.47	0.98
FM Ratio	0.50	0.30	0.47	0.98

Table 14 (continued)

SPL #: 130, Quartz-Sericite Alteration Zone

wt.(%)	Chlorite	Calcite[1]	Sericite	Opaques[1]
N[2]	(4)	(3)	(3)	(3)
SiO2	25.28	0.01	46.95	0.46
TiO2	0.10	0.00	0.26	67.29
Al2O3	21.96	0.00	34.46	0.06
Cr2O3	0.12	0.00	0.02	0.00
FeO	24.91	1.50	3.25	1.15
MnO	0.28	1.04	0.04	0.10
MgO	15.70	1.60	1.55	0.02
CaO	0.11	51.27	1.08	0.24
Na2O	0.00	0.00	0.59	0.00
K2O	0.04	0.00	7.38	0.00
Totals	88.49	54.72	95.58	69.81
# of ions on the basis of:				
	28(O)	6(O)	22(O)	6(O)
Si	5.271	0.001	6.195	0.026
Ti	0.016	0.000	0.026	2.930
Al	5.396	0.000	5.359	0.004
Cr	0.020	0.000	0.002	0.000
Fe	4.343	0.129	0.358	0.053
Mn	0.049	0.091	0.005	0.006
Mg	4.880	0.245	0.305	0.002
Ca	0.024	5.533	0.152	0.016
Na	0.000	0.000	0.150	0.000
K	0.011	0.000	1.242	0.000
Totals	21.010	5.999	13.795	3.039
Proportions				
Fe	46.97	2.19	43.94	69.01
Mg	52.77	4.15	37.39	2.23
Ca	0.26	93.67	18.67	28.76
FM Ratio	0.47	0.28	0.54	0.86

Table 14 (continued)

SPL #: 66, Iron Chlorite Alteration Zone

wt.(%)	Chlorite	Sericite	Opaques[1]
N[2]	(6)	(2)	(1)
SiO2	24.34	48.81	0.09
TiO2	0.12	0.27	51.59
Al2O3	22.81	37.11	0.03
Cr2O3	0.08	0.06	0.00
FeO	33.13	1.62	35.33
MnO	0.37	0.00	5.94
MgO	7.97	0.88	0.01
CaO	0.00	0.18	0.00
Na2O	0.00	1.23	0.00
K2O	0.07	6.65	0.00
Totals	88.89	13.65	92.99
# of ions on the basis of:			
	28(O)	22(O)	6(O)
Si	5.274	6.243	0.005
Ti	0.019	0.026	2.071
Al	5.826	5.594	0.002
Cr	0.014	0.007	0.000
Fe	6.003	0.173	1.577
Mn	0.068	0.001	0.269
Mg	2.573	0.167	0.000
Ca	0.000	0.025	0.000
Na	0.000	0.304	0.000
K	0.020	1.085	0.000
Totals	19.791	13.625	3.924
Proportions			
Fe	70.00	47.50	99.97
Mg	30.00	45.73	0.03
Ca	0.00	6.76	0.00
FM Ratio	0.70	0.51	0.85

Table 15. X-Ray Diffraction and Thin Section Staining Results.

Four samples were analyzed by X-Ray Diffraction by the Geological Survey of Canada's Mineralogy Section, Ottawa, Ontario for identification of Al-silicates.

Nine additional samples were analyzed at the University of Minnesota-Duluth to identify chlorite and carbonate species using a Picker Diffractometer with CuK_{α} radiation. Unoriented slide mounts were scanned from 6-60° at 1°/minute. Mineral identifications were made using Deer, Howie, and Zussman (1966), and identification tables of Berry (1974). Four of these samples, along with twelve others were stained with a potassium ferricyanide solution for identification of carbonate species.

Table 15. X-Ray Diffraction and Thin Section Staining Results.

XRF Analyses (Geological Survey of Canada)

SPL #	Al-Silicate Species
21	kyanite + andalusite
25	kyanite
221	kyanite
283	kyanite

XRF/Thin Section Staining

SPL #	Carbonate Species	Chlorite Species
Chloritoid Alteration Zone:		
11	ankerite	
167	ankerite	
220		Fe-ripidolite/chamosite
242	ankerite/calcite	Fe-ripidolite
226		chamosite
Quartz-Sericite Alteration Zone:		
96		Mg-ripidolite
257		Mg-ripidolite/clinoclore
Iron Chlorite Alteration Zone:		
59		Fe-ripidolite
72	ankerite?	Fe-ripidolite

Thin Section Staining (for Carbonate Species)

SPL #	Carbonate Species
Chloritoid Alteration Zone:	
10	ankerite
56	ankerite
150	ankerite
249	ankerite/calcite?
224	ankerite
Quartz-Sericite Alteration Zone:	
63	calcite
95	calcite/Fe dolomite
135	calcite/Fe dolomite
181	calcite
238	calcite
281	calcite/Fe dolomite?
282	calcite

Appendix IV.

Table 16. Normative Mineral Compositions

Normative mineral calculations were performed by the Geological Survey of Canada using chemical analyses listed in Table 12. The following parameters were applied in the calculations:

1. CO_2 is a permitted component,

2. H_2O has been removed and the remaining components normalized to 100%,

3. all ferric iron is not converted to ferrous iron,

4. ferric iron is unchanged,

5. an appropriate name for the normative composition is given according to the classification of Irvine and Baragar (1971).

As in Tables 12 and 13 of Appendix II, the last column of the following table represents a classification of each sample according to the sample's mineral assemblage (see Appendix I). The alteration assemblages coincide with those described in the text (Ch. III, Alteration) and with the alteration zones shown on Plate 2. The alteration types include: (1) Least Altered, (2) Quartz-Sericite, (3) Iron Chlorite, and (4) Chloritoid. Type (4) includes quartz-kyanite-bearing rocks locally found associated with chloritoid type alteration.

The following abbreviations are used:

Minerals	
Quartz	Q
Corundum	C
Orthoclase	OR
Albite	AB
Anorthite	An
Enstitite	EN
Ferrosilite	FS
Magnetite	MT
Ilmenite	IL
Chromite	CR
Apatite	AP
Pyrite	PY
Calcite	CC

Rock Name	
Tholeiitic	T
Calc-Alkaline	CA
Basalt	BA
Andesite	AND
Dacite	DAC
Rhyolite	RHY
K-poor Series	(KP)
K-rich Series	(KP)
Average Series	(AS)

Table 16. Normative Mineral Compositions

SPL #	Q	C	OR	AB	AN	EN	FS	MT	IL	CR	AP	PY	CC	NAME	ALT[1] TYPE
1	48.56	11.02	14.09	14.71		2.88	4.06	1.33	0.91		0.50	0.08	1.86	CA RHY (AS)	III
2	22.91	8.31	3.04	15.66	11.27	10.96	9.31	2.54	1.47		0.21	0.06	14.27	T AND (AS)	IV
3	27.85	11.66	3.95	14.13	6.28	8.99	15.58	1.97	1.94	0.05	0.41	0.06	7.12	T AND (KP)	III
10	21.67	10.03	0.55	19.30	3.43	14.33	9.92	1.65	1.87	0.05	0.27	0.19	16.74	T AND (KP)	IV
11	40.78	12.85	1.29	0.87		7.83	9.83	6.01	1.57	0.05	0.26	0.51	18.14	T DAC (AS)	II
12	38.04	7.16	9.84	39.46				0.61	0.64		0.26	0.13	3.69	CA RHY (KP)	IV
18*	59.16	12.38	12.58	12.17		0.58		0.54	1.21		0.60		0.23	CA RHY (AS)	IV
21	73.74	19.32	1.19	4.27		0.18			0.57		0.33	0.06		CA RHY (KP)	IV**
25	79.70	13.67	1.54	4.23	0.02				0.14		0.26	0.06		CA RHY (KP)	IV**
26	40.57	19.19	8.06	6.25	0.22	3.97	10.73	7.04	2.31	0.06	0.37	1.24		T DAC (AS)	IV
27	31.83	6.44	8.78	33.77	7.89	2.17	4.62	1.19	1.21	0.02	0.48		1.63	T DAC (KP)	III
29	32.45	12.18	8.19	0.87		10.88	7.44	4.05	1.28	0.05	0.17	0.13	22.33	T DAC (KR)	II
30	21.42	15.02	4.11	7.89		16.90	11.31	1.95	1.52	0.08	0.19	0.06	19.56	T AND (KP)	II
31	23.42	6.87	2.80	13.95	14.91	10.65	9.42	2.69	1.43		0.17	0.11	13.59	T BA (AS)	II
32	29.38	16.07	2.18	0.89		29.25	16.61	1.83	1.66	0.08	0.24	0.13	1.68	T AND (KR)	II
33	16.12	1.25	0.06	1.76	38.56	20.76	8.06	6.95	1.50	0.06	0.17		4.74	T BA (KR)	II
35	37.48	19.76	19.79	7.89	2.12	3.05	1.98	4.51	2.64	0.11	0.39	0.06	0.24	T DAC (KR)	IV
38	35.07	13.68	15.71	2.68		10.76	11.39	5.66	1.74	0.62	0.22	1.60	1.44	T DAC (KR)	III
45	54.51	18.36	5.62	4.37		2.74	3.84	4.79	3.67	0.03	1.56	0.06	0.47	T RHY (AS)	IV
49	49.93	13.86	11.89	1.76		5.14	10.67	2.71	2.30	0.02	0.87	0.15	0.71	T DAC (KR)	IV
50	58.11	13.27	21.39	1.70		0.67	1.37	1.78	0.82	0.02	0.38		0.47	T RHY (KR)	IV
51	54.49	17.48	4.17			5.04	11.21	4.81	1.99	0.01	0.22	0.06	0.47	T DAC (KR)	IV
54	21.42	15.03	6.19	17.71	2.47	12.17	10.55	1.82	2.07	0.05	0.24	0.26	10.00	T AND (KP)	IV
55*	2.10		0.18	7.01	39.44	20.07	8.20	4.36	1.20	0.12	0.14	0.23	1.18	T BA (KR)	I
56	33.15	14.84	8.27			6.20	8.93	2.83	1.78	0.09	0.22	0.06	23.63	T RHY (KR)	IV
57	23.30	7.77	2.96	15.56	12.28	10.51	9.42	2.52	1.42	0.02	0.24	0.08	13.94	T AND (AS)	II
61	16.63	11.35		27.31		19.27	14.45	2.72	1.84	0.09	0.17		6.16	T AND (KP)	II
63	17.98	11.15		18.69	0.14	20.76	14.64	2.75	1.60	0.06	0.17	0.08	11.97	T AND (KP)	II
71	23.57	7.50	0.12	16.65	13.58	11.84	13.42	2.40	2.10	0.06	0.22	0.06	8.48	T BA (KP)	III

[1] Alteration Type: (I) Least Altered, (II) Quartz-Sericite, (III) Iron-Chlorite, (IV) Chloritoid.

*Also,
SPL # 18 reported 0.55% Hematite.
SPL # 55 reported 11.63% Diopside, 4.14% Hedenbergite

**Quartz-kyanite-bearing rocks associated with Chloritoid-type alteration.

Table 16 (continued).

SPL #	Q	C	OR	AB	AN	EN	FS	MT	IL	CR	AP	PY	CC	NAME	ALT[1] TYPE
79*	48.08	13.91	24.19	8.74		0.45			0.40	0.02	0.74	0.06	1.64	CA RHY (KR)	II
80	47.42	13.20	18.99	7.92	0.21	3.50	0.93	3.62	1.13		0.72		2.36	CA RHY (KR)	III
85	31.92	15.15	13.24	2.67	0.23	7.25	20.79	2.44	4.07	0.03	1.98		0.24	T AND (KR)	III
86	30.74	14.78	10.08	2.65		12.73	14.05	2.12	1.75	0.08	0.24	0.09	10.70	T AND (KR)	II
88	34.97	26.06	3.77			4.87	18.44	7.54	2.86	0.02	1.01		0.48	T AND (KR)	IV
89	18.27	29.68	11.36	1.80	0.67	5.63	18.01	9.99	3.97	0.05	0.34		0.24	T AND (KR)	IV
90*	5.39			11.38	34.21	22.08	10.56	3.74	1.35	0.08	0.17	0.15	4.22	T BA (KP)	I
95	47.88	11.72	16.79	6.91		5.17	2.45	2.37	0.99		0.43	0.17	5.11	CA RHY (KR)	II
96	22.87	7.15	2.83	14.65	13.83	11.14	9.31	2.51	1.47		0.21	0.13	13.9	T BA (AS)	II
97	39.54	9.42	17.76	13.87		7.44	3.69	1.64	0.92		0.50	0.08	5.13	CA RHY (AS)	II
99	58.86	9.93	21.44	0.87				1.34	0.56		0.24	0.06	6.75	CA RHY (KR)	III
102	17.23	12.11	0.99			16.95	18.99	3.20	1.34	0.05	0.19	0.52	28.43	T AND (KR)	III
104	20.10	14.15	5.11	9.80	1.30	18.56	14.05	1.80	1.56	0.08	0.17	0.11	13.17	T AND (AS)	II
106*	10.39		0.06	5.22	40.11	7.43	2.33	7.90	1.37	0.06	0.14	0.15	4.21	T BA (KR)	II
112	53.56	11.72	15.59	2.62		7.49	3.68	1.20	1.04		0.43	0.09	2.59	CA RHY (KR)	II
116*	6.59		0.49	6.14	40.37	25.08	11.22	3.46	1.48	0.08	0.14	0.04	1.89	T BA (KR)	I
117	28.01	13.56	10.40	4.43		17.26	9.47	2.58	2.07	0.02	1.24	0.50	10.47	T AND (KR)	II
118	51.53	11.67	11.79	7.90		8.10	3.42	1.35	0.91		0.36	0.04	2.83	CA RHY (AS)	II
126	64.06	11.01	14.72	3.45		1.99	0.78	1.77	0.47		0.09	0.04	1.62	CA RHY (KR)	II
127*	23.42	7.34	2.87	12.22	15.38	11.53	9.33	2.54	1.51	0.02	0.24	0.23	13.37	T BA (AS)	II
129	39.51	7.73	15.90	31.99		1.11		0.98	0.51		0.17		1.86	CA RHY (KP)	II
132	21.43	11.88	0.87	16.83	5.66	17.73	15.13	2.28	1.85	0.08	0.19	0.13	5.95	T AND (KP)	II
139	21.42	10.87	1.05	12.36		20.41	13.94	2.12	1.14	0.06	0.19	0.04	16.38	T AND (KP)	I
144	28.20	12.95	3.45	5.38	7.22	16.29	20.85	1.99	1.85	0.08	0.17	0.11	1.45	CA BA (KR)	III
146	25.70	20.93	33.37	5.42		1.29					1.91	0.18	0.24	T RHY (KR)	IV
148*	43.51	16.58	18.27	4.37	3.92	2.83	3.50	2.09	2.51	0.02	0.62	0.02	1.65	CA AND (KR)	IV

*Also,
SPL # 79 reported 0.83% Hematite.
SPL # 90 reported 4.74% Diopside, 1.98% Hedenbergite.
SPL # 106 reported 16.22% Diopside, 4.43% Hedenbergite.
SPL # 116 reported 2.17% Diopside, 4.3% Hedenbergite.
SPL # 127 reported 0.25% Hematite.
SPL # 148 reported 9.29% Hematite.

Table 16 (continued).

SPL #	Q	C	OR	AB	AN	EN	FS	MT	IL	CR	AP	PY	CC	NAME	ALT[1] TYPE
149	45.25	18.52	23.87	6.99		0.04			3.00	0.02	0.24		0.47	T RHY (KR)	IV
153	44.32	9.52	18.49	20.87		1.34	1.13	1.49			0.43	0.02	1.40	CA RHY (AS)	II
156	56.60	12.10	23.39			1.14	1.09	1.49	1.79		0.60	0.65	1.17	T RHY (KR)	IV
157*	8.65			6.16	42.13	19.42	8.74	5.28	1.68	0.08	0.19	0.51	6.39	T BA (KR)	III
159	44.54	17.95	15.67	0.88		2.23	3.40	7.68	2.19	0.09	0.19	0.21	4.96	T RHY (KR)	IV
161	23.15	7.56	2.96	13.84	14.09	10.95	9.91	2.22	1.48		0.24	0.11	13.49	CA BA (AS)	III
163	39.82	14.50	5.54			8.72	13.23	4.38	1.35	0.08	0.17	1.09	11.13	T DAC (KR)	IV
167	39.95	14.19	16.18	4.35		4.74	7.01	2.83	1.74	0.08	0.19	0.09	8.66	T RHY (KR)	IV
171	31.13	15.70	6.83			27.12	13.79	2.54	2.25	0.02	1.16		0.48	T AND (KR)	II
176*	6.41			16.63	33.25	22.35	9.74	7.34	1.53	0.06	0.22	0.06	1.88	T BA (KP)	I
182*	2.84		0.55	20.88	31.86	21.47	14.82	2.98	1.91	0.08	0.22		1.64	T BA (KP)	I
187	15.14	12.29	6.69	19.49	1.65	17.75	15.12	1.97	1.77	0.09	0.19	0.24	7.62	T AND (KP)	II
193*	0.99		1.08	20.60	30.61	13.79	9.28	3.53	1.64	0.08	0.14	0.25	2.77	T BA (KP)	I
195	13.29	9.42	0.19	23.19	3.05	21.98	14.19	1.99	1.66	0.17	0.17		10.79	T AND (KP)	I
210*	2.90		2.40	15.46	32.44	13.28	8.85	3.98	1.95	0.06	0.26	0.02	0.46	T BA (KR)	I
211	15.62	10.03	2.63		9.43	28.99	17.39	3.22	1.17	0.08	0.17	1.18	10.11	T BA (KR)	II
218*	58.90	13.26	16.34	6.93	0.29	0.89		0.94	1.28	0.02	0.69	0.30		CA RHY (KR)	IV
219	49.99	17.18	10.53	13.21	1.34	1.40	0.54	3.32	1.54	0.02	0.92	0.02		T RHY (AS)	IV
220	24.91	16.40			0.24	17.40	22.63	16.35	1.15	0.02	0.67		0.24	T BA (KR)	IV
221*	74.71	19.84	0.71	2.55		0.08					0.65	0.02		T RHY (KP)	IV**
222	27.88	9.55	2.91	10.42	9.80	10.83	9.37	2.38	1.54		0.21	0.17	14.93	T BA (AS)	IV
224	34.88	10.88	15.05	11.38	4.45	3.86	6.57	1.95	3.91	0.02	1.39	0.02	5.64	T AND (KR)	III
226*	42.35	13.81	0.13	1.81		16.30					0.17	0.36	0.49	T AND (KP)	IV

*Also,
SPL # 157 reported 0.56% Diopside, 0.22% Hedenbergite.
SPL # 176 reported 0.38% Diopside, 0.14% Hedenbergite.
SPL # 182 reported 0.48% Diopside, 0.29% Hedenbergite.
SPL # 193 reported 9.61% Diopside, 5.64% Hedenbergite.
SPL # 210 reported 11.35% Diopside, 6.60% Hedenbergite.
SPL # 218 reported 0.17% Hematite.
SPL # 221 reported 0.74% Rutile.
SPL # 226 reported 0.69% Rutile, 23.89% Hematite.
**Quartz-kyanite-bearing rocks associated with Chloritoid-type alteration.

Table 16 (continued).

SPL #	Q	C	OR	AB	AN	EN	FS	MT	IL	CR	AP	PY	CC	NAME	ALT[1] TYPE
227	47.76	13.07	10.38	7.81	8.46	2.94	0.41	0.45	3.80	0.02	1.19		3.73	CA AND (KR)	III
229*	31.29	21.44		2.66	0.40	10.36					0.73	1.05	0.24	T AND (KP)	IV
230	64.88	10.62	7.25	4.32	1.92	3.11	4.86	1.93	0.72		0.31	0.08		T DAC (KR)	IV
231	35.63	11.86	5.62	2.65	13.29	8.45	12.89	2.42	3.25	0.03	1.53		2.38	T BA (KR)	III
232*	42.97	13.55	7.65	6.28	3.59	10.37					0.07	0.32	1.21	T AND (KR)	IV
233	47.07	13.55	4.79	4.34	13.16	6.14	4.97	0.45	1.93	0.08	0.21	0.04	3.26	CA BA (KR)	II
234	40.07	14.53	8.25	4.37	9.47	6.87	8.66	0.90	2.06	0.09	0.17	0.09	4.47	CA BA (KR)	III
235	48.26	13.25	14.32	5.23		4.99	7.81	1.20	1.68	0.06	0.17	1.86	1.17	T RHY (KR)	III
236	45.12	17.51	0.74	0.88	1.73	8.80	12.33	5.26	1.83	0.08	0.19	0.81	4.72	CA BA (KR)	IV
237	16.61	10.38	0.93	28.30	3.56	16.85	14.25	2.58	1.79	0.08	0.07		4.52	T AND (KP)	I
238	24.27	11.79	5.19	6.11		13.85	11.71	1.95	1.43	0.05	0.19	0.13	23.24	T DAC (AS)	II
239	31.39	14.11	5.82	5.20		5.09	5.18	2.82	1.69	0.08	0.21		28.42	T RHY (AS)	IV
240	40.79	14.29	6.09	2.59		5.42	4.97	3.85	1.61	0.08	0.14		21.18	T RHY (KR)	IV
241	25.28	8.89	3.22	12.17	11.98	10.88	9.61	2.09	1.54	0.02	0.19	0.11	14.02	CA BA (AS)	II
242	28.92	11.55	5.95	5.21		6.75	7.31	1.79	1.29	0.06	0.17	0.21	30.81	T RHY (AS)	IV
246	57.40	6.40	8.26	21.66	1.45	0.76	2.49	0.59	0.45		0.14	0.06	0.46	T RHY (KP)	I
247	27.55	10.28	4.25	14.02	8.41	8.15	14.57	1.65	1.81	0.06	0.22	0.13	8.71	T AND (AS)	III
248	24.45	10.37	1.64	13.03	0.63	7.52	13.08	2.09	1.91	0.05	0.26	0.08	14.88	T AND (KP)	IV
249	21.99	12.11	4 21	12.21		12.18	12.21	1.64	1.64	0.06	0.22	0.45	21.09	T DAC (KP)	III
250	25.69	8.27	2.80	12.21	12.31	10.68	9.07	2.84	1.45		0.22	0.17	14.29	T BA (AS)	III
251	51.37	13.19	17.51	8.64		2.72	2.84	1.63	1.14		0.71	0.21	0.23	CA RHY (KR)	IV
253*	69.94	28.04	0.65								0.43	0.21	0.23	T RHY (KR)	IV
263	43.89	3.37	24.28	23.85	1.22	0.80	0.13	1.02	0.23		0.12	0.27	0.92	CA RHY (AS)	IV**
265	39.27	19.82	9.63	6.14	6.89	4.60	5.53	4.36	2.36	0.12	0.24	0.09	0.94	CA AND (KR)	IV
273*	21.71	10.94	11.11	19.63		1.89					0.21	1.11	4.27	T AND (KP)	III
279	28.06	10.07	6.75			5.16	3.98	2.18	1.64	0.03	0.23	0.49	41.42	T RHY (KR)	IV
283	23.39	11.22	5.95	4.39		15.36	14.22	1.80	1.81	0.06	0.24	0.11	21.45	T AND (AS)	II

*Also,
SPL # 229 reported 2.83% Rutile, 29.01% Hematite.
SPL # 232 reported 0.85% Rutile, 13.14% Hematite.
SPL # 253 reported 0.60% Rutile, 0.12% Wollastonite.
SPL # 273 reported 0.85% Rutile, 28.28% Hematite.

**Quartz-kyanite-bearing rocks associated with Chloritoid-type alteration.

Table 16 (continued).

SPL #	Q	C	OR	AB	AN	EN	FS	MT	IL	CR	AP	PY	CC	NAME	ALT[1] TYPE
289*			9.22	16.38	27.02	13.41	8.71	3.55	1.55	0.06	0.19	0.19	2.78	T BA (KR)	I
290*	10.67		0.31	9.68	36.15	15.87	12.66	4.53	1.88	0.05	0.19	0.02	3.31	T BA (KR)	I
291	30.18	17.71	8.91		0.21	10.12	26.16	3.54	2.08	0.09	1.01			T BA (KR)	IV
292	44.43	14.21	13.85	4.38	0.60	6.04	12.26	1.65	2.07	0.02	0.26		0.24	T DAC (KR)	III
293	24.54	15.37	10.04	5.35	0.53	9.42	24.06	3.36	2.02	0.11	0.88		4.32	T AND (KR)	III
294*	19.46	23.32	40.44	13.25		0.42			0.17	0.05	0.12	0.02	0.24	CA RHY (KR)	IV
295	45.86	13.10	17.33	7.88		3.99	8.00	1.05	1.59	0.02	0.29	0.41	0.47	T RHY (KR)	IV
296	24.49	16.73	0.38	1.81	1.59	13.04	32.68	5.11	1.89	0.11	0.79	1.14	0.24	CA BA (AS)	IV
297*	5.56	26.68	40.32	22.36	0.75	0.50			0.07	0.23	0.54		0.24	CA RHY (KR)	II
298*	16.55	21.17	42.33	14.96		0.25			2.72	0.20	0.39		0.24	CA RHY (KR)	IV
299	22.64	7.39	2.84	16.44	12.66	10.06	9.37	2.67	1.46	0.02	0.24	0.04	14.19	T AND (AS)	IV
300	62.75	10.67	13.72	2.59		2.34	4.18	1.33	1.49	0.03	0.24	0.42	0.23	T RHY (KR)	IV

*Also,
SPL # 289 reported 1.66% Forsterite, 1.14% Fayalite, 9.01% Diopside, 5.10% Hedenbergite.
SPL # 290 reported 2.76% Diopside, 1.92% Hedenbergite.
SPL # 294 reported 1.90% Rutile, 0.63% Hematite.
SPL # 297 reported 2.03% Rutile, 0.74% Hematite.
SPL # 298 reported 0.27% Rutile, 0.94% Hematite.